miRNA-7 Inhibition Restores *Pax6* Levels in Murine Haploinsufficient Islets

by

Kevin Yongblah
BSc Hons, University of Essex, 2012

A Thesis Submitted in Partial Fulfilment
of the Requirements for the Degree of

Master of Science

in the Department of Biochemistry and Microbiology

Supervisory Committee

miRNA-7 Inhibition Restores *Pax6* Levels in Murine Haploinsufficient Islets

by

Kevin Yongblah
BSc Hons, University of Essex, 2012

Supervisory Committee

Dr Perry Howard, Department of Biochemistry & Microbiology
Supervisor

Dr Caren Helbing, Department of Biochemistry & Microbiology
Departmental Member

Dr Robert Chow, Department of Biology
Outside Member

Abstract

Supervisory Committee

Dr Perry Howard, Department of Biochemistry & Microbiology
Supervisor

Dr Caren Helbing, Department of Biochemistry & Microbiology
Departmental Member

Dr Robert Chow, Department of Biology
Outside Member

Aniridia is a rare genetic disorder that affects the development of the eye and is caused in most cases by mutations in the *PAX6* gene. Patients with a heterozygous mutation in their *PAX6* gene are born without irises. Aniridia patients are also prone to other eye diseases over their lifetimes such as cataracts and glaucoma. Aniridia's progressive nature suggests that therapeutic intervention aimed at restoring *PAX6* expression may be effective at ameliorating the progression of this disease.

PAX6 is necessary for the development and maintenance not only of the eye, but also the pancreas. Patients with aniridia have an increased likelihood of developing glucose intolerance and diabetes. Indeed, genetic studies in rodents have confirmed that haploinsufficient animals for *Pax6* develop glucose intolerance due to an ongoing requirement for *Pax6* expression in the pancreas and gut.

This thesis is a proof-of-concept study designed to determine the effects of repressing miRNA regulation of murine *Pax6*. *Pax6* is regulated by miRNA-7 and miRNA-375. I hypothesized that repression of miRNA-7 and miRNA-375 would restore *Pax6* expression and that this strategy might be useful in treating some of the progressive symptoms that emerge in aniridia patients in adulthood. As a first step towards evaluating miRNA inhibition as a therapeutic strategy for the treatment of aniridia, my first

objective was to confirm whether miRNA-7 and miRNA-375 regulate *Pax6* expression in pancreatic cells and tissue. My second objective was to determine whether these miRNAs could be efficiently inhibited. My third objective was to determine whether repression of miRNA-7 or miRNA-375 alters endogenous PAX6 protein levels in pancreatic cell lines. My final objective was to determine whether target protectors, delivered to explants of pancreatic islets through an adeno-associated virus (AAV) vector, could be used to restore *Pax6* expression in murine haploinsufficient islets. From this study, I have confirmed that miRNA-7 and miRNA-375 regulate *Pax6* in pancreatic cells that these miRNAs can be specifically inhibited, and that inhibition leads to an increase in *Pax6* on both the reporter and protein levels. I have shown that target protectors against the miRNA-7 and miRNA-375 binding sites within the *Pax6* 3'UTR are effective at increasing the levels of PAX6 protein in pancreatic cell lines. Finally, I have also shown that a target protector against the miRNA-7 binding site can increase PAX6 protein levels in islets from murine haploinsufficient islets to near wild-type levels. My thesis lays the groundwork for the development of anti-miRNA-based therapies aimed at restoring *PAX6* expression in the eye and pancreas.

Table of Contents

List of Tables

List of Figures

List of Appendices

List of Abbreviations

AAV- Adeno-associated virus
AAVS1- Adeno-associated virus Integration Site 1
Ago2- Argonaute 2
AK -Aniridic keratopathy
BCA- Bicinchoninic acid
BGS- Bovine growth serum
Bp- Base pairs
cDNA- Complementary DNA
CNS- Central nervous system
CMV- Cytomegalovirus
CTS- C-terminal subdomain
CT-S -Centrotemporal spikes
Dey- Dixie's
DMEM- Dulbecco's modified eagle media
DNA- Deoxyribonucleic acid
EGFP- Enhanced green fluorescent protein
Ey- Eyeless
EX- Embryonic day X
GCG- Glucagon
GFP- Green fluorescent protein
GIP- Gastric inhibitory polypeptide
GLP- Glucagon like peptide
Glut- Glucose transporter
GSIS- Glucose stimulate insulin secretion
GTT- Glucose tolerance test
GWAS- Genome wide association study
HBSS- Hank balanced salt solution
HCV- Hepatitis C virus
HD- Homeodomain
HeLa- Henrietta Lacks
HEK- Human Embryonic Kidney
HOMA- Homeostatic model assessment
Huh- Hepatocarcinoma
HRP- Horseradish peroxidase
ICA- Independent component analysis
IEE- Intercistronic expression element
Ins-Insulin
ITR- Inverted terminal repeats
Kb- Kilo bases
kDa- KiloDalton
LB- Luria-Bertani
LCA- Leber's congenital amaurosis
LNA- Locked nucleic acid
MIN6- Mouse insulinoma

miRNA- MicroRNA
miR-375- mmu- miRNA-375-3p
miR-375-OE – Overexpression vector for mmu- miRNA-375-3p
miR-7- mmu-miRNA-7-5p
miR-7-OE- Overexpression vector for mmu-miRNA-7-5p
MODY- Mature onset of diabetes in youth
MOI- Multiplicity of infection
MTNP Myotrophin
mRNA- Messenger RNA
Neu- Neuherberg
NMD- Nonsense mediated decay
NTS- N-terminal subdomain
ORF- Open reading frame
OGTT- Oral glucose tolerance test
PAX4- Paired box 4
PAX6- Paired box 6
PBS- Phosphate buffered saline
PBTB- PBS, BSA, Triton-X 100
PC1/3- Proprotein convertase 1/3
PCR- Polymerase chain reaction
PD- Paired domain
PDK1- 3-phosphoinositide dependent protein kinase-1
PDX1- Pancreatic and duodenal homeobox 1
PFA- Paraformaldehyde
Pol II- Polymerase II
Pol III- Polymerase III
PP- Pancreatic polypeptides
PPI- Prepulse inhibition
Pre-miRNA - Precursor miRNA
Pri-miRNA - Primary miRNA
PST- Proline serine threonine
PTC- Premature termination codon
rAAV- Recombinant AAV
RE- Rolandic epilepsy
RISC- RNA-induced silencing
RNA- Ribonucleic acid
RNAi- RNA inference
RPC- Retinal progenitor cells
RPE- Retinal pigment epithelium
RPE65- Ribulose-phosphate-3-epimerase 65
SDS- Sodium dodecyl sulfate
SDS -PAGE- SDS-polyacrylamide gel electrophoresis
Sey- Small-eye
Sey-dey- Small-eye-Dixies
SNP-Single nucleotide polymorphisms
SOP- Standard operating protocol

SV40- Simian vacuolating virus 40
TBS-T- Tris-buffered saline-Tween 20
tRNA- Transfer RNA
TP- Target protector
TP-375- Target protector for mmu-miRNA-375 binding site
TP-7- Target protector for mmu-miRNA-7 binding site
Tud- Tough Decoy
Tud 375- Tough decoy with miRNA binding site against mmu-miRNA-375
Tud 7- Tough decoy with miRNA binding site against mmu-miRNA-7
Tud MT- Control Tough decoy, with miRNA binding site mutated to guanine
UTR- Untranslated region
WAGR - Wilms tumour, aniridia, genitourinary anomalies, and retardation
ΔPD- Paired-less

Chapter 1: Introduction

The paired box 6 *(PAX6)* gene encodes for a transcription factor which is critical for the development of the eye, the brain, and the pancreas. Haploinsufficiency of the *PAX6* gene, in humans leads to aniridia, a rare eye disorder named for the lack of an iris. However, there is a spectrum of symptoms in aniridia that are associated with *PAX6* mutations which include: foveal hypoplasia, corneal disease, glaucoma, and cataracts such that most of the major eye structures are impacted[1,2]. Patients are born with low vision primarily due to hypomorphic fovea, but will frequently experience progressive loss of vision due to cataracts, corneal clouding, and glaucoma, even with medical intervention[1,2]. This is thought to reflect an on-going requirement for *PAX6* expression in the eye. In addition, aniridia is associated with several non-ocular conditions such as obesity, glucose intolerance, and anosmia[3,4,5]. The postnatal requirement for *PAX6* suggests there may be a therapeutic window for interventions aimed at increasing the expression of *PAX6*.

In my thesis, I examine whether the inhibition of miRNA-7 and miRNA-375 sites within the 3'UTR of *Pax6* can be used to increase murine *Pax6* expression as a potential therapeutic strategy for aniridia. In chapter 1, I will provide a general background on *PAX6*, its role in aniridia syndrome, focussing on the role of *PAX6* in the pancreas and its association with diabetes. This is followed by current and potential strategies to treat the progressive component of aniridia syndrome, leading to the background on the strategy I have tested. This is followed by the hypothesis and objective. In Chapter 2, I describe the materials and methods used for the thesis. Following this is the results chapter that

provides evidence that the miRNA inhibition strategy used can restore *Pax6* levels to close to wild type. The thesis is concluded with a discussion reviewing the results, and lays out the future directions that can follow from the data I have collected.

1.1-*PAX*6 Regulates Development and Maintenance of Multiple Organs

PAX6 is a paired-box transcription factor that has a key role in regulating development and maintenance in the eye, the pancreas, and the brain. Human *PAX6* is located on chr11p13 (see Figure 1a), occupies a 28 kb stretch of DNA and spans 16 exons[6]. *PAX6* is highly conserved in humans, mice, rats, zebrafish, quail, and the fly *Drosophil*a where it plays an essential role in eye development[7]. For example, at the amino acid level, human and rodent PAX6 are 100% identical, while chick and zebrafish PAX6/Pax6 share 96% and 93% identity with human PAX6, respectively[7].

1.2-*PAX6* Transcription

Transcription of *PAX6* involves three promoters and alternative splicing. The two main promoters for *PAX6* expression are: P0 and P1[8,9], which transcribe two individual 13 exon-long transcripts (see Figure 1b). Despite the differences between the two transcripts, they both encode the same polypeptide since translation starts at exon 4[8,9]. The two transcripts are regulated differently during embryonic development and may provide spatiotemporal control ensuring the correct expression of *PAX6* during development and maintenance of numerous organs. A third promoter, termed promoter α, is found in an intronic sequence amidst exon 4 and 5, and results in the translation of a truncated PAX6 protein isoform (see Figure 1c)[10,11].

Additional regulatory elements are found upstream of the promoters and regulate tissue specific expression[12,13]. In addition to these upstream regulatory elements, distal

regulatory components have been discovered[14,15]. For example, there is a tissue-specific enhancer more than 120 kb downstream of the *PAX6* gene[14]. This multi-layered regulation is thought to fine-tune control of *PAX6* expression in specific tissues during defined windows of development.

1.3-PAX6 Isoforms and Their Roles

The three isoforms of *PAX6* include the canonical *PAX6*, *PAX6(5a)* and *PAX6* (ΔPD or paired-less) (see Figure 1c). The canonical isoform is expressed by both P0 and P1 and consists of the paired domain and the homeodomain that binds to DNA. These domains are connected by a glycine-rich linker domain. This form also contains a transactivation domain, called the P/S/T domain, which is rich in proline/serine/threonine[9,16]. The alternative *PAX6(5a)* isoform is due to an alternative splicing event that produces a 14-amino-acid insert in exon 5 within the paired domain and has different DNA binding activity from that of the canonical form[9]. The canonical isoform interacts preferentially with DNA at the N-terminal subdomain of the PAIRED domain, whilst the amino-acid insertion causes the *PAX6(5a)* isoform to interact preferentially with DNA at the C-terminal subdomain of the paired domain[17]. The *PAX6*(ΔPD) isoform is expressed by Pα and does not contain the paired domain; instead, it is comprised of the DNA-binding homeodomain and the PST domain[10,18,19]. The purpose of the distinct isoforms is not known; however, it has been shown that *Pax6*(5a) plays a distinct role in lens and iris development[20]. Although its physiological role is still unknown, overexpression of the truncated form results in disrupted development and in microphthalmia[18,19].

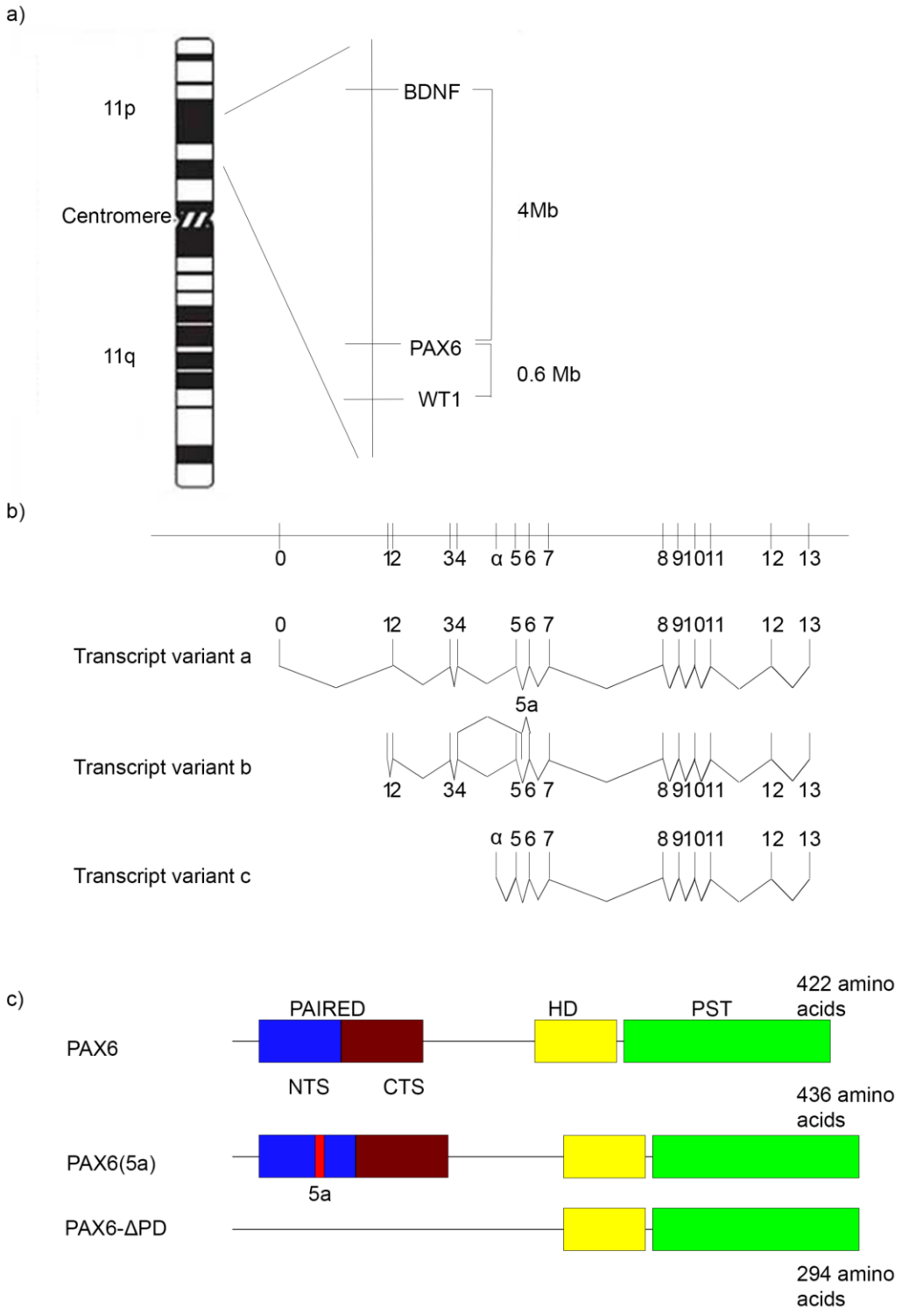

Figure 1: The *PAX6* genomic location, transcripts, and isoforms. a) A Schematic diagram of chromosome 11. *PAX6* is located on the p arm of chromosome 11 at position 12. *PAX6* is situated between brain-derived neurotrophic factor (BDNF) and Wilm's tumour gene 1 (WT1). (b) Transcript variants of *PAX6*. *PAX6* contains 14 exons; alternative promoter use results in the

three unique transcripts. Variant b undergoes an alternative splicing event at intron 5 and results in the inclusion of a 14-amino-acid insert. Additionally, the transcript variant c starts from the α promoter generates a unique isoform (PAX6-ΔPD). (c) PAX6 protein isoforms. Canonical PAX6 protein contains two paired box (PAIRED) domains and paired-type homeodomain (HD- in yellow), and a carboxyl-terminal transactivation domain, that is proline, serine, and threonine (PST- in green) rich. The second isoform contains a 14-amino-acid insert, which alters the DNA-binding activity of the PAIRED domain. The difference created by the insertion results in different DNA-binding activity to either the CTS (C-terminal subdomain - in dark red) or NTS (N-terminal subdomain - in blue). PAX6-ΔPD isoform is created by transcription from an internal promoter α.

1.4-PAX6 Expression Pattern

PAX6 is expressed early in development and is restricted to the central nervous system (CNS), the eye, the olfactory bulb, and the endocrine pancreas. In mice, *Pax6* expression starts at E8.5, in the neuroepithelium of the dorsal part of the telencephalic primordium[9]. At E10, expression is also seen in the developing eye and pancreas[20,21,22], and is maintained into adulthood in the endocrine islets and multiple components of the eye.

In humans, *PAX6* is first expressed in multiple components of developing eye with expression starting at the 6th week of gestation[23]. *PAX6* expression is maintained into adulthood in the endocrine pancreas and in the retina, lens and cornea[24,25]. This early expression of *PAX6* provided the first indication that *PAX6* would play a crucial role in the development of the eye, brain and pancreas.

1.5-*PAX6* Role in Eye Development

The function of *Pax6* has been studied most thoroughly in the developing eye, where *Pax6* transcriptionally interacts with several genes to coordinate their expression. For example, during lens development in chicken embryos, *Pax6* and *Sox2* interact with δ-crystallin enhancer (DC5 enhancer) resulting in the expression of δ-crystallin[26]. *Pax6* has also been shown to have a role in determining cell fate. Tissue-specific (neuroretina)

inactivation of *Pax6* in mice via Cre-LoxP excision showed that *Pax6* was required to maintain a pluripotent phenotype in retinal progenitor cells (RPCs). The loss of *Pax6* shortly after RPCs have formed alters the fate of these cells, resulting in only amacrine interneurons which are generated at the expense of other retina-neuron cell types[27].

1.6-Aniridia and the Loss of *PAX6*

As stated previously, the critical role of *PAX6* in eye formation is indicated by the phenotypes caused by mutations of *PAX6*. Homozygous mutations are lethal causing mice to die within minutes of birth, because of perturbed development of the brain and pancreas[28,29]. In humans a complete loss of *PAX6* is rare, with only two reports of patients surviving birth with mutations in both *PAX6* alleles[30,31]. In these instances, the patients died within a few weeks of birth because of multiple organ defects, complications such as neonatal diabetes mellitus, and complex brain abnormalities. In contrast, heterozygous mutations resulting in loss of function of *PAX6*, resulting in reduced PAX6 protein[32] and lead to aniridia in humans and the small-eye (*Sey*) in mice[28].

Aniridia is a rare, congenital, pan-ocular disorder that affects approximately 1/40,000 to 1/100,000 people[6]. While the disease is named after the underdeveloped or absent iris that is its presenting clinical feature, hypoplasia of the macula and optic nerve are also frequently present and impact visual acuity. In addition to these congenital features, the majority of aniridic patients will suffer from progressive deterioration of vision due to a delayed onset of glaucoma, cataracts, corneal clouding, and aniridic keratopathy (AK)[6]. These latter two phenotypes are the result of limbal stem-cell deficiency, which impairs the ability of the cornea to regenerate[2,33,34]. These progressive degenerative conditions frequently result in progressive vision loss despite therapeutic

interventions. It is thought that the delayed onset of these conditions indicates an ongoing requirement of *PAX6* for the maintenance of the eye. Consequently, aniridic patients will often require many surgeries during their lifetimes, and the outcomes of these surgeries are poorer than those same surgeries in the general population. For these reasons, there is considerable interest in therapies aimed at correcting the underlying genetic defect.

1.7-Mutations in Aniridia

Aniridia has a strikingly high penetrance; therefore, patients with *PAX6* mutations are likely to show phenotypic abnormalities; however, aniridia has a highly variable expressivity, resulting in some patients having a mild phenotypic expression, while other patients have more severely affected phenotypes. This highly variable phenotypes are reflected in the large number of unique mutations of *PAX6* that cause aniridia (433 unique mutations)[35]. Aniridia is mainly transmitted in an autosomal dominant fashion because of the haploinsufficiency of *PAX6* (approximately 70% of cases), while spontaneous mutation accounts for the remaining cases (approximately 30% of cases)[6]. Haploinsufficiency of *PAX6* results in patients only having one functional copy of the *PAX6* and the single functional copy does not produce enough protein to bring about wild-type condition resulting in a disease state. The non-functional copy results in aberrant gene product that is either degraded, or results in abnormally functioning protein. The majority (66%) of mutations occur within the *PAX6* coding region. According to the Human PAX6 Mutation database, approximately 48% of mutations occur in the paired domain, 12% in the linker region, 18% in the homeodomain, and 12% in the PST region (see Figure 2a)[35,36]. Of these mutations, approximately 36% are nonsense mutations, 14% are splice mutations, 23% are frame-shifting insertions or

deletions, 5% are in-frame insertions or deletions, 18% are missense mutations and 4% are run-on mutations of the *PAX6* gene (see Figure 2b)[35,36]. Other patients may have chromosomal rearrangements or deletions that disrupt or remove the *PAX6* gene, as seen in patients who suffer from the Wilm's tumour-Aniridia-Genitourinary anomalies, and Retardation (WAGR) Syndrome. These cases involve deletions encompassing the *PAX6* gene and several distal genes including the Wilm's Tumour (*WT1*) locus (see Figure 1a). These patients have developmental defects in the eye, including aniridia and loss of visual acuity. These patients also have abnormalities of the genitalia and urinary tract, intellectual disability and elevated risk for kidney tumours[6].

The other 33% of mutations that do not occur in the *PAX6* coding region are likely due to mutations that disrupt the *PAX6* regulatory sequences that are found in introns or are found distal and proximal from the gene. Examples of this have been seen in patients that have chromosomal rearrangements which disrupt 11p13 but spare the *PAX6* transcription unit. One example is a breakpoint located 3′ to *PAX6*, designated as SIMO, which is located ~124 kb 3′ of the *PAX6* polyadenylation sites and disrupts an element that is required for *PAX6* expression[14].

1.8-Aniridia Syndrome: Loss of *PAX6* Affects Multiple Organs

While historically aniridia has been viewed as a pan-ocular disease, there is growing appreciation within the field that it is more properly classified as a syndrome which impacts the function of multiple organs, including the eye, the brain, the gut, and the pancreas[5,6,25,37]. As a consequence, these patients have behavioural abnormalities[38,39,40], anosmia may occur[5,41], obesity is common[3], and glucose intolerance and diabetes are also prevalent and segregate with the mutant *PAX6* allele[42]. Genetic

studies in mice and rats have now confirmed that these extra ocular phenotypes are due to *Pax6* deficiency in the affected organs[43,44,45,46].

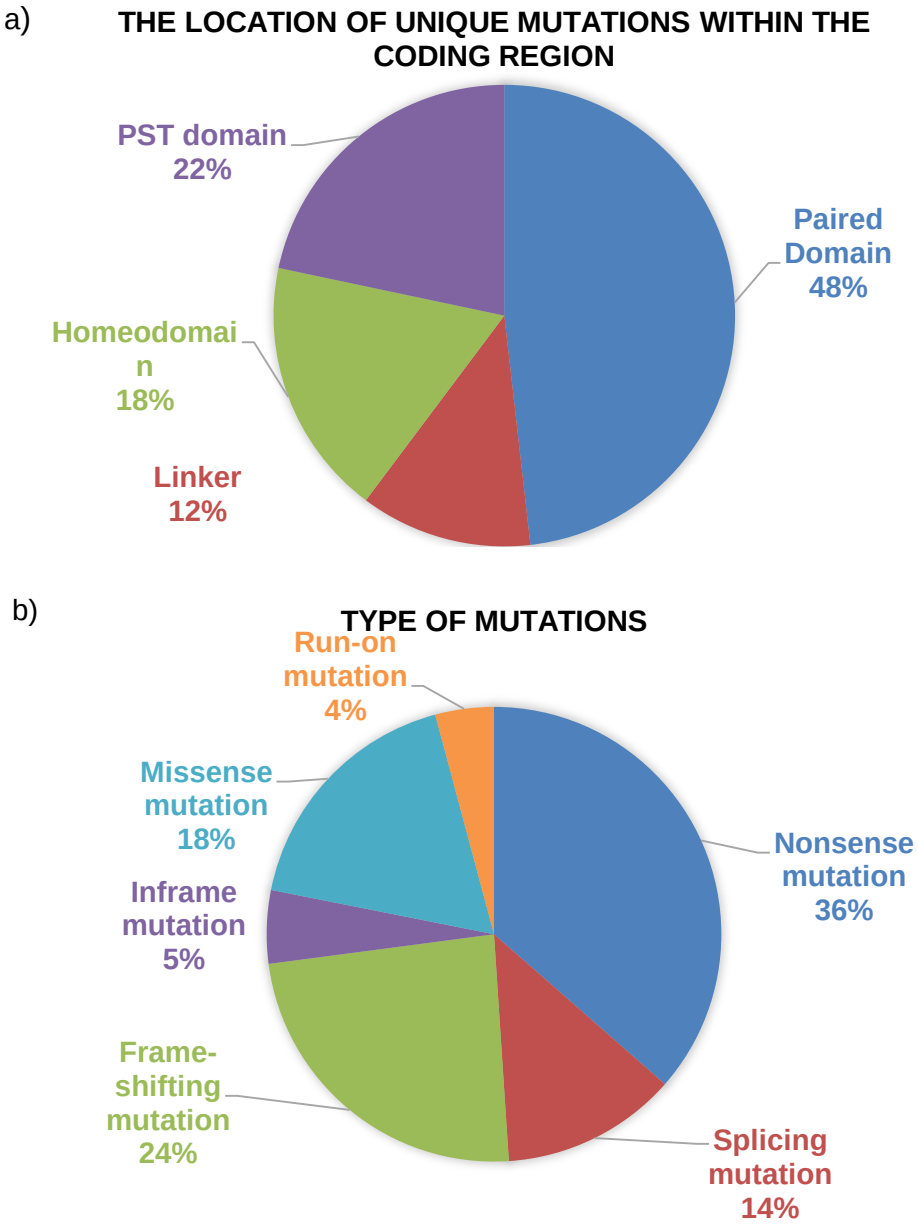

Figure 2: Mutation distribution of *PAX6*, from the Human *PAX6* Allelic Variant Database. (a) Domain distribution of mutation within the coding region of *PAX6*, from the Human *PAX6* Allelic Variant Database. (b) Distribution of different mutation types in the *PAX6* gene from the Human *PAX6* Allelic Variant Database.

1.9-*PAX6* and the Brain

Aniridic patients may have abnormalities in brain structure, such as structural defects in the corpus callosum, the olfactory bulb, the cerebellum, and the pineal gland[5,6,40,47]. Haploinsufficiency of *PAX6* causes the decreased volumes of the corpus callosum, absence or underdevelopment of the anterior commissure, and smaller brain size. *Pax6* heterozygous mutant (*rSey*^{2}/+) rats show impaired prepulse inhibition (PPI). These rats also exhibited more aggression and withdrawal behaviour during social interaction, and had impaired rearing activity and fear-conditioned memory[46]. Additionally, there is now evidence that *PAX6* may be linked to rolandic epilepsy (RE). This is a genetic focal epilepsy found in children and is characterized by centrotemporal spikes (CT-S). This syndrome accounts for approximately 15% of all epilepsies in children, and symptoms include clonic movement of the lower face, dysarthria, and hypersalivation, these seizures occur mainly during sleep, and go into remission by the age of 15 years. In a recent study, a single nucleotide polymorphism (SNP rs662702) was found within the *PAX6* 3'UTR that associated with RE. The homozygous mutant allele was seen at a higher frequency in patients that suffer from RE (4%) than the control (0.6%). Those who had a homozygous mutant allele had 12-fold increased odds of having CT-S after correction for sex and population stratification and it appears that the homozygous allele is highly penetrant. It is postulated that in the affected cohort, an increase of *PAX6* expression is due to reduced binding of microRNA-328 that leads to RE[48]. Disruption of this miRNA-328 site has been previously shown to increase *PAX6*[49] and is associated with myopia[50].

PAX6 is expressed in the adult cortex, which implicates it in brain function[51]. Indeed, Sisodiay et al.[5] showed by magnetic resonance imaging (MRI) that heterozygous *PAX6* patients had an absence of or malformed anterior commissure and reduction in the

callosal area. Furthermore, via the Pennsylvania Smell Identification test, this study found only two of the patients (out of 14) had normal olfaction function, whilst the rest had varying degrees of anosmia[5]. This study adds to one previously reported case[41] and evidence seen in the mice. In mice, the volume of the main olfactory bulb was significantly reduced, and the effect was more pronounced as the mice aged[52]. Additionally, MRI analysis has shown that patients with heterozygous mutations of *PAX6* have abnormal cortical patterning, reduction in the cortical area, and reduction in cortical thickness that is not associated with age[40].

1.10-*PAX6* and the Pancreas

A number of studies have shown the key role of *PAX6* in the development and maintenance of the pancreas. Mice that are *Pax6* null die shortly after birth because of several developmental defects, including overt diabetes. When *Pax6* is conditionally inactivated in the pancreas during development, mice fail to produce mature pancreatic endocrine cells (α, and β cells) and do not express glucagon, or insulin. As a result, these mice develop hyperglycaemia and hypoinsulinemia and die of overt diabetes shortly after birth[53].

Consistent with the glucose intolerance and diabetes seen in human patients, there are a number of pancreatic defects in mice due to haploinsufficiency of *Pax6*. Mice that have only a single copy of *Pax6* have reduced levels of insulin mRNA (40-60% reduction), reduced insulin protein levels (25% reduction) in β cells[43], and reduced levels of glucagon mRNA (30% reduction) in α cells[45].Additionally *Pax6* has been shown to be able to bind and activate both insulin[43] and glucagon promoters[45]. This is due to both direct and indirect transcriptional regulation of these genes by *Pax6*. In addition to the

requirement of *Pax6* in the pancreas for glucose homeostasis, there is also evidence that *Pax6* is required in the gut for the development of gastric inhibitory peptide (GIP) and glucagon-like peptide-1 and -2 (GLP-1 and GLP-2 respectively) producing cells[45,37]. *Pax6* is also implicated in the processing of GIP and proglucagon[54,37]. Another critical gene in glucose homeostasis which is regulated by *Pax6* is glucose transporter, *Glut2*[44]. *Pax6* has been shown to directly regulate *Glut2* expression; thus, *Pax6* deficiency may also impair the ability of the pancreas to sense high glucose as well as respond to that condition.

In human patients, *PAX6* has been implicated in glucose intolerance and diabetes. A study by Yasuda et al.[4] found five unrelated aniridic patients who had glucose intolerance or diabetes. The patients who had glucose intolerance had no family history of diabetes in their families. In these patients, glucose intolerance appeared to be due to defects in insulin secretion[4]. Stronger evidence was identified by Wen et al.[25], who found an opal mutation within arginine 240 of *PAX6* in a study of 19 aniridic patients from a single pedigree. Within this family, age-dependent glucose intolerance or diabetes segregated with the *PAX6* allele. To confirm the relationship between aniridia and glucose intolerance or diabetes, the authors generated a small-eye mouse strain with a similar opal mutation within arginine 266 of *Pax6*. Strikingly, these mice developed age-dependent glucose intolerance corroborating what was seen in the human pedigree. Wen et al.[25] went on to show that both patients and mice with this mutation had defects in pro-insulin processing due to a deficiency of *PC1/3*[25]. It is important to note that the development of the pancreas is morphologically normal in haploinsufficient animals[25]. However, *Pax6* deficiency results in glucose intolerance and diabetes through a direct

and ongoing requirement for *Pax6* to maintain multiple steps in the expression and processing of insulin, glucagon, and somatostatin[25,43,44,53]. As *Pax6* regulates both glucagon and insulin, loss of *Pax6* could result in an equal reduction of glucagon and insulin balancing the effect on glucose homeostasis, and not resulting in glucose intolerance or diabetes. However, insulin and glucagon expression, processing and secretion are regulated by multiple factors, and reduction of *Pax6* levels may disrupt glucose homeostasis resulting in glucose intolerance or diabetes by multiple pathways. As discussed earlier *Pax6* controls PC1/3 which in the pancreas is required to process proinsulin to insulin[25], and loss of *Pax6* may result in higher levels of proinsulin meaning that even with equal expression of glucagon and insulin the balance between the two is lost due to increase proinsulin : insulin ratio, resulting in higher levels of glucagon and higher hepatic glucose production. Indeed an increase in proinsulin : insulin ratio has been seen in *Pax6* mutant mice[25]. Another potential pathway that loss of *Pax6* can result in disrupted glucose homeostasis is through disrupted regulation of glucagon and insulin by GLP-1. GLP-1 increases insulin secretion and inhibits glucagon secretion, and *Pax6* has been shown to be crucial for GLP-1 expression[45,37]. Loss of GLP-1 expression may also alter glucagon: insulin ratio resulting in an increase in glucagon levels with a loss of insulin resulting in hyperglycaemia and consequently diabetes. Indeed, *Pax6* mutant mice have reduced levels of GLP-1 and these mice develop diabetes[45]. Upon treatment with a GLP-1 agonist alleviates the diabetes in these mice[45].

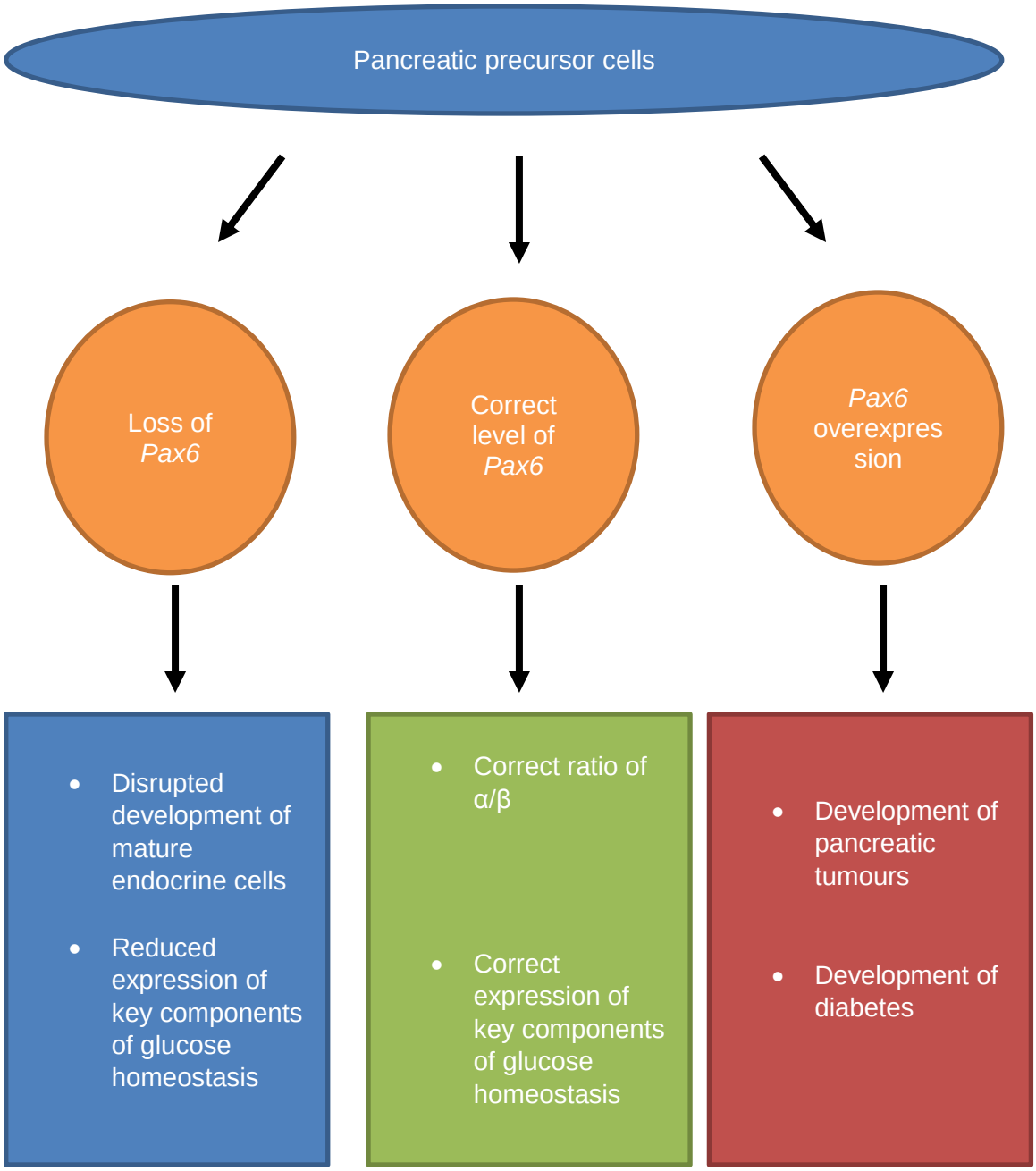

Figure 3: *Pax6* role in the development of pancreatic cells. *Pax6* is key for ensuring the maturation of correct endocrine cell population. *Pax6*-null mice have disrupted pancreatic development; they fail to produce mature pancreatic endocrine cells, with a loss of *Pax6* resulting in a near absence of α cells, and a reduced number of β cells, and a reduction in expression of key components of glucose homeostasis. Whilst overexpression of *Pax6* is also detrimental resulting in the formation of pancreatic tumours and diabetes in mice. The correct level of Pax6 is needed to ensure the correct development of endocrine islet cell population occurs
.

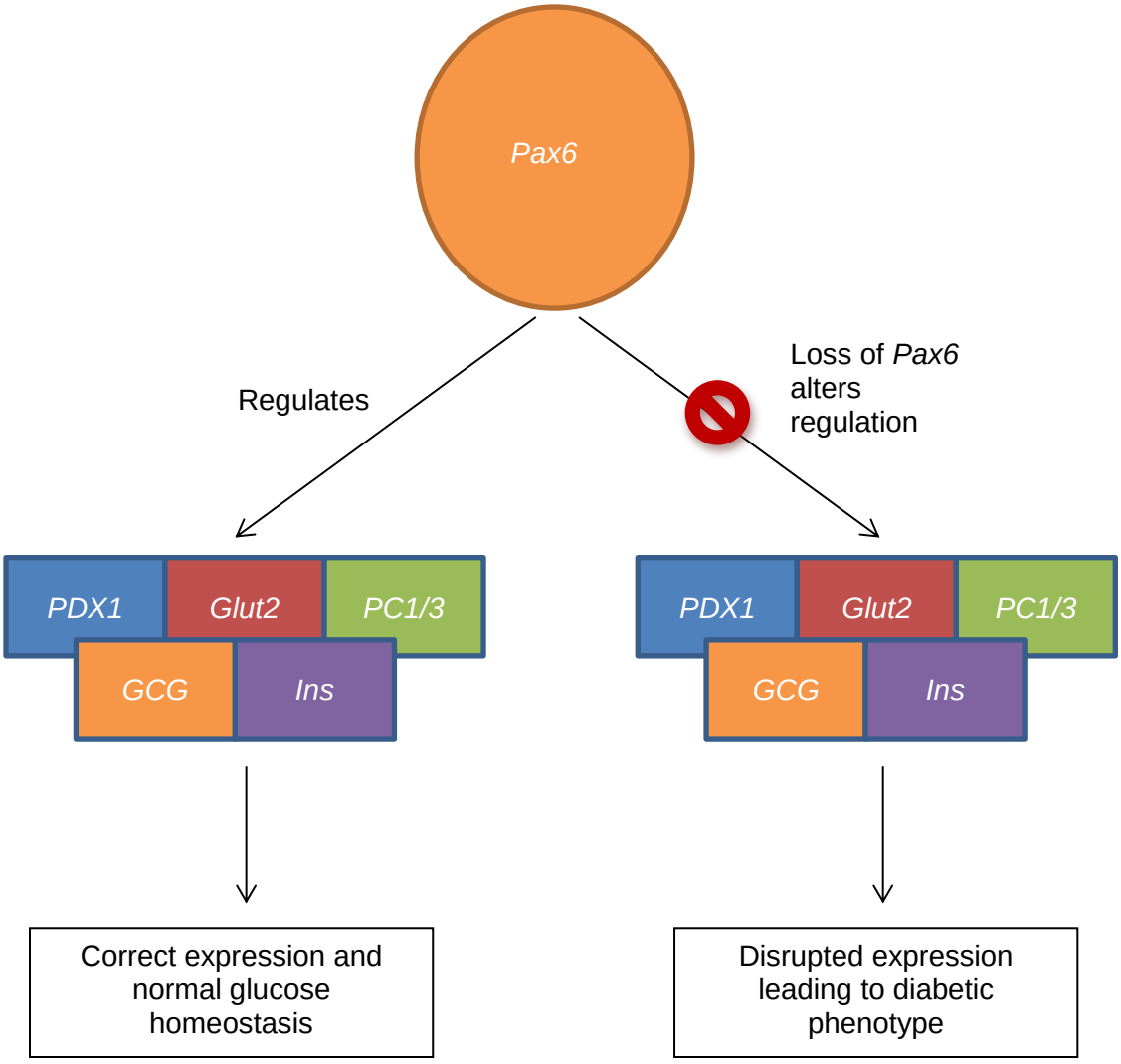

Figure 4: ***Pax6* role in maintaining glucose homeostasis.** *Pax6* regulates several key factors in glucose homeostasis. Loss of *Pax6* in adult mice results in reduced expression, abrogating glucose homeostasis - e.g., insulin secretion and processing - resulting in mice having classic diabetic symptoms.

1.11-Mature Onset of Diabetes in Youth (MODY)

It is now clear given the involvement of *PAX6* with glucose intolerance and diabetes that *PAX6* belongs to a collection of genes which cause a rare form of monogenetic diabetes known as Mature Onset of Diabetes in Youth (MODY). MODY is characterized by the onset of glucose intolerance and diabetes typically in the early to mid-teens, although there are extreme examples of onset in early childhood[56]. The

majority of genes implicated in MODY are, like *PAX6*, transcription factors that regulate glucose homeostasis. MODY differs from type 1 and type 2 diabetes in its monogenetic nature and in the fact that it typically exhibits with aspects of both insulin deficiency and insulin resistance[56].

Interestingly, penetrance in MODY is highly variable, suggesting that environmental and behavioural factors may influence it. In support of this, it was recently shown that mice which are haploinsufficient for *Pax6* develop glucose intolerance on a normal diet after six months, but on a high-fat diet the development of glucose intolerance is exacerbated with the onset occurring starting at 6 weeks[57]. After 12 weeks of high fat diet mutant *Pax6* mice have an increased prevalence of diabetes (80%), whilst the wildtype mice had only a 10% prevalence of diabetes[57]. The mutant mice on the high fat diet showed impaired insulin secretion, insulin resistance, defective pro-insulin processing, and decreased GLP-1[57]. The dependency of this model on the diet, suggests these *Pax6* deficient mice may provide insight into the relationship between diabetes, genetics, and behavioural or environmental factors.

1.12-*PAX6* and Diabetes in the General population

There is now clear evidence that *Pax6* haploinsufficiency results in defective glucose homeostasis from defects in production, processing, and sensitivity of insulin and glucagon. In these cases, patients present with aniridia and pancreatic dysfunction is part of a syndrome of defects that need to be monitored. Intriguingly, there is now evidence that expression of *PAX6* may also be affected within a subset of the general population with diabetes. Genome-Wide Association Studies (GWAS) of Scandinavian populations from the Diabetes Genetics Initiative have shown an association between diabetes and a

single nucleotide polymorphism (SNP; rs68428) located 35kb upstream 5' of the *PAX6* gene[42]. This region is conserved and involved in *PAX6* regulation in mice (Elizabeth Simpson, personal communication). The allele is associated with increased fasting insulin and increased HOMA-insulin resistance. Moreover, *PAX6* was the only gene in the region whose expression was affected by the allele, and the allele is associated with impaired insulin response, reduced glucagon, and *PSCK1* expression in a comparison of human islets isolated from 6 diabetics and 42 non-diabetic organ donors[42]. Under the additive model tested, there was no association between the allele and an increased risk for developing type 2 diabetes. A recessive model could not be ruled out[42]. However, these results suggest that therapies aimed at increasing *Pax6* expression may be useful in controlling diabetes in the general population.

1.13-Therapy for Aniridia

Current treatments for aniridia and its associated ocular defects are based on the severity of the defects. In mild cases of aniridia, less-invasive treatments are used, ranging from corrective tinted lenses, to topical treatment for the early formation of glaucoma[2,58]. Patients with more severe symptoms may require complex surgeries. For example, patients with dense cataracts may have them extracted to improve visual acuity, while other patients who suffer serve corneal defects may need corneo-limbal transplants[2,58]. These treatments may require lifelong systemic immunosuppression and carry a risk of failure much higher than seen in the general population[58]. For example, after intraocular surgery, patients commonly develop aniridic fibrosis syndrome, which presents as a progressive development of fibrosis in the anterior chamber, resulting in the

thickening and scarring of the cornea[59]. For these reasons, there is a need for therapies aimed at fixing the underlying genetic problem.

1.14-The Addition of an Exogenous Gene to Replace the Non-functional Copy of *PAX6*

Haploinsufficiency of *PAX6* results in reduced PAX6 protein levels and one potential strategy to restore *PAX6* levels is gene replacement therapy, where an additional exogenous *PAX6* gene is added to replace the non-functional copy of *PAX6* and restore the PAX6 protein levels to normal (see Figure 5). A similar strategy has been successfully used in Leber's Congenital Amaurosis (LCA), which is a rare form of inherited blindness in which patients may have nystagmus (involuntary eye movement). One form of LCA is caused by a progressive loss of function of rods and cones due to insufficient RPE65 isomerase, which is required to form light-sensitive pigments. An initial success of exogenous gene therapy was seen when vision was restored in a dog[60]. Success has also been seen in human patients in three different studies, where patients who were treated with viral-vector expressing *RPE65* had improved vision and increased light sensitivity at the site of retinal gene transfer[61,62,63]. This therapy seems to be long-lasting since patients who had a follow-up examination after three years showed no reduction in any clinical parameters[64].

However, using exogenous gene therapy to restore *PAX6* levels will face difficulties not seen in this LCA treatment because there are several differences between *RPE65* and *PAX6.* First, *RPE65* is only expressed in the retinal pigment epithelial (RPE) cells and cone photoreceptors[65,66], while *PAX6* is expressed in multiple components of the eye (the retina, the cornea, the lens, the iris, etc.); hence, the areas to target within the eye are known for *RPE65* and this type of LCA, but in the case of *PAX6* the optimal

target tissue for gene therapy is still unknown. Furthermore, *PAX6* is a transcription factor whose regulatory function is very sensitive to gene dosage. Therefore, ensuring that the correct amount of *PAX6* is administered becomes crucial. Overexpression of *PAX6* has been shown to result in defects in several organs. For example, mice with multiple copies of *PAX6* have severe eye abnormalities[67]. In rabbit corneal epithelial cell lines, overexpression of *Pax6* suppresses cell proliferation and disrupts the cell cycle[68]. Moreover, conditional overexpression in pancreatic cells results in diabetes and pancreatic tumours in mice[69]. Human patients who have *PAX6* levels that are overexpressed also suffer defects. Patients with tandem duplication of *PAX6* exhibit developmental delay, mild facial, and eye abnormalities[70].

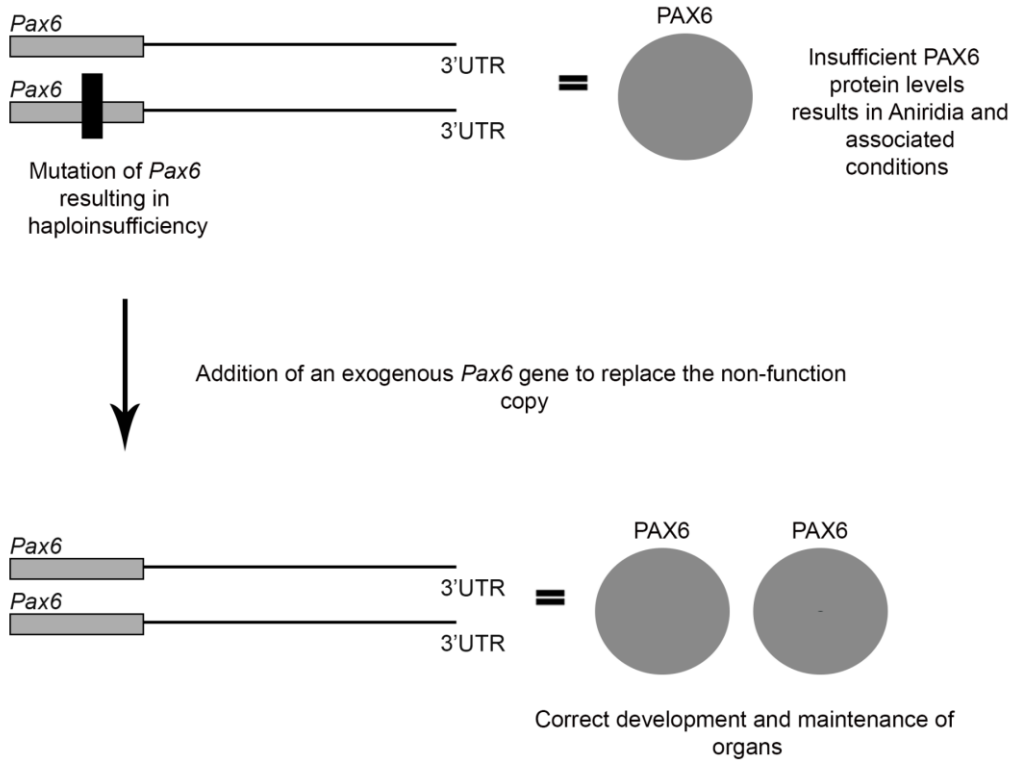

Figure 5: Gene therapy as a potential strategy to overcome the effects of reduced *Pax6* levels. Using exogenous *Pax6* to replace the non-functional copy of *Pax6* may produce more PAX6 protein. The *Pax6* mRNA transcript with the black bar represents a mutated copy of *Pax6*.

1.15-Targeting Nonsense-Mediated Decay

Another potential strategy to restore *PAX6* levels is to target the mutant *PAX6* allele, as a majority of *PAX6* mutations are a result of a premature stop codon, due to nonsense, splicing or frameshift mutations[36]. While transcripts containing a premature stop codon would be predicted to translate into a truncated protein, the transcript is not expressed because of Nonsense-Mediated Decay (NMD). NMD is a regulatory pathway in eukaryotes that degrades mRNA transcripts that contain premature stop codons reducing errors in gene expression[71].

Gregory-Evan et al.[32] have targeted the NMD pathway through the use of aminoglycosides (Ataluren)[32]. The aminoglycosides promote ribosomal read-through of the premature termination codon (PTC). Translation would normally be halted at the PTC, but in the presence of an aminoglycoside a conformation changes at the ribosomal decoding site, reducing ribosome discernment and forcing the use of closely related tRNAs. Therefore, the closely related tRNA may be inserted at the stop site allowing the ribosome to move past the premature stop codon and translation to continue[72]. An amino acid may be replaced by another amino acid that has very similar chemical properties, and if the PTC is not in a critical position for protein activity, the protein may still function normally. The mechanism is not fully known, but it is believed that aminoglycosides bind to ribosomes and perturb peptide elongation by making the ribosome more prone to errors during the elongation process[72] (see Figure 6).

Forcing ribosomal read-through has the potential to make a functional PAX6 protein. By suppressing nonsense mutations (via Ataluren) Gregory-Evans et al.[32] were able to reverse the disease progression in postnatal mutant mice, restoring the retina, the cornea, and lens morphology and restoring light sensitivity by the restoration of PAX6

protein levels from 50% to approximately 90% of wildtype PAX6 protein levels[32]. They showed that the murine eye retained remarkable plasticity postnatally and suggested that the eye remained sensitive to molecular remodelling[32]. This group is currently establishing a phase 2 clinical trial to test the efficacy of Ataluren in patients.

Despite the advances made in restoring ocular morphology and light sensitivity by NMD suppression there are still several limitations to this treatment. The first is the number of patients: the treatment is predicted to benefit only patients with an in-frame nonsense mutation of *PAX6*, which is approximately 50% of the aniridic population. Additionally, Ataluren only works on the opal stop codon UGA[73], which suggests that as few as 1/3 of the potential premature stop codons are the correct codon (approximately 15% of the aniridic population). Furthermore, Ataluren is only effective when the opal stop codon is followed by pyrimidine[73], which may reduce the effectiveness further to only about 5% of the aniridic population (see Figure 7). Also, the treatment may be ineffective if the premature stop codon is at a crucial codon/amino acid for the function of *PAX6*. Therefore, the forced ribosomal read through may still produce a non-functional protein. Because of these limitations, other strategies for increasing *PAX6* levels are still needed.

1.16-Suppression of miRNA as a Strategy for Restoring PAX6 Protein Levels

Our goal is to develop a therapeutic strategy to treat the progressive conditions associated with aniridia. My master's thesis is a proof-of-concept study for therapy based on microRNA (miRNA) inhibition. Specifically, I have been working on targeting miRNA regulation of *Pax6* in pancreatic cells which are haploinsufficient for *Pax6*.

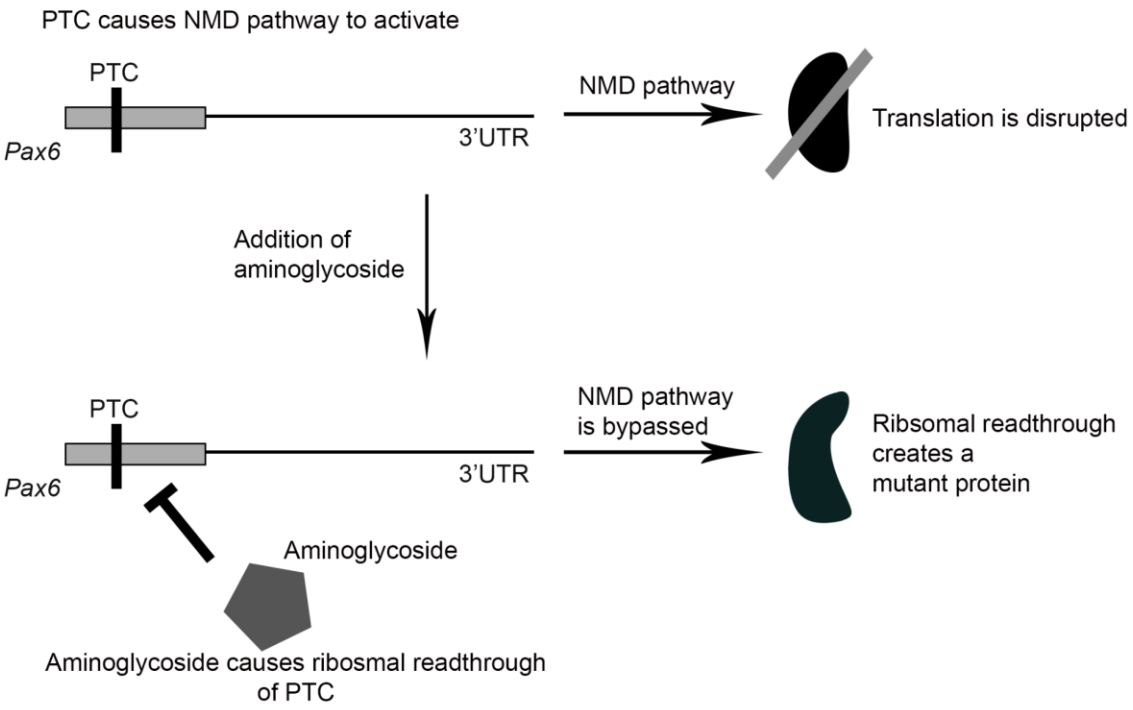

Figure 6: Suppression of nonsense mediated decay by aminoglycoside to increase PAX6 protein levels. Most mRNA transcripts that have PTC are degraded by the process of nonsense-mediated decay (NMD), and only a small proportion of the transcripts can be translated into truncated, non-functional peptides. However, aminoglycosides, such as Ataluren, stimulate ribosomal read-through of PTCs during translation, resulting in the translation of a mutant protein that may be functional.

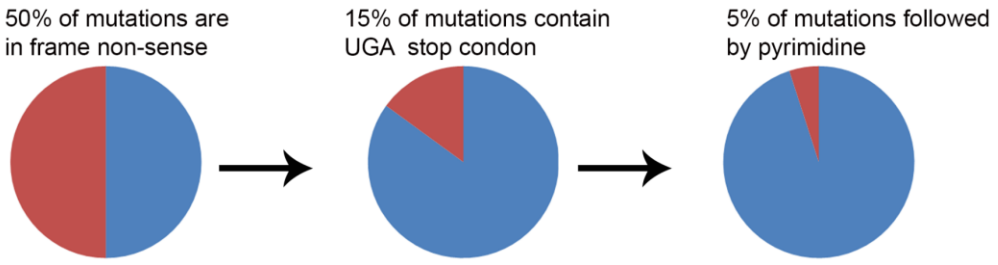

Figure 7: Limitations of Ataluren. The potential aniridic population that may be treated with Ataluren. Ataluren treatment only affects patients with an in-frame nonsense mutation of *PAX6*, which is approximately 50% of the aniridic population. Additionally, Ataluren only works on the opal stop codon UGA, resulting in treatment for approximately 15% of the aniridic population. Furthermore, Ataluren is only effective when the opal stop codon is followed by pyrimidine, which is the case with approximately 5% of the aniridic population.

1.17-miRNA

microRNAs (miRNAs) are small, non-coding RNA sequences (22-28 nucleotides in length), that typically downregulate gene expression by modestly regulating the amount of protein that a gene produces[74,75]. miRNA regulates gene expression in a sequence-specific manner through complementary binding to the target mRNA's 3'UTR via an 8-nucleotide seed sequence (seed sites) found at the 5'end of the mature miRNA transcript[74,75] (see Figure 7). In animals, miRNAs bind to multiple seed sites in 3'untranslated regions (3'UTR) with partial complementation to the target mRNA. There are four types of seed sites that when present have a high probability of being functional[76]. The seed site that is least efficient at regulating mRNA transcripts is a 6-mer site that contains a perfectly matched 6-nt miRNA seed; this seed is the base seed site and is located at position is 2-7 of the mature miRNA[76]. The second seed site is a 7mer-m8 site; this seed site has increased repression due to a Watson–Crick base-pair match to miRNA at nucleotide 8[76]. The next seed site is a 7mer-A1 site, at which the seed sites regulation is boosted by an A across from miRNA nucleotide 1[76]. Finally, the last seed site is an 8mer site, this seed site is comprised of both the m8 (Watson-Crick match at nucleotide 8) and the A1 (a supplemented A across from miRNA nucleotide 1)[76]. The miRNA seed site follows an order of regulator efficacy, with 8mer being the strongest followed by 7mer-m8, 7mer-A1; and finally 6mer[76]. The regulator order is also seen at the protein expression level[77].

RNA polymerase II transcribes the miRNA precursor, primary miRNA (pri-miRNA)[78]. The resulting transcripts undergoes subsequent processing by the RNase III-like enzyme, Drosha and DGCR8, an RNA-binding protein, resulting in ~60-70 nt premature miRNA (pre-miRNA)[79]. Pre-miRNA molecules are transported to the

cytoplasm via Exportin-5[80] and then processed by Dicer (also an RNaseIII-like enzyme) resulting in a 22-28 nucleotide mature miRNA[81]. The mature miRNA is processed further into a single-stranded transcript; in this form it interacts with the RNA-induced silencing complex (RISC). The resulting RISC-miRNA complex acts as a guide in targeting and interacting with its target mRNA 3'UTR. Based on complementarity, the RISC-miRNA complex will either cleave or bind to the mRNA target transcript, thus preventing translation, and repressing the mRNA transcripts expression. Generally, regulation by miRNA will lead to the inhibition of translation if the miRNA has moderate complementarity with the target mRNA, whereas miRNA regulation will lead to the degradation of the target mRNA if the miRNA has perfect or near-perfect complementarity with the target[82,83]. The role of miRNAs in regulation suggests that miRNAs act as rheostats, resulting in adjustments to expression and fine-tuning the translation of protein. Moreover, it has been shown that a single miRNA can regulate production of several proteins, but this repression is typically mild[84].

Because miRNA regulation is dependent upon the small 6- to 8-nucleotide seed site, a single miRNA can potentially regulate several mRNA targets and a single mRNA target can potentially be regulated by several miRNAs; therefore, a single miRNA will have a modest effect on the regulation of its target mRNA. This characteristic makes miRNA an alluring target for the development of therapies for diseases which result from insufficient protein levels and in which small changes in protein levels may prove beneficial. Such diseases include some cancers[85], type 1 diabetes (as several miRNAs are involved in regulation insulin secretion and biosynthesis, and β cell survival), [86,87,88] and monogenetic disorders such as aniridia.

The use of miRNA inhibitors as a therapeutic strategy is attracting interest, as successes have been seen in clinical trials. One of the most studied miRNAs is miRNA-122, which is abundant in the liver and plays a role in the metabolism of fatty acids, and cholesterol and in the replication of the hepatitis C virus (HCV) genome. Studies have shown that miRNA-122 expression likely stimulates the replication of HCV RNA. Unlike conventional miRNA, miRNA-122 interacts with the 5'end of the HCV RNA genome resulting in an increase of viral RNA[89,90]. Inhibition of miRNA-122 results in reduces HCV genome replication and infectious virus production in Huh-7.5 cells[91]. Based on the discovery of miRNA-122's role in viral replication, a locked-nucleic-acid based antisense (LNA) oligonucleotide has been developed. Treatment with LNA has been tested in non-human primates and has shown successful microRNA silencing in these animals and resulted in reduced viremia[92]. Furthermore, LNA treatment resulted in no histopathological changes and showed no associated toxicity. A trial of miRNA-122 inhibitor in humans identified no long-term safety issues[93]**.** A number of preclinical *in vivo* experiments have demonstrated the potential to treat various diseases by the use of miRNA therapies. For example, the use of miRNA-34 mimics for primary liver cancer treatment is currently undergoing in phase I clinical trials [94](ClinicalTrials.gov Identifier: NCT01829971)**.**

Our long-term goal is to develop a miRNA suppression strategy to counter the progressive effects of aniridia syndrome. By suppressing miRNA regulation of *Pax6*, we aim to increase *Pax6* expression in cells that are haploinsufficient for *Pax6*. This approach has several advantages in comparison to other strategies discussed earlier (a strategy of exogenous gene replacement and a strategy of NMD suppression). For

example, targeting miRNA regulation is not dependent on the type of mutation in the *PAX6* gene and should therefore be applicable to a larger aniridic population. Moreover, in contrast to an exogenous gene replacement strategy, suppressing miRNA ensures that *PAX6* is left under endogenous chromatin regulation. This may help to prevent overexpression of PAX6, which as discussed earlier has detrimental effects on several organs[67,68,69].

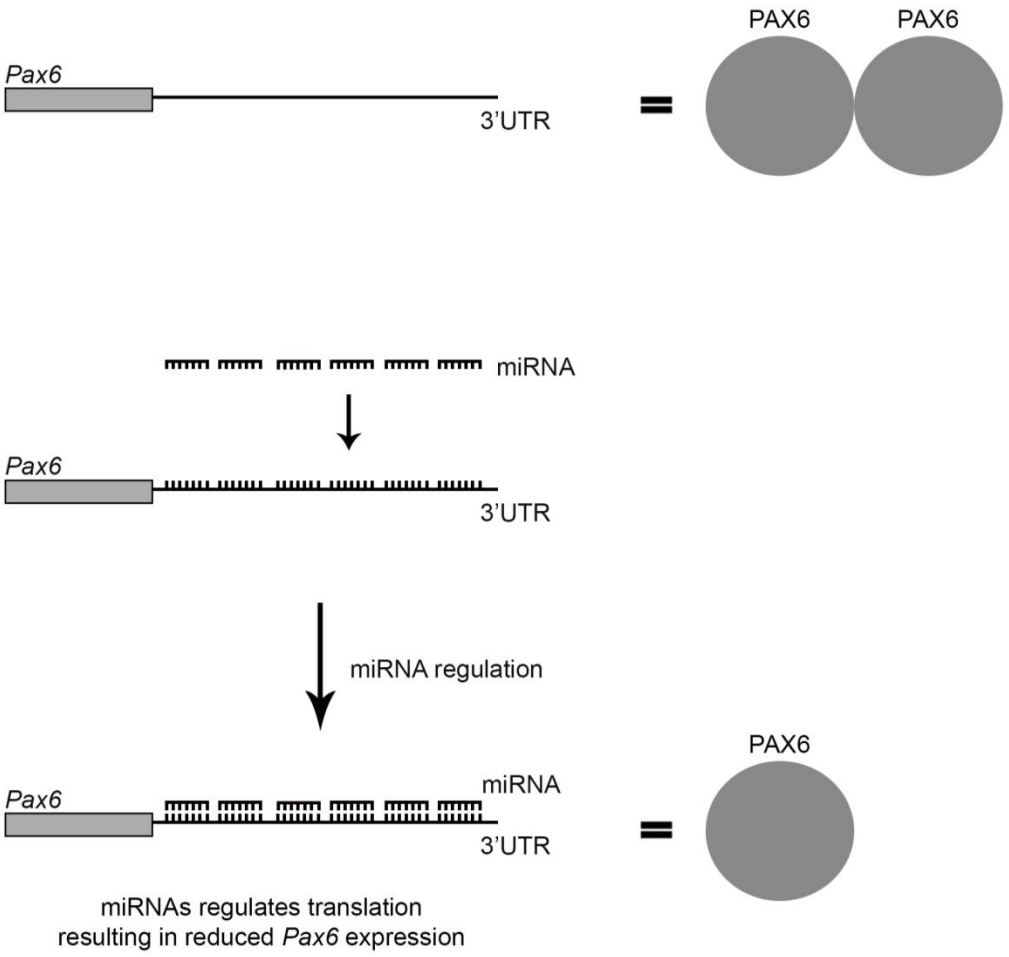

Figure 8: miRNA regulation of *Pax6*. *Pax6* translation is modestly regulated by miRNA; miRNAs regulate their mRNA targets in a sequence-specific manner, binding to the 3'UTR of their targets and reduces the amount of protein produced by translation inhibition or mRNA degradation.

1.18-Where to Target miRNA Inhibition.

We chose to test miRNA inhibition of *Pax6* in pancreatic cells as a starting point for several reasons: (1) pancreatic endocrine α and β cell lines are readily available; (2) *Pax6* is only expressed in the endocrine cells of the pancreas and not in the exocrine cells or the acinar cells, which facilitates targeting; (3) there are several read outs of treatment success, such as measuring glucose, glucagon, and insulin levels, and most importantly, (4) in contrast to those in the eye, some of the miRNAs regulating *Pax6* in the pancreas are known.

1.19-Identifying Target miRNA.

The first component of this project was to decide which miRNAs to target. To do this our collaborators in the Robert Chow laboratory at University of Victoria have undertaken a bioinformatics and literature analysis to generate and confirm a list of potential miRNAs which regulate *Pax6*. From the bioinformatics analysis, we identified the two top-scoring sites in the *Pax6* 3'UTR: a predicted miRNA-375 (with a 7mer-A1 target seed site) is one of the most abundant miRNAs in the pancreas and expression is restricted to endocrine cells. The miRNA-375 seed site is conserved in the 3'UTR of mammalian, chicken, and frog *Pax6/pax6,* all of which express *Pax6* in the pancreas[95,96]. This conservation increases the likelihood that the miRNA-375 seed site is functionally important. Furthermore, miRNA-375 is specifically expressed in the pancreas (and slightly, in the pituitary gland) and expression is restricted to endocrine cells[86,97]. The ability of miRNA-375 to target *PAX6 in vitro* has recently been confirmed through luciferase assays in HEK293 cells[102]. Thus, we know that miRNA-375 can target *PAX6* in at least one setting[98].

The second highly conserved miRNA site within the *Pax6* 3'UTR is a 7mer-m8 seed match for miRNA-7. Like miRNA-375, miRNA-7 has been shown to directly regulate the *Pax6* 3'UTR in heterologous reporter assays in HEK 293 cells and MIN6 pancreatic cells[98,99]. Knockdown of miRNA-7 in pancreatic explants resulted in a 22% increase in insulin mRNA and a 61% increase in glucagon mRNA suggesting that miRNA-7 is functional in pancreatic endocrine cells[99]. More recently it has been shown that repression of miRNA-7 in pancreatic islets in culture can increase *Pax6* levels[100]. These results indicate that *Pax6* is a bonafide target of miRNA-7. Based on this information, we chose to target miRNA-7 and miRNA-375 regulation of *Pax6* as the first step in our investigation.

1.20-miRNA Suppression Strategies

To test whether suppression of miRNA-7 or miRNA-375 can be used as a therapeutic strategy to increase *Pax6* expression, an efficient system for suppressing miRNA is needed. Currently, the primary agents for suppressing miRNA are synthetic miRNA antisense molecules of various chemical compositions that are fully complementary to mature miRNA. One type of agent is known as "antagomirs", which are 2' *O*-methyl, phosphorothioate, cholesterol-modified antisense oligonucleotides. These synthetic miRNA inhibitors have been used in several *in vitro* and *in vivo* studies on the effect of miRNA suppression[101,102]. The effect of these synthetic RNAs is transient, since a gradual loss of inhibition occurs because of degradation; thus, multiple administrations are required to obtain a constant effect. Lack of tissue-specific delivery is a further problem with these agents, and efficiency in some cell types further reduces the applicability of synthetic inhibitors in some uses[103]. Instead of synthetic miRNA

antisense molecules, we have opted for the "tough decoy" (Tud) system developed by Haraguchi et al.[104], using designed Tuds to target miRNA-7 or miRNA-375. The Tuds are a miRNA-suppression system based on sequestering a single miRNA from its target mRNAs, with the Tuds acting as decoy targets for miRNA[104]. The Tuds contain two miRNA-binding sites that are complementary to mature miRNA, including a 4-nucleotide insert ensures cleavage of the Tuds (by miRNA-RISC complex) does not occur. Furthermore, the Tuds were optimised to be expressed from a Pol III promoter to achieve high expression, and the miRNA-binding sites have been designed between stem loops, which helps export RNA into the cytoplasm via Exportin 5. Also, the Tuds contain a 4bp linker, and the stem length is also optimised to ensure efficient transport and thus increase the potency of the Tuds[104]. The Tuds have been shown to suppress miRNA for over a month. Additionally, these Tuds outperformed other inhibitors in a comparative study comparing Tuds to traditional chemically based miRNA inhibitors[105].

One potential undesired side effect of the Tuds is that they supress the broad function of a single miRNA. Given that a single miRNA can regulate numerous mRNAs, Tud suppression of a miRNA may affect multiple mRNA targets. This could result in positive or negative pleiotropic effects and off-targeting. To address this concern, we have also designed target protectors (TPs), which mask a specific mRNA 3'UTR. TPs interfere with miRNA-mRNA interaction, protecting the target from miRNA suppression. miRNA-mediated degradation does not occur as the TPs are not loaded into the RISC complex which triggers the destabilisation of mRNA via deadenylation complexes, however there is a possibility that the TPs may alter other regulator elements in the 3'UTR resulting in destabilisation of the mRNA transcript, this however has not been the

case in several other studies[106,107,108,109]. The TPs were also designed to express from Pol III-driven H1 promoter and produced a 60 bp RNA that is complementary to the miRNA-7 or miRNA-375 binding site in *Pax6* 3'UTR and binds to the 3'UTR of *Pax6* via Watson-Crick base pairing. The TPs have been widely used in zebrafish, and more recently in mammalian cells, to specifically block the effects of miRNA[107,108,109].

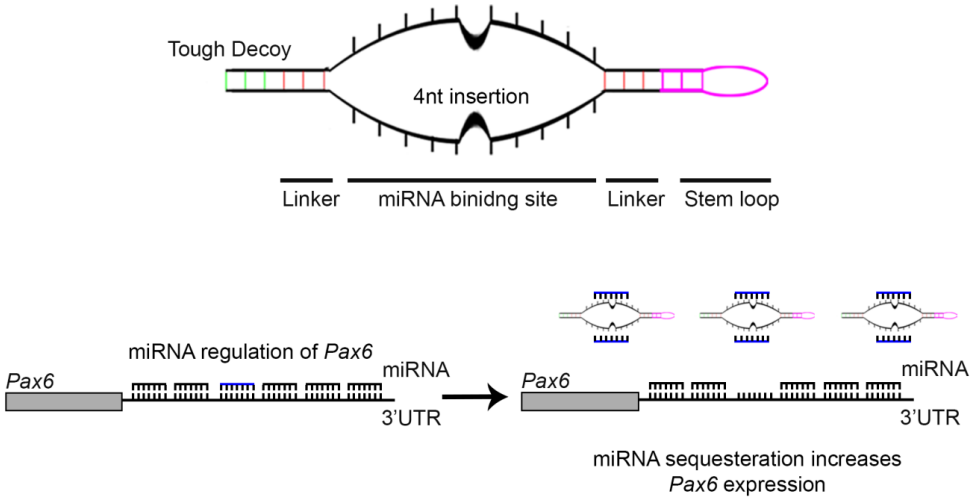

Figure 9: Tud suppression of miRNA to increase *Pax6* expression. Tough decoy (Tud) consisting of a stem (shown in green), the linkers (shown in red), two miRNA binding sites with a 4 nucleotide insert, and a stem loop (shown in pink). Specific miRNAs are sequestered from their targets resulting in an increase of target protein expression.

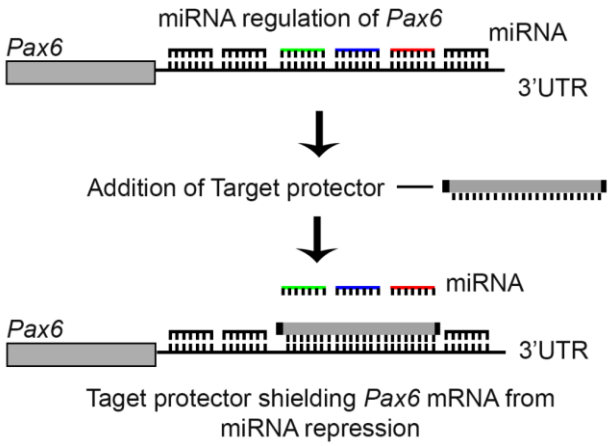

Figure 10: Target protector strategy to increase *Pax6* expression. Target protectors are 60-nucleotide RNA sequences that bind complementarily to the *Pax6* 3'UTR. Target protectors act as a shield, repelling miRNAs from reaching their target and increasing *Pax6* expression.

1.21-Using rAAV as Delivery Vector in a miRNA Suppression Strategy

The delivery system used to express a miRNA inhibitor is a crucial factor in testing our miRNA strategies in an *ex vivo* context. One delivery system uses a non-viral vector such as naked plasmid DNA, or electroporation which can be designed with a promoter to enable spatiotemporal expression. However, these vector systems have several disadvantages for application *in vivo,* including inefficient delivery for some cell types and tissues. In contrast, the use of a viral vector as a delivery system for inhibitors has several advantage, including being efficient and having the ability to infect a wide array of cell types[110]. Of the numerous viral vectors available, we have chosen to use the recombinant adeno-associated virus (rAAV) as a delivery system (see figure 11). AAVs are 20nm replication-dependent viruses that belong to the *Dependoparvovirus* genus. AAVs contain a single-stranded DNA genome (either positive or negative-sensed), made up of inverted terminal repeats (ITRs). Furthermore, AAVs contain two open reading frames: one containing *rep* and the other *cap* genes. The ITR sequence ensures efficient replication of the AAV genome and is required for efficient capsid formation to create the AAV particle. The *rep* gene produces various Rep proteins Rep78, Rep68, Rep53 and Rep40. These proteins have several functions, including strand and site-specific endonuclease activity, and ATP-dependent helicase activity, and are critical for specific integration into the host genome. The *cap* gene produces three capsid proteins: VP1, VP2, and VP3;[111] these proteins make up the AAV capsid, which is comprised of 60 capsid subunits. The VP1, VP2, and VP3 proteins are arranged in an icosahedral symmetry in a ratio of 1:1:8, with an estimated size of 3.9 MegaDaltons[111].

The rAAV vector has several advantages over other viral vectors for the introduction of miRNA inhibitors. One reason we have opted to use rAAV is its

adaptable capsid structure. The capsid can be adapted to produce different serotypes of AAV vectors which allows for potent transduction of many tissues[112,113], and improves the titre of AAV vector types[114]. An added benefit of rAAV as a viral vector is that the Rep gene and cis-active intercistronic expression element (IEE) are supplied *in trans* (from a plasmid and HEK293 cell lines respectively), to create the recombinant AAV (rAAV)[115]**.** The creation of a rAAV eliminates the wildtype AAVs ability to integrate into the host chromosome[116,117], causing the rAAV vector to exist as a double-stranded circular episome that does not associate with the host chromosome[118]. These episomes are maintained extra-chromosomally and develop a chromatin-like organization. Another benefit of rAAVs over other viral vectors is their ability to infect non-dividing cells and persist for a period of years without damaging the cells, resulting in long-term transgene expression in non-dividing cells[119]. Additionally, there is almost no immune response to AAV infection[120]. Clinical trials using AAV vectors are currently being undertaken for a number of diseases. As discussed earlier, AAV delivery of *RPE65* has been shown to be effective as a potential long-term treatment for one form of LCA. These vectors appear to be quite safe for use in humans.

1.22-The Use of the Small Eye Mouse Model to Characterise *PAX6* Functions

The mouse provides an excellent model for investigating the role of *Pax6* in various tissues. This is because of the numerous mutation of *Pax6* in the various models mirrors the wide range of mutations that occur in aniridia, and mutant mice are phenotypically similar. The small-eye mutation was first described in mice by Robert et al. in 1967[121]. The mice had a dominant mutation which differed from 16 of the 20 eye mutations in mice known at the time and the phenotypes presented were distinguishable

from three of the remaining known eye mutation. Unlike the known mutations at the time, these mice had closed eyelids at birth, showing the mutation was unique. The mouse model was named *Small eye (Sey)* because of the reduced eye size[121]. The authors noted the expressivity of the mutant phenotype was variable, which is also observed in patients affected by aniridia.

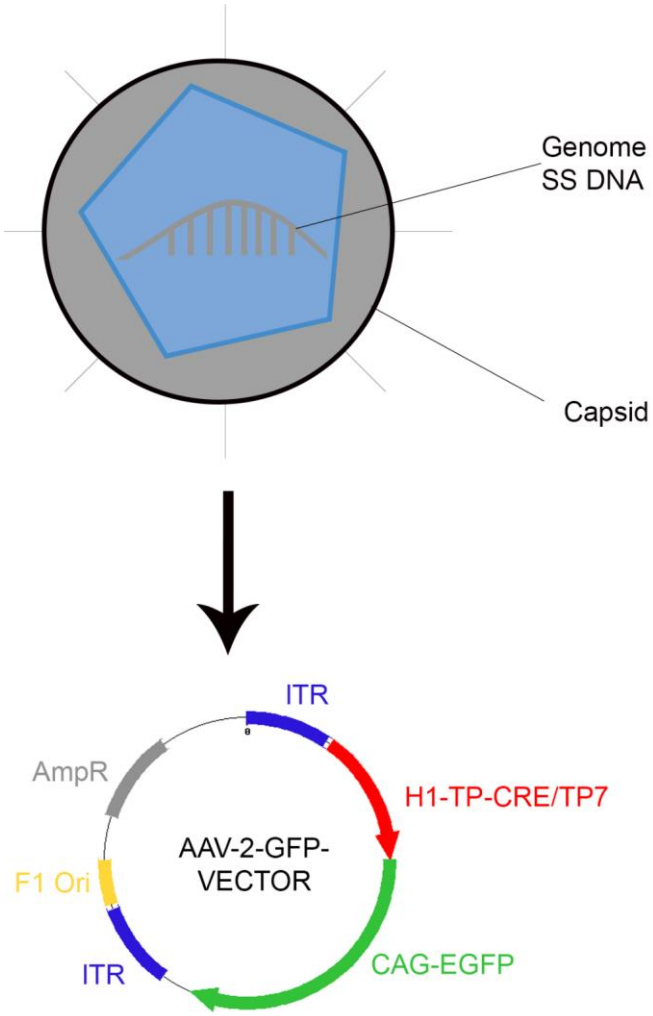

Figure 11: Schematic diagram of viral vector that will be used to test TP strategies in an *ex vivo* setting. An AAVs consists of a single-stranded DNA molecule. The viral vector does not have an envelope coating the genomic DNA; instead, it is stored within a membrane inside the capsid. This rAAV will express the vector map shown, and will express either TP-CRE or TP-7 contains GFP downstream in the use of suppressing miRNA regulation of *Pax6*.

Several studies have since shown that *Sey* and *Pax6* are homologous[28,121,122] and this discovery has spurred the development of multiple mouse model to further study the role of *PAX6* in greater detail. Table 4 provides several examples of the current mouse models that are available. One example is Small-eye Dickie ($Pax6^{Sey\text{-}dey)}$ mutant mouse model; these mice have a spontaneous semi-dominant deletion that encompasses *Wt1* as well as *Pax6*[123]. Homozygous mutants die during embryogenesis. Heterozygous mutant mice are characterized by the following features: they have distinctly small eye/eyes; the lens is also small and may present with cataracts; the retina may be abnormally folded and the anterior chamber is usually missing. Heterozygous mice also have impaired axonal growth and differentiation and delayed migration of preneuronal cells, which is an indirect consequence of reduced neural retina size. Formation of the lens and of the nasal cavity placodes is dependent on normal *Pax6* expression. These mice also have reduced body size[124]. Despite mutation in the *Wt1* gene, Small-eye Dixie mice do not develop tumours in the kidneys. They can be used to model the *PAX6-WT1* deletion seen in WAGR syndrome. Another example is the mouse model $Pax6^{(+/Sey\text{-}Neu)}$ which mimics aniridic keratopathy (AK)[125]. Adult heterozygous mutant mice have corneal epithelia that were thinner and had fewer layers. The stroma often contains lens tissue and display epithelial vacuolation. The corneal stroma is thicker centrally. A majority of heterozygous mice corneas are vascularized or contain cellular infiltrates. These corneal abnormalities are similar to those found in AK, and these mice can be used as a model for AK. Table 1 details several mutant mouse variants available from Jackson Lab that can be used to model aspects of aniridia.

Table 1: The ocular defects found in mouse models for aniridia syndrome.
Ocular phenotype and the mutation that causes the phenotype are listed for several mouse models of aniridia. Information was obtained from Mouse Genome Informatics (MGI) database - http://www.informatics.jax.org/

Allelic Composition	Ocular Phenotype	Mutation
Pax6$^{Sey\text{-}Dey/Pax6+}$	• Iris hypoplasia • Abnormal lens development • Cataract • Small lens • Microphthalmia • Abnormal retina morphology	A large deletion that also includes the neighbouring Wilm's tumour gene (Wt1)
Pax6$^{3Neu/Pax6+}$	• Irregularly shaped pupil • Corneal opacity • Corneal lens attachment • Cataract • Anterior polar cataracts • Microphthalmia	Insertion of single nucleotide (A) at exon 7, resulting in the deletion of linker region, homeodomain, and P/S/T domains
Pax6$^{4Neu/Pax6+}$	• Abnormal iris morphology • Irregularly shaped pupil • Anterior iris synechia • Cataract • Microphthalmia	T to C substitution in exon 10 resulting in a Ser to Pro substitution at amino acid position 273.
Pax6$^{Sey\text{-}Neu/Pax6+}$	• Iris hypoplasia • Abnormal cornea morphology • Corneal vascularization • Abnormal corneal epithelium morphology • Abnormal corneal stroma morphology • Abnormal lens vesicle development • Microphthalmia	G to T transversion at the +1 position of a splice donor site results. This results in the loss of 115 amino acids from the C terminus, including the transactivation domain.
Pax6$^{Sey/Pax6+}$	• Abnormal optic nerve morphology • Abnormal anterior eye segment morphology • Abnormal corneal epithelium morphology • Abnormal lens morphology • Microphthalmia	G to T transversion in codon 194 alters this position in the protein from a glycine to a stop codon, resulting in termination before the homeobox domain.

1.23-Hypothesis and Objectives

This thesis is a proof-of-concept study of miRNA suppression as a therapeutic strategy for the treatment of aniridia. My hypothesis is that inhibition of miRNA-7 and miRNA-375 can increase the expression of PAX6 protein in heterozygous cells to wild-type levels. In order to test this hypothesis, I had four objectives:

(1) To confirm the findings of previous studies showing that miRNA-7 and miRNA-375 regulate *Pax6*.

(2) To determine whether miRNA-375 and miRNA-7 can be repressed effectively.

(3) To determine whether repression of miRNA-7 or miRNA-375 alters endogenous PAX6 protein levels in pancreatic cell lines.

(4) To determine whether inhibition of miRNA-7 or miRNA-375 can restore levels of PAX6 protein to normal in haploinsufficient explants.

Chapter 2: Materials and methods

2.1-Animal Care Statement

This study was carried out under the guidelines of the Canadian Council on Animal Care. The protocol was approved by the University of Victoria Animal Care Committee (Permit Number: 2013-011-1). Euthanasia was carried out under isoflurane anaesthesia, and all efforts were made to minimize suffering. Breeding pairs for the generation of experimental mice (*Pax6* $^{sey\ -dey}$) were purchased from Jackson Lab.

2.2-Islet Isolation

Mice were anaesthetized and euthanized in accordance with approved standard operating procedure (SOP#AC2013 rodent-euthanasia). General anaesthesia was administered via inhalant of isoflurane. Anaesthetic depth was assessed by toe pinching and death was carried out by cervical dislocation once the animals were confirmed to be unconscious.

Euthanized mice were then skinned and a laparotomy was performed to reveal the abdomen region. The ribcage and the diaphragm were removed to ensure the liver was not blocking entry to the common bile. The entry into the duodenum (Ampulla of Vater) was clamped using a haemostat. Once the common bile duct was exposed, 2ml Liberase TL (Roche) at 1.08 Wünsch units per ml (that had been diluted in serum-free RPMI media) was perfused in to the pancreas via a 27-gauge needle. Once the pancreas is perfused, the pancreas was removed by peeling it away from the spleen, small intestine, stomach and liver. The perfused pancreas was placed on ice for up to one hour.

2.3-Digestion and Purification

Pancreas was digested by placing each perfused pancreas in a 37°C water bath for 14-18 minutes (predetermined to account for lot-to-lot variability, briefly two perfused pancreases were digested at one of the following times: 12,14,16,18,20 minutes. Islet yield and viability was analysed to determine digestion time). Once digestion was completed, pancreatic tissue was dissociated by shaking the tubes vigorously (40 inverts of the conical tube containing a pancreas in 10 second). The pancreas was then washed with G-solution (1XHBSS + 1%BSA + 0.357g/L sodium bicarbonate), to quench digestion. The digested pancreas was spun down at 290XG for 2 minutes at 4°C. After another wash step, dissociated tissue was passed through a 0.419 mm sieve (Canadawide scientific) to separate out non-digested tissue, fat and lymph nodes from the digested pancreas. After another wash, cells were then purified on an 1110 Histopaque (Sigma) gradient by spinning sample at 900XG for 20 minutes at 24°C, with slow acceleration and no braking. Islet cells were collected and washed again. Islet cells then underwent gravity sedimentation and were then handpicked under a microscope. When handpicking the size of the islets are estimated base on the size of a p200 pipette tip, and a homogeneous sample of sizes are collected and aliquoted for downstream processes.

2.4-Cell Culture

αTC1-6 and β-TC-6 cell lines were purchased from the American tissue culture collection (ATCC). αTC1-6 are differentiated pancreatic α cell line that produces glucagon. αTC1-6 was cloned from αTC1 cell line. Which was derived from an *Mus musculus* adenoma. β-TC-6 cell lines are pancreatic β cell derived from *Mus musculus* insulinoma cell lines that secretes insulin in response to glucose. These cell lines endogenous express miRNA-375, miRNA-7 and *Pax6*. αTC1-6 cell lines were cultured in growth medium consisting of

DMEM (Hyclone TM) supplemented with 10% heat inactivated bovine growth serum (BGS), 15mM HEPES, 0.1mM non-essential amino acids, 0.02% bovine serum albumin (BSA), 1.5g/L sodium bicarbonate, and 2.0g/L glucose. β-TC-6 cell lines were cultured in growth medium consisting of DMEM (Hyclone TM) supplemented with 15% heat inactive BGS and 1mM sodium pyruvate. Cells were cultured at 37°C and 5% CO_2. Islet cells were isolated from mice as described above, and were cultured in RPMI media (Gibco) supplemented with 10% heat inactivated BGS and 1% penicillin-streptomycin (Gibco). Islet cells were initially cultured at 27 °C and 5% CO_2 for 48 hours to reduced stress levels, and were moved to 37°C and 5% CO_2 following this recovery period.

2.5-Cell Line Passaging

All cell lines were passaged or seeded when they reached 80% confluence as follows: the media was removed, and cells were washed with $CaCl_2$, $MgCl_2$, and phenol red- free phosphate buffered saline (PBS) (Hyclone) and then trypsinized with 0.05% Trypsin-EDTA in PBS for 5 minutes at room temperature. Trypsin was quenched with appropriate growth media containing growth serum and cells were centrifuged at 300XG for 5 minutes. Supernatant was removed and cells were re-suspended in fresh growth medium. Cells were counted and plated at density depending on the plate size used – (96 well plate - $2.5x10^4$ cells per well, 24 well plate - $2.5X10^5$ cells per well, 12 well plate - $5X10^5$ cells per well, 6 well plate - $1X10^6$ cells per well).

For αTC1-6 cell lines, a similar procedure for passaging the cells was taken. Instead of using trypsin to detach the cells, an enzyme-free cell dissociation buffer (Gibco) in Hank's Balanced Salt Solution (HBSS) was used.

2.6-Luciferase Assay

αTC1-6 or β-TC-6 cell lines ($2.5x10^4$ per well in a 96 well plate) were transfected with Firefly Luciferase reporter plasmid (10ng per well), and Renilla Luciferase plasmid (40ng per well), using JetPrime transfection reagent based on the manufacturer's instructions. The growth media was removed 24 hours following transfection, and cells were treated with Dual-Glo Luciferase buffer and Dual-Glo Luciferase substrate mix (following the manufacturer's instructions). The reaction was incubated in the dark for 10 minutes, and then read on Perkin Elmer Victor^{3}V 1420 multi-label plate reader. Firefly Luciferase activity was normalized to the activity of Renilla Luciferase. Firefly luciferase has a peak emission at 560nm, and Renilla luciferase has a peak emission at 480nm. The settings for the plate reader are as followed: No filter, 10 second counting time, and normal emission aperture, based on manufactures recommendation.

2.7-Luciferase Assay – Tud Titration

Pancreatic cells were co-transfected with the following: Renilla luciferase, a Firefly luciferase reporter that contains the exact miRNA site (either miRNA-375 or miRNA-7) downstream; and either Tud 375 or Tud 7 at varying concentrating (10ng-40ng per well) or Tud MT. For lower concentration of Tud 375 or Tud 7, Tud Mt was added to compensate so that the total amount of DNA was constant. Bioluminescence was measured 24 hours post transfection as described above.

2.8-SDS-PAGE Detection of miRNA Inhibition on PAX6 Protein Levels

Cell lines were aspirated of media, then washed three times with PBS, then treated with 1XSDS buffer (0.05M Tris-HCl pH 6.8, 2% SDS, 10% glycerol, without bromophenol-blue and 2-β mercaptoethanol to carry out BCA assay. Bromophenol-blue and 2-β mercaptoethanol were added before boiling the samples) and protein inhibitor

cocktail and scraped. Whole cell lysate was incubated on ice for 30 minutes, and then placed on a nutator for 15 min at 4°C. Samples were then passed through an 18-gauge needle, and spun down at 20,000XG, for 30 minutes, and the soluble fraction was kept and the insoluble fraction was discarded. Protein concentration was determined by BCA assay (Pierce Fisher). Samples were diluted to equal concentration, and 0.01% bromophenol-blue, 2.5% 2-β mercaptoethanol was added. Afterwards the samples were boiled for 10 min at 95 degrees prior to electrophoresis. Samples were resolved on a 10-15% SDS-PAGE gel, and transferred to nitrocellulose using Towbin transfer buffer (0.025M TRIS, 0.192 M Glycine, and 20 % Methanol). Membranes were then stained with Ponceau S Staining Solution (0.1%(w/v) Ponceau S (Sigma) in 1%(v/v) acetic acid) and then washed with 1X Tris-buffered Saline (TBS - 50mM Tris-Cl pH 7.5, 150mM NaCl) for 5 minutes. Membranes were blocked in 2.0% casein in 1X TBS overnight at 4°C. Primary antibodies: anti-PAX6 1:100 (DSHB Hybridoma product PAX6) or, anti-β -ACTIN 1:4000 (sigma) were diluted in TBS–Tween20 (TBS-T), where Tween20 concentration was at 0.05 %. Blots were washed 3 times in TBS-T for 5 minutes and probed with anti-mouse IgG horseradish peroxidase (HRP) conjugate (R&D system) at a working dilution of 1:4000, or 1: 10,000 (depending on primary antibody). Antibody binding was detected using enhanced chemiluminescence western blotting substrate (Pierce) or Luminata Forte (Millpore) per the manufacturer's instructions. Blots were then exposed to film which was developed via an X-ray film developer (Kodak). For the islets, a small modification was made to the procedure. The islets were first centrifuged at 400Xg for 10 minutes at 4°C as islets were in suspensions, then washed twice with PBS and then treated as above. For Li-cor detection a similar process was undertaken, with a

small modification. After staining Ponceau S Staining Solution blots were washed with TBS, and then blocked with Blocking Buffer for Fluorescent Western Blotting (Rockland Inc.) overnight at 4°C. After incubation of the primary antibody, and wash steps the blot was then kept in the dark. The secondary antibody used was an Anti-MOUSE IgG (H&L) (GOAT) DyLight™ 680 Conjugated (Rockland inc.) at a dilution of 1:10,000, diluted in Blocking Buffer for Fluorescent Western Blotting solution (Rockland inc). After incubation with the secondary antibody, the blot was washed 3 times for 5 minutes each in TBS-T, and followed by 2 more washes in TBS for 5 minutes each. Blots were detected using Odessy Li-cor CLX in the 700nm channel. Quantification of blot was done by the image studio software.

2.9-Flow Cytometer

Adherent cells were detached from the plate via trypsin, digestion was quenched and cell counts were taken. Cells were spun down at 350XG for 5 minutes, the supernatant was removed and the cells were washed with PBS (all following wash step were done under these conditions unless stated). Cell were washed with PBS and then fixed with 1% Paraformaldehyde (PFA) in PBS. Cells were washed with PBS and then treated with (-20°C) cold 100% ethanol which was added drop wise whilst vortexing to a final concentration of 70%. Cells were then incubated in the dark at 4°C on a nutator for one hour. Cells were then spun down, and 3% BSA in PBS was added. The cells were spun down at 300XG for 10 minutes at room temperature. The supernatant was removed and cells were treated with 0.1% Triton-X 100 for 10 minutes on ice. 3% BSA was added and cells were spun down 300g for 10 minutes at room temperature. The supernatant was removed and cells were then blocked with 3% BSA for one hour on a nutator. Samples

were then washed with PBS-TB (PBS, 0.5%BSA, 0.1%Triton-X 100). Cells were then resuspended in solution with primary antibody: PBS-TB+ 1% goat serum + mouse anti-PAX6 (1:3000) (DSHB Hybridoma product PAX6) and/or PBS-TB+ 1% goat serum + anti chicken GFP (1:200) (incubated overnight on a nutator in the dark at 4°C). Samples were then washed with 3% BSA in PBS. Next the cells were spun down and the supernatant was removed. Cells were re-suspended in PBS-TB + 1% goat serum with the secondary antibody: Alexa Fluor® 647 conjugate F(ab')2-goat anti-mouse IgG (H+L) (1:1000) and/or Alexa Fluor® 488 AffiniPure F(ab') fragment donkey anti-chicken IgY (IgG) (H+L) (1:100) and incubated in the dark at 4°C for two hours on the nutator. Samples were then washed with 3%BSA in PBS, and then spun down and re-suspended in 0.5% BSA in PBS, and passed through cell strainer before loaded onto the flow cytometer. For the islets, the protocol above was used by with small modification. Islets were collected and centrifuged for 10 minutes 400XG. Islet containing pellet was washed with PBS. Islets were treated with 0.01 % trypsin-EDTA for 5 min to dissociate the islets; trypsin was quenched with appropriate cell culture media containing FBS. Primary antibody condition was used at a higher concentration: PBS-TB+ 1% goat serum + mouse anti-PAX6 (1:100) (DSHB Hybridoma product PAX6). The secondary antibody conditions were the same. Cells were then treated as described above. The program used for acquisition of the cells was BD cellquest^{tm} pro and analysis of events was carried out via FlowJo.

2.10-Viral Transduction

Media was aspirated and replaced with serum free media. The cells were then transduced with AAV vectors at MOI of 10^6 Genomic Copies (GC) per cell. Serum free

media was replaced after 6 hours. Cells were processed three days after transduction. For islets a similar procedure was undertaken, however, islets were processed after five days post transduction and treated at a higher MOI of 10^8 GC per islet cell.

2.11-Statistics

Statistics were done using Flow Jo, or GraphPad Prism 6. Quantification of western blot was done by image J, and li-COR image studio software.

2.12-Vector, Reporters and Plasmid Sequences

The luciferase reporters were subcloned into pMir-Luc purchased from Signosis. The Tuds and TPs were subcloned into pAAV-Lacz vector purchased from Agilent technology. The TPs and Tuds were designed to be expressed from the Pol III driven H1 promoter. The TPs produce a 60 bp RNA that is complementary to the region containing miRNA-7 or miRNA-375 seed matches within the *Pax6* mRNA 3'UTR. The target protector 7 (TP-7) anneals to region 650-710 of the 3'UTR, whilst the target protector 375 (TP-375) anneals to region 180-240 within the 3'UTR. To control for non-specific effects, we used a target protector complementary to the bacterial CRE recombinase cDNA which will not anneal to with any mammalian transcripts (TP-CRE). The firefly SV40 luciferase reporter was purchase from Signosis, and the full mouse *Pax6* 3'UTR was subcloned into this reporter to produce the wildtype *Pax6* 3'UTR luciferase reporter.

Table 2: Luciferase Reporter Sequence.
Sequence for the following: *Pax6* 3'UTR at the location denoted, or mutation (in bold) for reporter, bases that were mutated are in bold. Seed site for exact miRNA 375 reporter and miRNA 7 reporter.

PAX6 3'UTR position 186-207	5'-GCACGGUAUCAGUUGGAACAAA-3'
203 Mutant Reporter	5'-GCACGGUAUCAGUUGG**GG**CAAA-3'
PAX6 3'UTR position 501-524	5'-UAAAAACUAUCUGUUGGUUUUCCA-3'
517 Mutant Reporter	5'-UAAAAACUAUCUGUUGGUUUU**GG**A-3'
PAX6 3'UTR position 640-662	5'-AAAAUGUAAGUAUUUGUCUUCCC-3'
655 Mutant Reporter	5'-AAAAUGUAAGUAUUUGUC**GG**CCC-3'
Exact miR 375 reporter	5'-CCUUGUUU-3'
Exact miR 7 reporter	5'-GUCUUCCC-3'

Table 3: Target Protector Sequence.
Insert sequence that was cloned into pAAV-Lacz vector. Containing the 60 nucleotide insert for TP-375 and TP-7 that covers to the miRNA binding site for miRNA-375 and miRNA-7 respectively. TP-CRE sequence corresponds to an Enterobacteria phage P1 CRE gene for CRE recombinase.

TP-CRE	5'-GGGACCGATTTCGACCAGGTTCGTTCACTCATGGAAAATAGCGATCGCTGCCAGGAGCG-3'
TP-375	5'-AGAAGGCACGGTATCAGTTGGAACAAATCTTCATTTTGGTATCCAAACTTTTATTCATTT -3'
TP-7	5'-TTAAACAGAAGGGATCTTTAGGAGTCTTACTAAAGATATTATTTCAATTAAAGTAAATATA -3'

Table 4: Tud constructs.
The Tud construct sequences were cloned into pAAV-LacZ vector. The tough decoys are composed of a stem shown in green; the linker is shown in red; miRNA binding sites are shown in black; the blue depicts a 4 nucleotide insert and, the pink sequence denotes the stem loop. Tud MT is not predicted to interact with known miRNA that are expressed in the pancreas based on miRbase analysis.

Tud MT	5'-GACGGCGCTAGGATCATCAACAGGGGGGAATCAC ATCTTAGTCTTCCCAAGTATTCTGGTCACAGAATACAAC GGGGGGAATCACATCTTAGTCTTCCCAAGATGATCCTAGCGCCG TC -3'
Tud 375	5'-GACGGCGCTAGGATCATCAACTCACGCGAGCCG ATCTAACGAACAAACAAGTATTCTGGTCACAGAATACAAC TCACGCGAGCCGATCTAACGAACAAACAAGATGATCCTAGCGCC GTC-3'
Tud 7	5'-GACGGCGCTAGGATCATCAACCAACAAAATCAC ATCTTAGTCTTCCACAAGTATTCTGGTCACAGAATACAAC CAACAAAATCACATCTTAGTCTTCCACAAGATGATCCTAGCGCC GTC -3'

Chapter 3: Results

This data in the following chapter is being used for the preparation of the following paper:

"**Protecting the *Pax6* 3'UTR from miR-7 is effective at restoring PAX6 expression in haploinsufficient islets in mice.**

"Kevin Yongblah[#], Spencer Alford[#], Bridget Ryan[*], Bob Chow[*], and Perry Howard[#]
Department of Biochemistry and Microbiology, University of Victoria. PO Box 1700 STN CSC Victoria BC V8W2Y2 Canada.
*Department of Biology, University of Victoria. PO Box 1700 STN CSC Victoria BC V8W Canada"

I have performed all experiments and generated the data and figures in this thesis as well as writing of the manuscript with the following exceptions:

- Spencer Alford generated all luciferase reporters, Tud and Target protector constructs. Additionally, Spencer ran preliminary experiments analysing miRNA binding site within the *Pax6* 3'UTR, this data is not presented in this thesis.
- Bridget Ryan a PhD student in Dr Robert Chow laboratory carried bioinformatic analysis of *Pax6* 3'UTR and putative miRNA targets, from these miRNA-7 and miRNA-375 were chosen to be further investigated.
- Dr Perry Howard provided input on experimental design and preparation of the manuscript.
- Dr Robert Chow provided assistance in experimental design and writing of the manuscript.

3.1- miRNA-375 and miRNA-7 Regulates *Pax6* in Pancreatic Cells

Previous work has implicated miRNA-375 and miRNA-7 in regulating *Pax6* pancreatic endocrine cells[53,99,100]. In mice, there is a single miRNA-375-5p (7mer-A1) site at position 178-207. There are also two miRNA-7-5p seed sites: one site at 7mer-m8 at position 633-661, which was previously identified, and an additional 8-mer site was identified at position 516-523. We first sought to determine whether these two miRNAs regulate *Pax6* expression in pancreatic cells. To confirm the ability of these miRNA-7 and miRNA-375 to regulate *Pax6*, we analysed the miRNA-7 and miRNA-375 putative binding sites in the *Pax6* 3'UTR to determine if they were functional. To do this, we generated luciferase reporters in which the putative miRNA binding sites were mutated individually, or mutated both miRNA-7 binding site to generate a double miRNA-7 mutant (see Figure 12a). We transiently expressed each of the reporters in pancreatic cell lines which endogenously express both miRNA-7 and miRNA-375, and compared the expression of the mutant reporters to the wild-type *Pax6* 3'UTR reporter. The mutation of the miR-7-site-2 binding site increased luciferase expression approximately two-fold relative to the WT *Pax*6 3'UTR reporter in β-TC-6 cells (see Figure 12b). In contrast, the mutated miR-7-site-1 reporter was not significantly elevated over wild type. Nor was the double mutant reporter, in which both miRNA-7 binding sites (*Pax6* 3'UTR site 517 and 655) were mutated, significantly elevated over the single miR-7 site 2 reporter. These results confirm that the miRNA-7 binding site at position 633-661 is the primary site of miRNA-7 regulation of *Pax6* in pancreatic cell lines. Similarly, the miR-375-site mutant reporter was also significantly increased relative to wild type reporter (1.9-fold increase), indicating this site is also functional in pancreatic cells. Together our data confirm that

both miRNA-375 and miRNA-7 regulate *Pax6* expression in pancreatic cells. A similar result was obtained in α-TC1-6 cells (see Appendix Figure 1c).

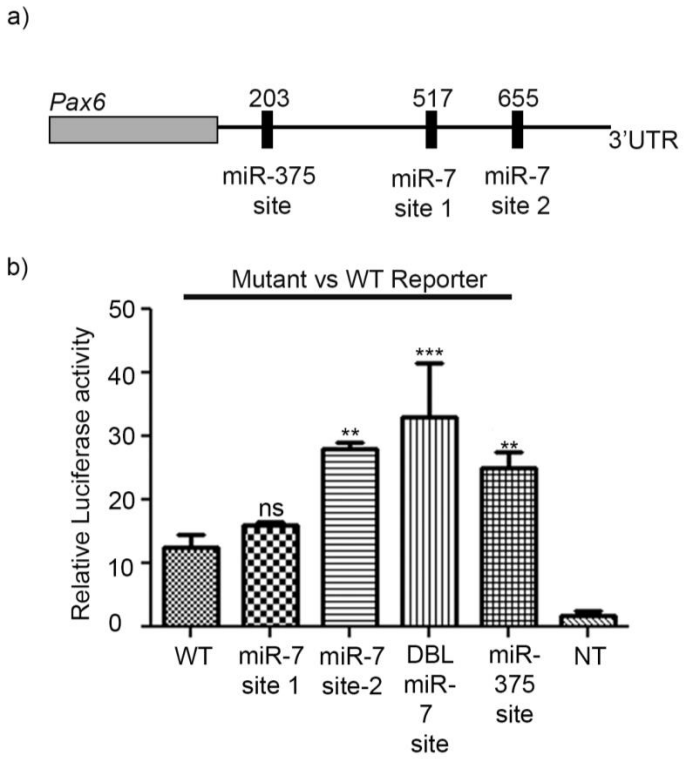

Figure 12: miRNA-375 and miRNA-7 can target *Pax6* 3'UTR in β-TC-6 cells. (a) Schematic diagram of miRNA-375 and miRNA-7 binding sites. The seed sites are located at 201-207 (miR-375), 516-521 (miR-7-site-1), and 655-660 (miR-7-site-2). (b) Representative luciferase reporter assays of β-TC-6 cells 24 hours after transfection of the wild-type *Pax6* 3'UTR or mutated *Pax6* 3'UTR at miRNA 7 or miRNA-375 seed sites, A one-way analysis of variance (ANOVA) was conducted with the following results: (F [5,12]) =28.19; P<0.0001) followed by Dunnett's multiple comparison test comparing each condition to control (WT) was used to determine whether there were significant differences between groups and control in panel (b) p<0.01=**, P<0.001=***. The number of experimental repeats =3.

To confirm that miRNA-7 and miRNA-375 regulate *Pax6* transcripts, miRNA-7 or miRNA-375 were overexpressed in the pancreatic α-TC1-6 cell line (see Appendix Figure 1a-b) and β-TC-6 cell line and endogenous PAX6 protein levels were examined (see Figure 13a). Overexpression of either miRNA-7 or miRNA-375 decreased PAX6 protein levels in pancreatic cells to 50% or 70% of wild-type PAX6 levels respectively

(see Figure 13b). These data confirm that both miRNA-375 and miRNA-7 are functional and regulate *Pax6* expression in pancreatic cells.

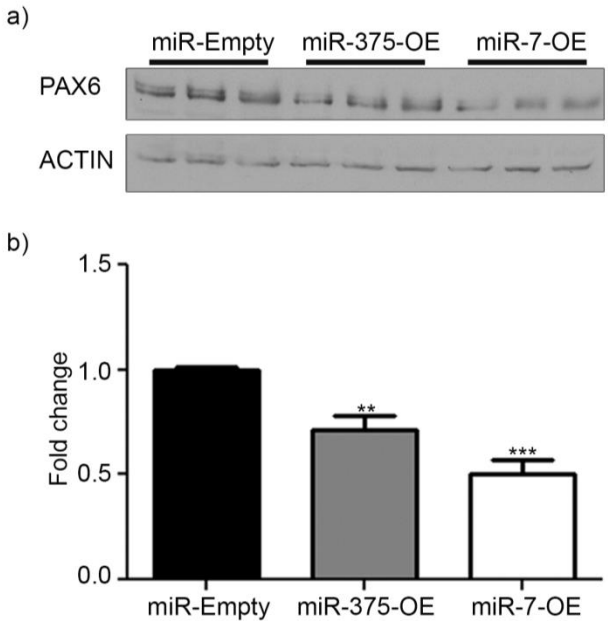

Figure 13: miRNA overexpression decreases the levels of PAX6 protein in β-TC-6 cells. (a) Representative western blot analysis of the effect of miRNA-375 or miRNA-7 overexpression on PAX6 protein levels in β-TC-6 cells; β -actin was used as a loading control. Each lane represents protein sample extracted from a well in a 6 well plate. (b) Quantification via Image J of a western blot: fold change is relative to miR-Empty. The fold change was calculated by dividing the ratio of PAX6:ACTIN signal of each condition (miR-Empty, miR-375-OE, miR-7-OE) by the average ratio of PAX6:ACTIN for miR-Empty. The resultant fold change for each condition was averaged. A one-way ANOVA (F [2,6]) =61.96; P<0.0001) followed by Dunnett's multiple comparison test comparing each condition to control (miR-Empty) was used to determine whether there were significant differences between groups to controls (b) p<0.01=**, P<0.001=***. The number of experimental repeats =3.

3.2-Tough Decoys Against miRNA-7 and miRNA-375 Increase Expression of *Pax6* reporter

We next determined the impact of inhibition of miRNA-375 or miRNA-7 on PAX6 protein levels in pancreatic cell lines. Utilizing the strategy developed by Haraguchi et al[104], we designed miRNA-7 and miRNA-375 inhibitors called tough decoys (Tuds) (see Figure 9). We first validated the ability of Tuds to inhibit their specific miRNA. To do this, we first began by transfecting a luciferase reporter that

contained the miRNA-7 seed site downstream of luciferase cDNA into α-TC1-6 cell lines (see Appendix Figure 2a-d) and β-TC-6 cell lines. This reporter was co-transfected with either a control plasmid; which expressed RNA from bacterial CRE recombinase under the control of the H1 promoter (TP-CRE); a vector-expressing a Tud backbone with the seed site has been mutated to guanines abrogating miRNA binding (Tud Mt); or Tud 7 at increasing concentration. Increasing concentration of Tud 7 increased the expression of the miRNA-7 site reporter (exact miR-7 reporter) in β-TC-6 cells up to a two-fold relative to the TP-CRE or Tud MT (see Figure 14a). In contrast, Tud 7 had no effect on a luciferase reporter that contained the miRNA-375 seed site downstream of luciferase cDNA (exact miR-375 reporter) when expressed at the highest concentration (see Figure 14b) confirming that Tud 7 is specific for miRNA-7. Similarly, Tud 375 was able to increase the expression of the miRNA-375 site reporter (exact miR-375 reporter) in β-TC-6 cells (see Figure 14c) but had no effect on the exact miR-7 site reporter (see Figure 14d). These results indicate that Tud 7 and Tud 375 are effective at specifically blocking the actions of their respective miRNAs.

With these data we have shown that miRNA-375 and miRNA-7 can target *Pax6* and that the identified miRNA-375 and miRNA-7 binding sites are functional. Additionally, we have shown that miRNA-375 and miRNA-7 can be repressed by Tuds. This demonstration accomplishes the first and second objectives itemized above (under Hypothesis and Objective). The next step was to see whether miRNA repression altered PAX6 levels in endogenous cells.

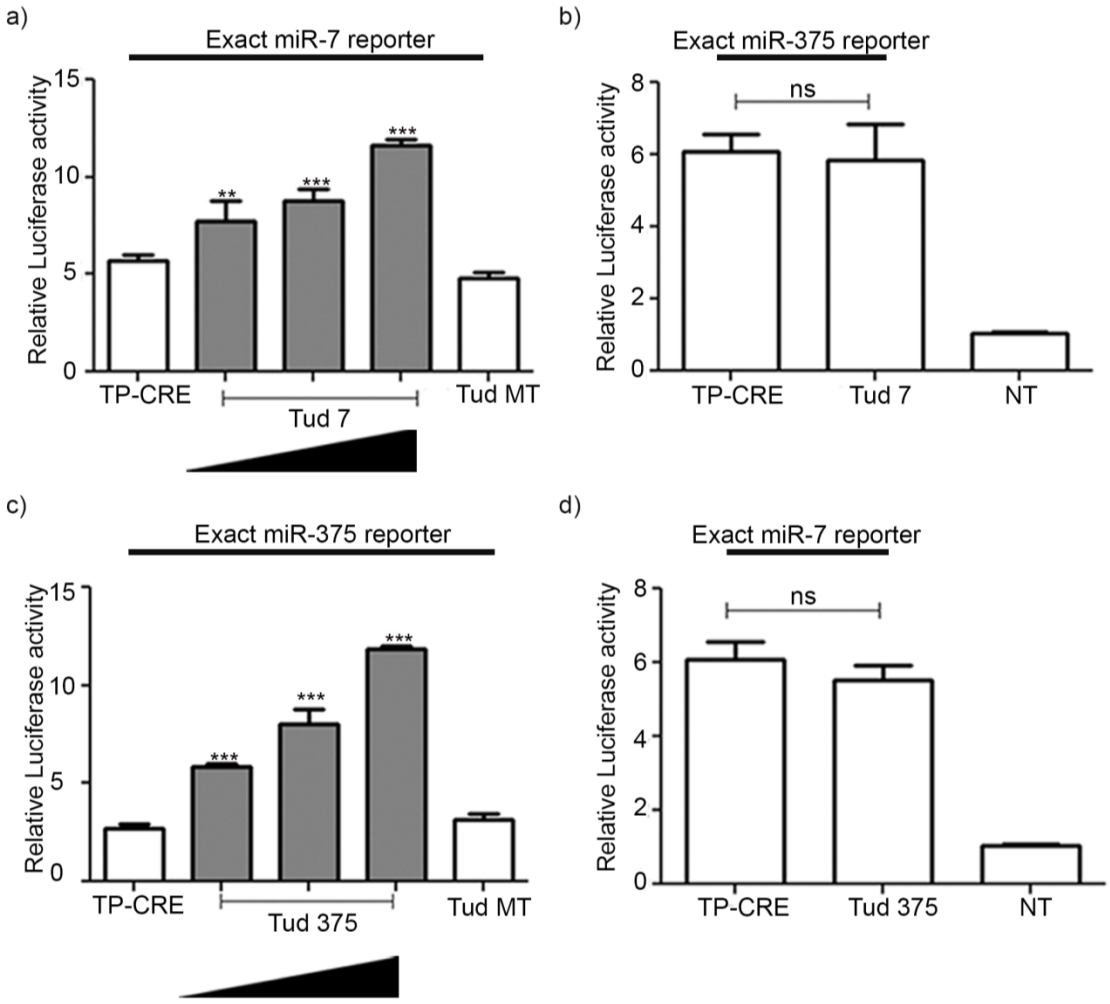

Figure 14: Tuds repress specific miRNA. (a) Representative luciferase reporter assays of β-TC-6 cells 24 hours after co-transfection of the exact miR-7 reporter and either control TP-CRE, Tud MT or increasing concentrations of Tud7. (b) Representative luciferase reporter assays of β-TC-6 cells 24 h after co-transfection of the exact miR-375 reporter and either control TP-CRE or Tud 7 (at the highest concentration tested previously). (c) Representative luciferase reporter assays of β-TC-6 cells 24 hours after co-transfection of the exact miR-375 reporter and either control TP-CRE, Tud MT or increasing concentrations of Tud 375. d) Representative luciferase reporter assays of β-TC-6 cells 24 hours after co-transfection of the exact miR-7 reporter and either control TP-CRE or Tud 375 (at the highest concentration previously tested). For each set of data, a one-way ANOVA was conducted with the following results: F [4,10] =47,45; P<0.0001 (a), F [2,6] =61.10; P<0.0001 (b), F [4,10] =59.35; P<0.0001 (c), F [2,6] =28.19; P<0.0001). One-way ANOVA was followed by Dunnett's multiple comparison test comparing each condition to the appropriate control (Tud Mt or TP-CRE) was used to determine whether there were significant differences between groups to controls (P<0.01=**, P<0.001=***, non-significant =n.s). The number of experimental repeats for each panel =3.

3.3-Suppression of miRNA Alters PAX6 Levels.

To study the effects of inhibition of miRNA-7 and miRNA-375 on *Pax6* expression, we examined Tud-mediated miRNA inhibition on a luciferase reporter that contains the *Pax6* 3'UTR immediately downstream of the luciferase cDNA. As expected, both Tud 7 and Tud 375 were able to specifically block the actions of miRNA-7 or miRNA-375 on the *Pax6* 3'UTR, increasing reporter expression in β-TC-6 cells by 2.2 or 1.8 times, respectively, relative to Tud MT (see Figure 15a). The effects on the reporter were specific as neither of the Tuds had any effect on the SV40 3'UTR luciferase reporter (SV40 reporter), which does not contain seed sites for miRNA-7 or miRNA-375 (see Figure 15b). A similar result was seen in α-TC1-6 (see Appendix Figure 2e-f).

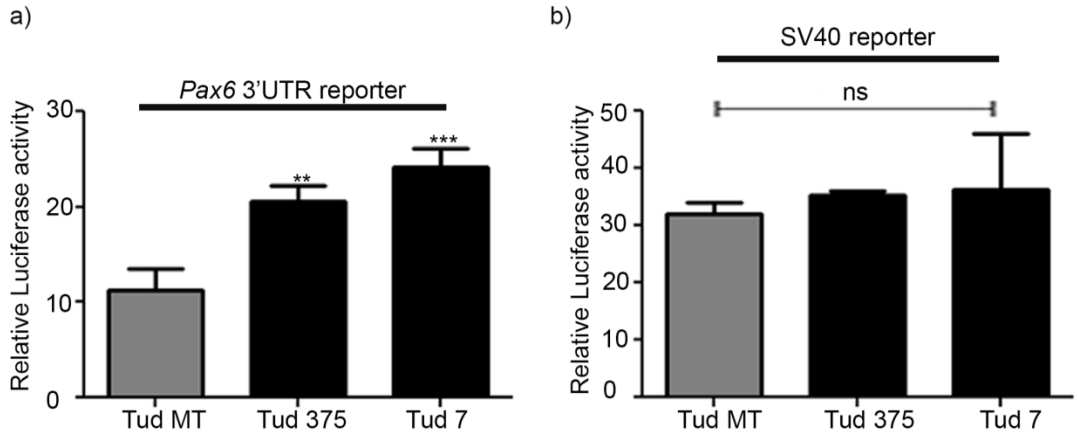

Figure 15: Tud-mediated miRNA repression increases *Pax6* 3'UTR reporter levels. **(**a) Representative luciferase reporter assays of β-TC-6 cells 24 hours after co-transfection of wild-type *Pax6* 3'UTR and Tud constructs. (b) Representative luciferase reporter assays of β-TC-6 cells 24 hours after co-transfection of SV40 reporter and Tud constructs. For both conditions a one-way ANOVA was carried out with the following results: F [2,6] =33.69; P<0.0001 (a), F [2,6] =0.4674; n.s (b), followed by Dunnett's multiple comparison test comparing all column to control (Tud Mt) was used to determine whether there were significant differences between groups to control in panel, P<0.01=**, P<0.001=***, non-significant = n.s. The number of experimental repeats for each panel =3.

The next step was to determine whether the effect of repression of miRNA on the *Pax6* 3'UTR reporter was translated to a difference in protein levels. To do this, we tested whether Tud 7 and Tud 375 were able to affect endogenous *Pax6* expression in pancreatic cells. β-TC-6 cells that were treated with Tud 7 or Tud 375 constructs expressing GFP. Cells that were positive for GFP were gated and the PAX6 protein levels were measured. Cells treated with either Tud 375 or Tud 7 showed an approximately 1.3-fold increase in PAX6 protein levels relative to the control Tud using flow cytometry (see Figure16 a-d), based on geometric mean. Western blot analysis of β-TC-6 cells that were treated with Tud 7 or Tud 375 constructs showed an approximately 1.5- or 1.3-fold increases in PAX6 protein levels, respectively, relative to Tud MT, confirming the flow cytometry data (see Figure16e-h). A similar result was seen in α-TC1-6 (see Appendix Figure 3a-d). Cumulatively, our data indicate that miRNA-7 and miRNA-375 regulate expression of *Pax6* in pancreatic β-TC-6 cells and that blocking this regulation may be effective at modestly increasing the level of PAX6 protein.

3.4-miRNA-7 and miRNA-375 Target Protectors Increase Pax6 Expression

Having established the suitability of targeting miRNA-7 and miRNA-375, we next sought a strategy to specifically limit the effects of this targeting to the *Pax6* 3'UTR. Accordingly, we designed target protectors (TPs) for the *Pax6* 3'UTR that specifically interfere with the miRNA-7-655 binding site or the miRNA-375 binding site. TPs are approximately 60-70 bp RNA molecules which are complementary to the target RNA and prevent miRNA binding (see the Introduction, above, for a more detailed discussion of TPs).

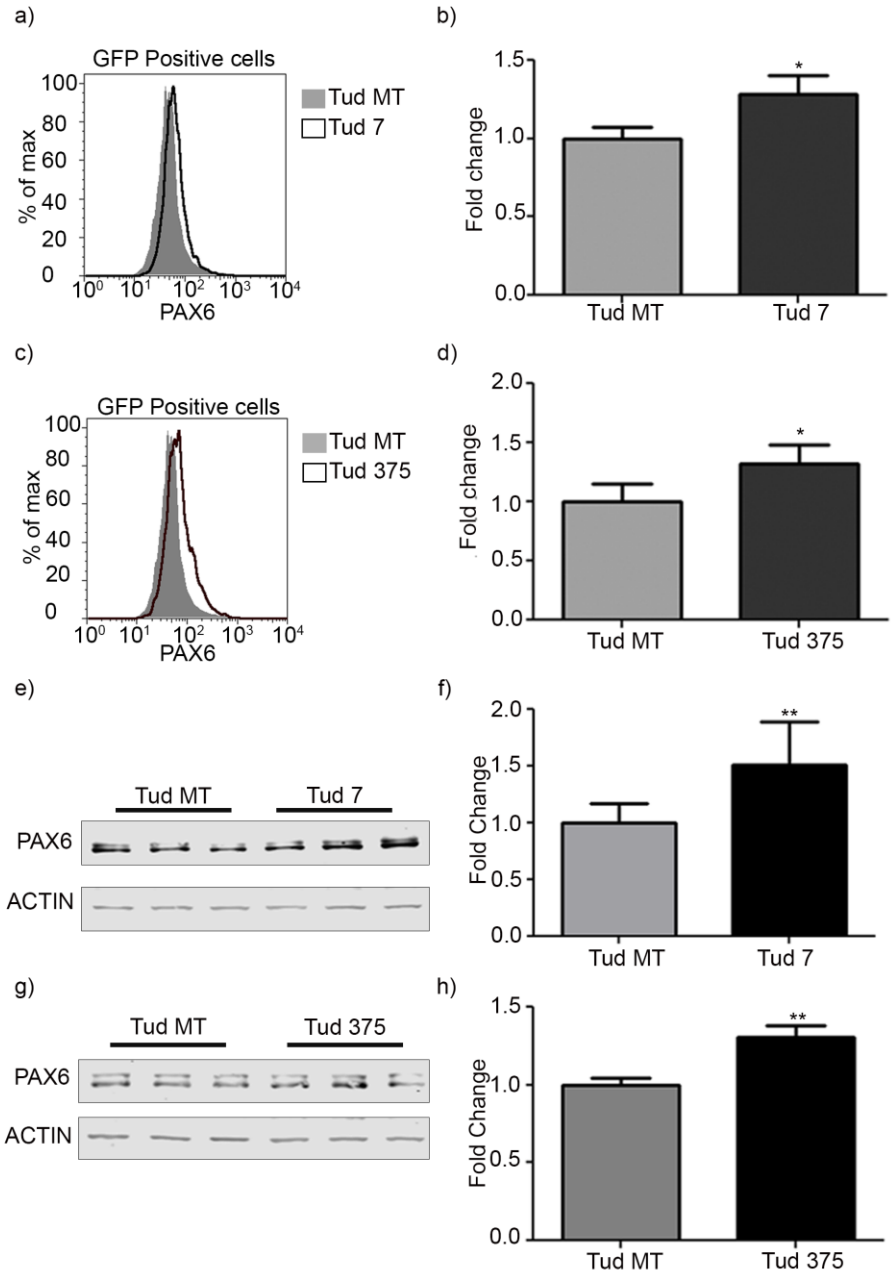

Figure 16: Tud-mediated inhibition of miRNA increases PAX6 protein levels in β-TC-6 cells. (a, and c) Representative PAX6 histogram from β-TC-6 cell population. The shaded histogram represents cells treated with Tud MT, while the non-shaded histogram with the dark line represents cells treated with (a) Tud 7 or (c) Tud 375 for each flow cytometer experiment 10^5 cell were collected and analysed, GFP% of positive cell was TMT - 75%, Tud 375 – 55.2%, Tud 7 – 62.3%. (b and d) Quantification of histogram for Tud Mt vs. (b)Tud 7 or (d)Tud 375 showing the PAX6 fold change relative to Tud MT. The fold change was calculated by dividing the geometric mean from three separate experiment of each condition by the average geometric mean Tud MT (from three separate experiment). The resultant fold change for each condition was averaged. (e and g) Representative western blot analysis of the effect of Tud-mediated

repression of (e) miRNA-7 or (g) miRNA-375 on PAX6 protein levels in β-TC 6 cells; β -actin was used as a loading control. Each lane represents protein sample extracted from a well in a 6 well plate. (f and h) Quantification of Li-cor western blot analysis, showing the effects of (f) Tud 7 and (h) Tud 375 on PAX6 protein levels, showing the PAX6 fold change relative to Tud MT. The fold change was calculated by dividing the ratio of PAX6:ACTIN li-Cor signal intensity from each condition by the average ratio of li-Cor signal intensity of PAX6:ACTIN for Tud MT. The resultant fold change for each condition was then averaged. . A two-tailed t-test was used to determine whether there was a significant difference between either Tud Mt and Tud 7 (b and f) or Tud 375 (d and h) in panel (b): t (4) =3.559 P=0.0236, panel (d): t (4) =3.281 P=0.0305, panel (f): t (16) =3.718 P=0.0034, panel (h): t (22) =3.351 P=0.0024. P<0.05=*, P<0.01=**. The number of experimental repeats for each panel =3.

The expression of TP-375 and TP-7 increased the expression of the *Pax6* 3'UTR luciferase reporter in β-TC-6 cells by 1.8- or 2.2-fold, respectively (see Figure 17a). Neither TP had any effect on the SV40 reporter, showing that the effects of the TPs are specific to *Pax6* 3'UTR (see Figure 17b). A similar result was seen in α-TC1-6 was seen (see Appendix Figure 4a-b).

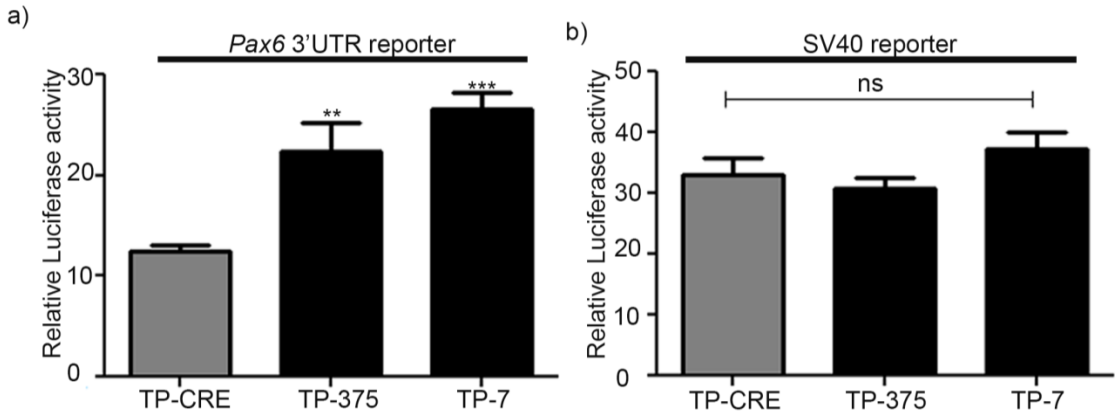

Figure 17: Shielding miRNA-binding sites within the *Pax6* 3'UTR increases *Pax6* 3'UTR reporter levels. (a) Representative luciferase reporter assays of β-TC-6 cells 24 h after co-transfection of wildtype *Pax6* 3'UTR reporter and TP constructs. (b) Representative luciferase reporter assays of β-TC-6 cells 24 hours after co-transfection of SV40 reporter and TP constructs. For all panels a one-way ANOVA was conducted with the following results: F [2,6] =43.00; P=0.0003 (a), F [2,6] =0.67276; non-significant (n.s). This was followed by Dunnett's multiple comparison test comparing all column to control (TP-CRE) was used to determine whether there were significant differences between groups to control, P<0.01=**, P<0.001=***, non-significant = n.s. The number of experimental repeats for each panel =3.

We next sought to determine the effect of the TPs on PAX6 protein levels in these cells. Western blot analysis revealed that, consistent with their ability to target more than one miRNA, both TP-375 and TP-7 could increase the levels of PAX6 protein, causing 40% or 80% increases in β-TC-6 cells, respectively (see Figure.18 a-b). These increases are higher than those achieved with the Tuds. A similar result was seen in α-TC1-6 (see Appendix Figure 4c-f). These results demonstrate that the target-protector strategy is effective at increasing levels of PAX6 protein within the twofold range we sought for therapeutic potential.

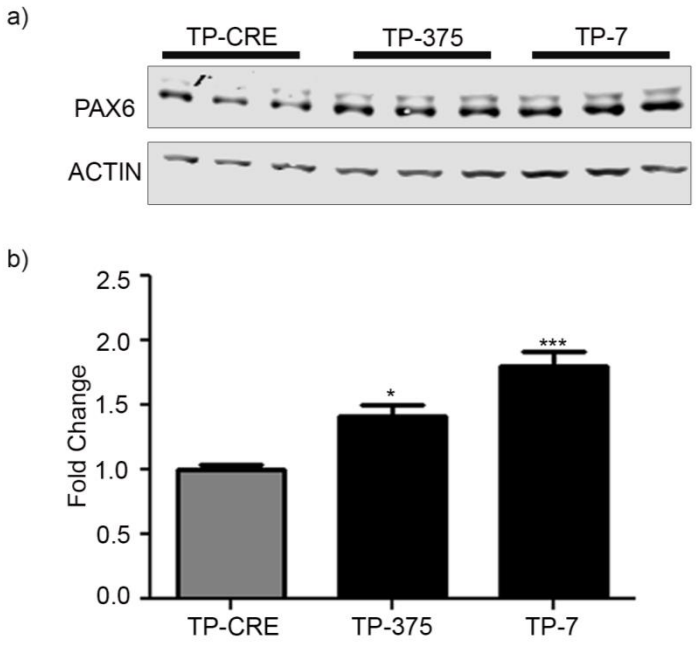

Figure 18: Shielding miRNA-binding sites of *Pax6* 3'UTR increases the levels of PAX6 protein.(a) Representative western blot analysis of the effect of TP-mediated repression of miRNA-7 or miRNA-375 on PAX6 protein levels in β-TC-6 cells; β -actin was used as a loading control. Each lane represents protein sample extracted from a well in a 6 well plate. (b) Quantification of western blot analysis, fold change relative to TP-CRE. The fold change was calculated by dividing the ratio of PAX6:ACTIN LiCor signal intensity from each condition by the average PAX6:ACTIN ratio li-Cor signal intensity of TP-CRE. The resultant fold change for each condition was averaged. For panels (b)a one-way ANOVA was conducted with the following results: F [2,6] =23.17; P=0.0015. This was followed by Dunnett's multiple comparison test comparing all column to control (TP-CRE) which was used to determine whether

there were significant differences between groups to control in panel (b), $P<0.01$=**, $P<0.001$=***. The number of experimental repeats for each panel =3.

3.5-Viral Delivery of Target Protectors Against miRNA-7 Increase *Pax6* Expression

An important question is whether the target-protector strategy can be used to restore PAX6 protein levels in cases of haploinsufficiency of *Pax6* as seen in aniridia patients. In the cornea and retina of $Pax6^{sey+/-}$ mice have approximately 50% protein levels of wildtype mice[32], therefore it is reasonable to infer that a two fold increase of protein levels in heterozygous cell will be needed to reach wildtype levels, and this will be the level of increase in protein we will be looking to achieve. Another important factor to address is the possibility that in *Pax6* haploinsufficient cells miRNA regulation may already be adjusted through feedback mechanisms to compensate for low *Pax6* levels. If this is the case, interfering with miRNA regulation of *Pax6* may be of no benefit. To address this question, we sought to restore *Pax6* expression in islets from mice heterozygous for the *Pax6* with mice that have Small-eye Dickie ($Pax6^{sey/dey}$) mutation (see The Use of Small Eye Mouse Model to Characterise *PAX6* Functions section for detail on mutation and phenotype). To test the TPs as a miRNA-suppression strategy in a heterozygous setting, we first needed to develop a vehicle to deliver the TPs into islets. We developed a targeting vector, which contained a GFP cassette in which GFP is driven by the CAG-CMV promoter and a TP cassette in which TP expression is controlled by the RNAP III-dependent H1 promoter. We then tested the ability of AAV2, and AAV8 to target pancreatic endocrine cell lines. We found that AAV2 was most effective at targeting α-TC1-6 cell lines (Appendix Figure 5), and that AAV2 could target islets *ex vivo* based on GFP fluorescence (see Figure 19b). The targeting efficiency was approximately 35% of the dissociated islet cells (see Figure 19c).

To confirm the ability of the viral AAV-2-TP-7-GFP or AAV-2-TP-CRE deliver TPs into a β cell derived lineage, we transduced the β-TC-6 cells, gated for GFP, and measured PAX6 expression using flow cytometry. AAV2-TP-7 was very effective at increasing PAX6 expression (2 fold increase) in these cells, relative to the TP-CRE control (see Figure 20a). Furthermore, PAX6 protein levels in targeted wild-type islet cells TP7 AAV were also increased (see Figure 20b).

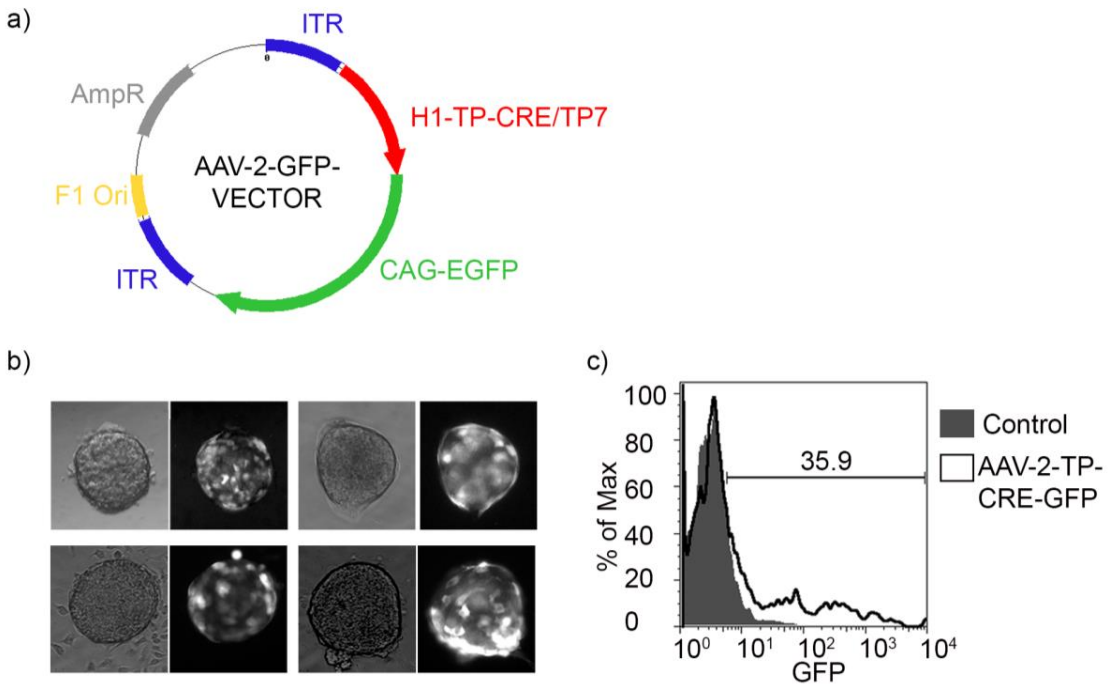

Figure 19: AAV-2 viral vector is an efficient delivery system for ex vivo islets. (a) The vector map of rAAV plasmid used to express TP-CRE-GFP or TP-7-GFP. (b) Representative images of isolated islets treated with AAV2 expressing GFP 5 days post transduction. (c) Representative histogram of dissociated islet cells; the shaded histogram represents non-infected (N.I) islet cells, while the non-shaded histogram with the dark line represents cells treated with AAV-2-TP-CRE-GFP. The number of cell collect and analysed in flow cytometer analysis was 10^5. The number of experimental repeats for panel b) =3, c)=2.

This result was replicated in a blind test in which we see a similar result (see Appendix Figure 6). Based on these results, we next compared the effect of TP-7 on

PAX6 protein levels on islets isolated from wild-type with its effect on islets isolated from *Pax6*$^{SeyDey\ +/-}$ mice (see The Use of Small Eye Mouse Model to Characterise *PAX6* Functions section for detail on mutation and phenotype). Islets from wildtype and heterozygous *Pax6*$^{SeyDey+/-}$ mice were isolated and treated with either TP-7 or TP-CRE. After treatment with TP-7, heterozygous islets had an increase of PAX6 protein to ~70% of wildtype levels, as shown by western blot analysis (see Figure 20c). One difficulty with protein quantification from whole-cell lysates is that one cannot discern between increases in expression in the majority of cells and substantial overexpression in a small minority of cells. This is an important issue since overexpression of PAX6 can have deleterious consequences[67,68,69]. To address this issue, we performed flow cytometry on infected islet cells. As shown in Figure 20d, the heterozygous islets had reduced number of cells expressing high levels of PAX6 (in comparison to wildtype islets treated with TP-CRE) and a geometric mean of 77.1. Treating heterozygous islets with TP-7 resulted in an increase in the geometric mean to 121 due to an increase in the number of cell that expressed high levels of PAX6. This resulted in heterozygous islets treated with TP-7 having 81% of PAX6 protein levels of WT islets treated with TP-CRE (geometric mean = 149). Collectively, our data show that a target-protector strategy directed against the miRNA-7 binding site in the 3'UTR of *Pax6* is effective at restoring PAX6 protein levels to near wild-type levels while minimizing the overexpression of PAX6.

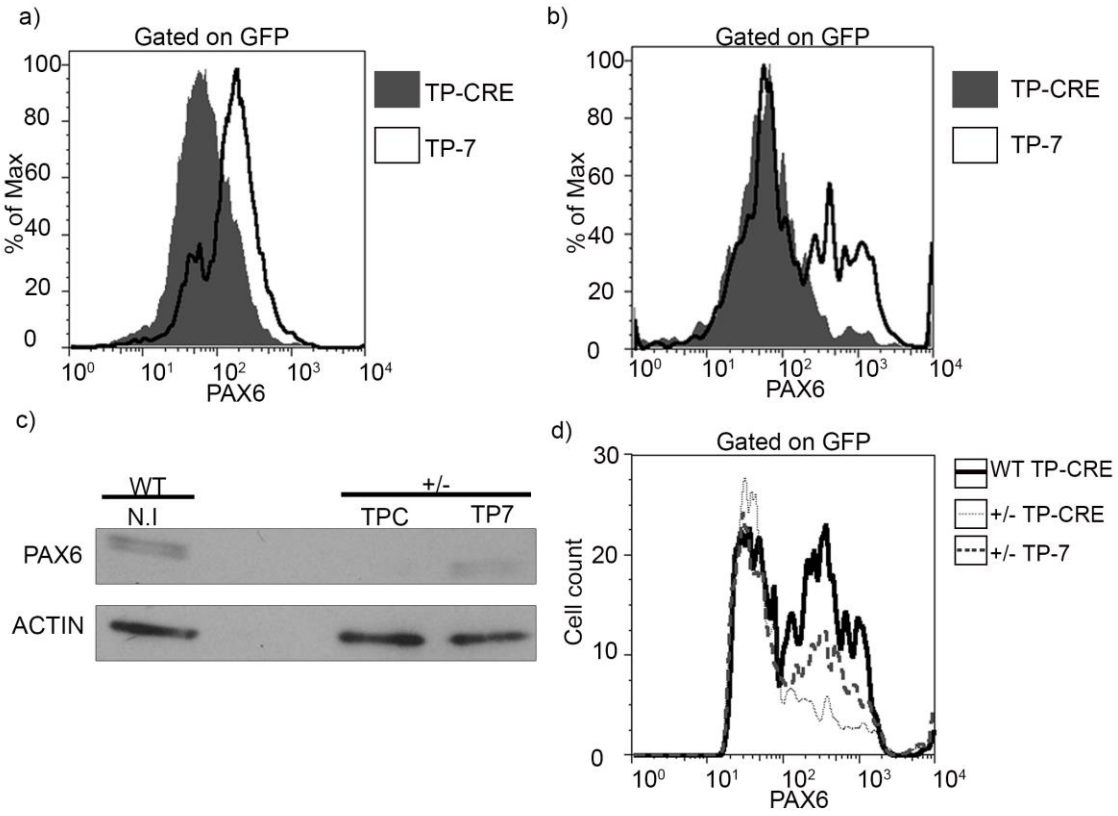

Figure 20: Shielding the miRNA-7 binding site within the *Pax6* 3'UTR increases PAX6 protein levels in haploinsufficient islets. (a) PAX6 histogram from GFP positive cells; the shaded histogram represents β-TC-6 cells treated with TP-CRE, and the non-shaded histogram with the dark line represents cells treated with TP-7. Number of cell collected and analysis was 10^4, GFP positive cell = TP-CRE - 87.4%, TP-7 – 84.7% (b) PAX6 histogram from GFP positive cells; the shaded histogram represents dissociated wild-type islet cells treated with TP-CRE, and the non-shaded histogram with the dark line represents cells treated with TP-7. Number of cell collected and analysis was 10^4, GFP positive cell = TP-CRE – 25.3%, TP-7 – 20.6% (c) Western blot analysis of the effect of TPs on PAX6 protein levels in heterozygous islet cells; β - actin was used as a loading control. (d) PAX6 histogram from GFP positive cells, the histogram with the solid black line represents dissociated wild-type islet cells treated with TP-CRE, the histogram with grey lines represents dissociated islets from heterozygous mice treated with TP-CRE, and the histogram with large dashed lines represents dissociated islets from heterozygous mice treated with TP-7. Number of cell collected and analysis was 5X10^5, GFP positive cell = WT-TPC -23.1%, +/- - TPC -18%, +/- - TP7 -19.7%. The number of experimental repeats for each panel a), b) =3, c), d) =2.

Chapter 4: Discussion

PAX6 is a crucial transcription factor that is involved in the development and maintenance of the eye and the pancreas. Haploinsufficiency of *PAX6* results in aniridia and its associated ocular and non-ocular defects, the latter including glucose intolerance and diabetes. Developing a method to suppress miRNA-directed gene regulation of *Pax6* opens the possibility of genetic therapies to increase *PAX6* levels in aniridic patients. Several synthetic miRNA inhibitors are currently being investigated in clinical trials[93,94] (ClinicalTrials.gov Identifier: NCT01829971), and data from this study provides more evidence that miRNA-suppression systems may be applicable in a therapeutic setting. The overall purpose of this study was to assess a miRNA-suppression strategy for murine *Pax6*. We hypothesised that suppression of miRNA-7 and/or miRNA-375 could restore *Pax6* levels in islets that were haploinsufficient for *Pax6*.

We have confirmed that miRNA-7 and miRNA-375 regulate *Pax6*, specifically we have shown that inhibition of miRNA-7 or miRNA-375 increases *Pax6* reporter and protein levels, and that an mRNA-specific miRNA-suppression system (TPs) can be used to increase *Pax6* levels in pancreatic cells. Using the TP strategy we have demonstrated that PAX6 protein levels in islets from heterozygous mice can be increased to 70% of wild-type levels. The TPs open a number of potential avenues for the development of therapies; they also serve as tools to help investigate specific miRNA-mRNA interactions. The TPs can be used in various tissues and developmental systems and can be delivered in many ways. However, this study does not address several questions that only *in vivo* studies can answer.

4.1-Confirmation of miRNA-375 and miRNA-7 Regulation of *Pax6*

We have confirmed that both miRNA-375 and miRNA-7 are functional regulators of *Pax6* in pancreatic endocrine cells. Overexpression of these miRNAs resulted in a reduction of protein levels, while luciferase assays evaluating the miRNA-binding sites within the *Pax6* 3'UTR revealed that the regulation of *Pax6* expression was dependent on the conserved miRNA seed site in the *Pax6* 3'UTR. Furthermore, Tud-mediated inhibition of miRNA resulted in an approximately twofold increase in both *Pax6* 3'UTR reporter levels and approximately 1.3-fold increase in PAX6 protein levels. This data confirms the findings of previous studies, which have shown that miRNA-7 can regulate *Pax6* in both the pancreas and brain[53,99,100].

miRNA-7 also has been shown to play a role in glucose homeostasis in mice. Loss of miRNA-7a2 in mice increase glucose tolerance due to increase in insulin secretion[126]. This increased insulin secretion was because of an increase of insulin exocytosis. The increased exocytosis was due to increased activity of soluble N-ethylmaleimide-sensitive factor attachment protein receptor (SNARE) complex[127]. The SNARE complex primary role is to mediate vesicle fusion to cell membrane. miRNA-7a2 regulation SNCA which has been shown to promote the formation of SNARE complex assembly. Loss of miRNA-7a2 resulted increase SNCA expression and in turn increased SNARE activity[126]. Inhibition of miRNA-7a expression did not alter β cell proliferation and apoptosis[126]. In contrast to increase insulin secretion, overexpression of miRNA-7a resulted in impaired insulin secretion and in diabetes in mice[126]. Additionally in islets from diabetic human and mice have reduced miRNA-7a levels[126]. All together these data indicate miRNA-7a has a role in glucose homeostasis and insulin secretion.

This thesis provides more evidence that endogenous miRNA-375 can regulate *Pax6* in the pancreas. Previously, Chevigny et al[98], showed that overexpression of miRNA-375 reduced *Pax6* 3'UTR reporter levels in HEK 293 cells[98]. Therefore, the data we have presented provides evidence that miRNA-375 regulates *Pax6* in pancreatic endocrine cells.

miRNA-375 also has a role in glucose homeostasis in mice. Mice that lack miRNA-375 develop hyperglycaemia because of an expansion in α cell numbers at the expense of β cell mass, and because of impaired cellular function[128]. These mice develop hypergluconeogenesis in the liver and have increased plasma glucagon levels. Additionally, there is an overall increase in insulin secretion to compensate the decrease in β cell mass[128]. Whilst overexpression of miRNA-375 resulted in suppression of glucose stimulated insulin secretion (GSIS) and reduction of myotrophin levels. [128] Myotrophin is necessary for insulin exocytosis, and inhibition of myotrophin in the pancreas mimicked the effects of miRNA-375 on insulin secretion. This data suggests miRNA-375 has a role in insulin secretion in mouse pancreas. miRNA-375 has also been suggested to have a role in cell proliferation and apoptosis in the pancreas. El Ouaamari *et al*.[129] showed that miRNA-375 can regulate PDK1, which is component in PIK3/PKB signaling cascade that is important in pancreas development[130] and maintenance of pancreatic cell mass and glucose homeostasis[131]. Loss of PDK1 result in diabetes and reduced number of β cell[131]. miRNA-375 can target PDK1, and overexpression of miRNA-375 in β cell lines reduced PDK1 protein levels accompanied with reduced downstream signalling resulting in reduced β cell and viability, additionally miRNA-375 overexpression reduced glucose ability to stimulate insulin mRNA production[129]. In

contrast inhibition of miRNA 375 resulted in an increase in PDK1 protein levels, insulin mRNA levels, and cell proliferation[129]. All together these data suggest that miRNA-375 may have a role in pancreatic development and β cell maintenance by regulating PDK1, as well as role in insulin secretion via the regulation of myotrophin. A link between *Pax6* and miRNA-375 has also been indicated by an independent component analysis (ICA) of miRNA regulation on gene expression in a model for type 1 Diabetes[132]. All these results are consistent with miRNA-375 regulation of *Pax6* in the pancreas.

4.2-Target Protectors Increase PAX6 Protein Levels in Heterozygous Islets.

We have shown that repression of miRNA-7 increases PAX6 protein levels in haploinsufficient islets. Treatment with a viral vector expressing TP-7, revealed a restoration of PAX6 levels to approximately 70% of wildtype levels. The data we have presented shows that shielding the miRNA-7 binding site in the 3'UTR of *Pax6* from miRNA regulation is effective at restoring PAX6 protein levels in haploinsufficient islets to near wildtype levels. This suggests that TPs against miRNA-7 binding sites may be potential targets for future work in the development of miRNA based therapeutics.

Inhibition of miRNA-7 in pancreatic endocrine cells by circular RNAs that act as a miRNA sponge has been shown to be effective *in vivo*[100]. Xu et al.[100] demonstrated that inhibition of miRNA-7 in islets from four month-old mice increased *Pax6* mRNA levels, and increased *PAX6* protein levels in pancreatic endocrine MIN6 cells. Furthermore, inhibition of miRNA-7 resulted in an increase in insulin expression, insulin content, and insulin secretion[100]. These data support the finding of this thesis; that repression of miRNA-7 can increase *Pax6* levels in pancreatic islets.

The use of circular RNAs as a potential miRNA-inhibition therapeutic strategy holds some promise, since circular RNAs, like Tuds sequester miRNA from its mRNA target, therefore, these miRNA-inhibitors may be useful at increasing gene expression to combat diseases that are caused by reduced gene expression. Mockenhaupt et al.[133] have shown that Tuds can reduce HCV replication in Huh 7.5 cells[133]. Although their study was based on cell culture, it suggests that miRNA inhibition can be used as a therapeutic strategy. Both Tud and circular-RNA-sponge strategies to sequester miRNA have the potential problem of lack of specificity, which may lead to pleiotropic effects. This problem should not occur, however, when TPs are incorporated into a therapeutic strategy, giving this approach a distinct advantage over miRNA inhibitors based on sequestering miRNA targets.

4.3-The Limitations of Target Protectors

As TPs cover a 60-base-pair region within the 3'UTR, multiple miRNAs may be blocked from regulating *Pax6*. Our miRNA-7 TP (TP-7) is predicted to interfere with adjacent miRNA-219, miRNA-182, miRNA-96, miRNA-382, and miRNA-876. Similarly, our miRNA-375 TP (TP-375) is predicted to block the adjacent miRNA-182, miRNA-365, miRNA-212, miRNA-369, and miRNA-374 sites. Since it is specific for *Pax6*, the target-protector therapeutic strategy may benefit from repressing multiple miRNAs. However, because multiple miRNAs are suppressed from targeting *Pax6* mRNA, overexpression of *Pax6* may occur, which can be detrimental[67,68,69]. This potential problem can be overcome by: targeting different miRNA sites, using a lower dosage, decreasing the size of the TP, and altering the promoter. It is unclear how much overexpression of PAX6 is required for pathology. Previous studies of overexpression

found that multiple copies of PAX6 are necessary to cause defects; 5-20 copies of *Pax6* were required to cause detrimental effects in the pancreas[69]. Therefore, if treatment with TPs results in *Pax6* overexpression that is below a detrimental level, it may still hold value as a therapeutic strategy. This question should be addressed in future *in vivo* studies.

4.4-Future Direction for Research

4.4.1-Suppression of miRNA-7 in Pancreatic Tissues by AAV-TP-7 *in vivo,* to Determine the Effects on *Pax6*

The next step, in the development of TPs for therapy would be to test them *in vivo*. This will provide insight to their effects on a living subject and account for variables, such as the breakdown of the TPs in the liver. The first objective would be to determine and optimise the efficiency of delivering the TPs into the pancreas. Toward this end a number of factor including: AAV serotypes, the dosage necessary to get efficient expression and methods of delivery of the TPs would be tested. Numerous studies have evaluated the transduction efficiency of several AAV serotypes at infecting pancreatic endocrine cells. These studies have found that three serotype: AAV8, AAV6, and AAV9 can efficiently transduce the pancreas[134,135,136]. In addition intra-ductal delivery of the AAV vectors resulted in efficient transduction, resulting in the highest GFP expression when compared to alternative delivery method[135]. These variables will be optimised at the same time and will be tested to corroborate the previous studies.

Furthermore, we can test multiple dosages, and monitor any side effects that may occur. The efficiency of transduction will be determined by flow cytometry analysis after the dissociation of islets, as was done in the current study. Before dissociation, a sample of islets will be fixed and analysed for any morphologic or hormonal expression

abnormalities, this analysis will be conducted by immunohistochemistry, and measurement of insulin, glucagon, and *PDX1* expression will be observed. Once these variables have been optimised and efficient transduction into endocrine cells is achieved, we would move to a mouse model more suitable for determining *in vivo* whether haploinsufficient of *Pax6* can be corrected by the TP strategy and whether a potential improvement of *Pax6* levels can meliorate the disease phenotype. For example, heterozygous *Pax6* mice fed on a high-fat diet develop diabetes at an exacerbated rate[57]; we can use this model to investigate whether restoring *Pax6* levels can alleviate a disease state. To this end, several measurements will be taken, including blood glucose levels, total plasma insulin levels, and the oral glucose tolerance test will be taken. To determine whether insulin secretion has been affected, glucose stimulated insulin secretion (GSIS) test would also be undertaken. Furthermore, the expression of components of insulin secretion, such as PC 1/3, as well as pro-insulin levels will be measured. In addition, the mechanism of action will be determined by confirming which endocrine islet cell population (α cells, β cells, or others) are affected. Moreover, *Pax6* regulates multiple targets in different cell types; for example, *Pax6* regulates glucagon in α cells, but in β cells it regulates insulin[44,126]. Therefore, increasing *Pax6* levels may have pleiotropic effects. To study this phenomenon, the GFP positive islets will be stained for cell markers of α and β cell population, glucagon and insulin, respectively. The islets will be analysed by immunohistochemistry and flow cytometry to determine whether co-localisation occurs and, if so, to what degree it occurs; indicating what cell types are being more affected by TPs.

4.4.1.2-Expected Outcomes and Potential Pitfalls

Haploinsufficiency of *Pax6* in humans and rodents causes a disruption to glucose homeostasis that is mediated by defective α and β cell regulation in the pancreas. The experiments discussed in the preceding section will determine whether increasing *Pax6* expression by suppressing key miRNAs can restore *Pax6* levels to wild-type, and thereby restore insulin and glucagon regulation in *Pax6* haploinsufficient mice. One possibility is that suppression of miRNA-7 alone is not sufficient to restore *Pax6* to wildtype levels and alleviate diabetic symptoms. In this case, we have several routes to explore in an attempt to increase expression. First, we can determine whether a combination of miRNA-375 and miRNA-7 suppression will work to increase suppression and restore *Pax6* expression**.** Alternatively, we can look at improving expression by increasing dosage or by altering promoter usage.

Another potential outcome is that miRNA repression by the TPs may result in overexpression of *Pax6*, which has been shown to detrimental to the pancreas[69]. If this occurs, several treatment parameters can be adjusted so as to reduce expression of TPs and *Pax6*; these parameters include AAV serotype, dosage, miRNAs target for suppression, size of TPs, and altering promoter usage.

If miRNA-inhibition treatment is successful in restoring *Pax6* levels and alleviating the symptoms associated with reduced *Pax6* levels, this will prove a significant step in the development of therapies for human patients, as miRNA inhibition may be used to restore *PAX6* expression in the aniridic population, which might alleviate the systemic symptoms current treatments struggle to deal with. Additionally, the increasing evidence that *PAX6* has a role in pathogenesis among a subpopulation of

diabetics, and as *PAX6* has properties similar to those of other MODY genes, suggest that TPs aimed at increasing *Pax6* expression may be useful in controlling diabetes.

The experiments discussed in this section will be designed to obtain data necessary to determine whether suppression of miRNA-7 regulation of *Pax6* is a potential target for the treatment of *Pax6* haploinsufficiency in the pancreas. This marks the first step in unlocking the potential of miRNA for the treatment of aniridia.

4.4.2-Suppression of miRNA in the Eye by adapting AAV-TP

If the TP strategy works in the pancreas, the next step would be to adapt the TPs to treat defects in the eye. Adapting the TPs to this purpose faces several challenges not seen in the pancreas. The first challenges would be determining what part of the eye to target; since *Pax6* is expressed in multiple components of the eye, it is difficult to determine what area to target to get the best therapeutic effect.

To address this question, we need to ensure that efficient transduction of an AAV-TP in multiple components of the eye can be achieved. There are several variables that can be altered to enable delivery of AAV to different components of the eye. Several studies have looked at the route of the administration and how this affects the viral vector's ability to target these components[137,138,139]. For example, to provide access to the cornea, AAVs have been applied in topical eye drops or by intra-stromal injection[137,138]. Expression of AAV into the retina of mice has been shown to be possible by systemic injection (into the tail vein)[137] as well as sub-retinal and intravitreal injections[139].

Additionally, a number of serotypes have been shown to exhibit cell tropism; for example, AAV5 is effective at infecting photoreceptors and the cornea[140,141,142]. Promoter alteration can also be used to customize what part of the eye gets targeted. For example,

the use AAV with hGRK1 promoter allowed for efficient expression of transgene in cones, and rod cells[141]. With these tools, effective transduction of the eye should be possible.

4.4.2.1-What miRNA to Target in the Eye to Increase Pax6 Expression

In order to test the TP strategy in the eye, we need to know what miRNA to target. One potential target is miRNA-7, which is expressed in the eye of adult mice[143], and in conjunction with the present study and previous studies[98,99,100], we know that miRNA-7 is a regulator of *Pax6*; therefore, targeting miRNA-7 to enhance *Pax6* levels may be a valid option. Another miRNA target in the eye that holds potential for restoration of *Pax6* levels is miRNA-328. A mutation in the *PAX6* 3'UTR increases the binding of miRNA-328 results in a reduction of *PAX6* levels and is associated with the development of myopia[49]. Myopia has been seen in several aniridic patients who had a mutation in *PAX6*[144,145,146], therefore, there appears to be a relationship between miRNA-328, *PAX6* and myopia. Additionally, it has been shown that miRNA-328 has the ability to target to wild-type *PAX6* 3'UTR, while the mutant allele that is related to increased binding and myopia had a stronger response to miRNA-328. Moreover overexpression of miRNA-328 results in reduced PAX6 protein levels[49]. This suggests that miRNA-328 regulates *Pax6* and, consequently, that targeting its binding site for protection may be a useful element in the TP strategy to restore *Pax6*.

4.4.2.2-What Component of the Eye to Target?

The final hurdle to overcome is to determine what component of the eye to target. Testing the strategies in a component of the eye that exhibits a disease state will allow us to determine whether increasing the levels of PAX6 protein can improve the affected

phenotype. This will be crucial to expand our knowledge of whether increasing the levels of *Pax6* can alleviate the defects associated with aniridia. Aniridic patients may develop keratopathy, a defect characterised by corneal ulceration, chronic pain and blindness[147]. The primary cause of aniridic keratopathy (AK) is a dysfunction of limbal stem cells. Recently, it has been shown that loss of *PAX6* results in limbal stem cells differentiating to skin-like epithelium cell. Moreover, *PAX6* is absent in congenital teratoma which alters cornea to skin lineage[34]. Additionally, overexpression of *PAX6* in skin epithelial stem cells causes them to resemble limbal stem cells[148]. If the TPs are successful in increasing *Pax6* expression in the cornea, this may alter the limbal stem cell fate and alleviate the symptoms of AK. The mouse models: $Pax6^{Sey\text{-}Neu/Pax6+}$ displays similar corneal defects (see The Use of the Small Eye Mouse Model to Characterise PAX6 Functions section for more details). This mouse model can be used to test TPs to increase *Pax6* levels and measure changes in corneal features[127]. Therefore, testing the TP strategy to increase *Pax6* expression in the cornea appears to be a valid area to investigate, as the cornea is easy to target, viral vectors have been shown to be able to infect corneal tissue, and a measurement of success is available.

I propose testing the ability of TPs to protect either the miRNA-7 or the miRNA-328 binding site in the *Pax6* 3'UTR to alleviate phenotype associated with AK. First, we need to confirm that these miRNAs are expressed in the cornea, that they are functional, and they can target *Pax6*. This can be achieved through experiment with corneal epithelial cell lines. If these miRNAs are functional and target *Pax6*, the next step is to determining whether TPs can restore PAX6 protein levels in these cell lines. Afterwards, the TPs should be tested in a relevant mouse model, namely $Pax6^{Sey\text{-}Neu/Pax6+}$ mice[125] . The

best route of administration for efficient transduction will be determined, along with the appropriate serotype using fluorescent microscopy or flow cytometry. PAX6 protein levels will be measured by western blot, flow cytometry, and the success of treatment to reduce the symptoms caused by *Pax6* mutations will be determined by comparative analysis of the ocular structures.

Bibliography

1. Hingorani, M. & Moore, A. in *GeneReviews(®)* (eds. Pagon, R. A. et al.) (University of Washington, Seattle, 1993).
2. Lee, H., Khan, R. & O'Keefe, M. Aniridia: current pathology and management. *Acta Ophthalmol. (Copenh.)* **86,** 708–715 (2008).
3. Netland, P. A., Scott, M. L., Boyle IV, J. W. & Lauderdale, J. D. Ocular and systemic findings in a survey of aniridia subjects. *J. Am. Assoc. Pediatr. Ophthalmol. Strabismus* **15,** 562–566 (2011).
4. Yasuda, T. *et al.* PAX6 mutation as a genetic factor common to aniridia and glucose intolerance. *Diabetes* **51,** 224–230 (2002).
5. Sisodiya, S. M. *et al.* PAX6 haploinsufficiency causes cerebral malformation and olfactory dysfunction in humans. *Nat. Genet.* **28,** 214–216 (2001).
6. Hingorani, M., Hanson, I. & van Heyningen, V. Aniridia. *Eur. J. Hum. Genet.* **20,** 1011–1017 (2012).
7. Heyningen, V. van & Williamson, K. A. PAX6 in sensory development. *Hum. Mol. Genet.* **11,** 1161–1167 (2002).
8. Plaza, S., Dozier, C., Turque, N. & Saule, S. Quail Pax-6 (Pax-QNR) mRNAs are expressed from two promoters used differentially during retina development and neuronal differentiation. *Mol. Cell. Biol.* **15,** 3344–3353 (1995).
9. Glaser, T., Walton, D. S. & Maas, R. L. Genomic structure, evolutionary conservation and aniridia mutations in the human PAX6 gene. *Nat. Genet.* **2,** 232–239 (1992).

10. Carriere, C. *et al.* Characterization of quail Pax-6 (Pax-QNR) proteins expressed in the neuroretina. *Mol. Cell. Biol.* **13,** 7257–7266 (1993).

11. Anderson, T. R., Hedlund, E. & Carpenter, E. M. Differential Pax6 promoter activity and transcript expression during forebrain development. *Mech. Dev.* **114,** 171–175 (2002).

12. Dimanlig, P. V., Faber, S. C., Auerbach, W., Makarenkova, H. P. & Lang, R. A. The upstream ectoderm enhancer in Pax6 has an important role in lens induction. *Dev. Camb. Engl.* **128,** 4415–4424 (2001).

13. Kammandel, B. *et al.* Distinctcis-Essential Modules Direct the Time–Space Pattern of thePax6Gene Activity. *Dev. Biol.* **205,** 79–97 (1999).

14. Kleinjan, D. A. *et al.* Long-range downstream enhancers are essential for Pax6 expression. *Dev. Biol.* **299,** 563–581 (2006).

15. Lauderdale, J. D., Wilensky, J. S., Oliver, E. R., Walton, D. S. & Glaser, T. 3′ deletions cause aniridia by preventing PAX6 gene expression. *Proc. Natl. Acad. Sci.* **97,** 13755–13759 (2000).

16. Walther, C. & Gruss, P. Pax-6, a murine paired box gene, is expressed in the developing CNS. *Dev. Camb. Engl.* **113,** 1435–1449 (1991).

17. Epstein, J. A. *et al.* Two independent and interactive DNA-binding subdomains of the Pax6 paired domain are regulated by alternative splicing. *Genes Dev.* **8,** 2022–2034 (1994).

18. Davis, N. *et al.* Pax6 dosage requirements in iris and ciliary body differentiation. *Dev. Biol.* **333,** 132–142 (2009).

19. Kim, J. & Lauderdale, J. D. Analysis of Pax6 expression using a BAC transgene reveals the presence of a paired-less isoform of Pax6 in the eye and olfactory bulb. *Dev. Biol.* **292,** 486–505 (2006).

20. Singh, S. *et al.* Iris hypoplasia in mice that lack the alternatively spliced Pax6(5a) isoform. *Proc. Natl. Acad. Sci. U. S. A.* **99,** 6812–6815 (2002).

21. Bäumer, N. *et al.* Retinal pigmented epithelium determination requires the redundant activities of Pax2 and Pax6. *Development* **130,** 2903–2915 (2003).

22. Jensen, J. *et al.* Independent development of pancreatic alpha- and beta-cells from neurogenin3-expressing precursors: a role for the notch pathway in repression of premature differentiation. *Diabetes* **49,** 163–176 (2000).

23. Nishina, S. *et al.* PAX6 expression in the developing human eye. *Br. J. Ophthalmol.* **83,** 723–727 (1999).

24. Zhang, W., Cveklovam, K., Oppermann, B., Kantorow, M. & Cvekl, A. Quantitation of PAX6 and PAX6(5a) transcript levels in adult human lens, cornea, and monkey retina. *Mol. Vis.* **7,** 1–5 (2001).

25. Wen, J. H. *et al.* Paired box 6 (PAX6) regulates glucose metabolism via proinsulin processing mediated by prohormone convertase 1/3 (PC1/3). *Diabetologia* **52,** 504–513 (2009).

26. Kamachi, Y., Uchikawa, M., Tanouchi, A., Sekido, R. & Kondoh, H. Pax6 and SOX2 form a co-DNA-binding partner complex that regulates initiation of lens development. *Genes Dev.* **15,** 1272–1286 (2001).

27. Marquardt, T. *et al.* Pax6 Is Required for the Multipotent State of Retinal Progenitor Cells. *Cell* **105,** 43–55 (2001).

28. Hill, R. E. *et al.* Mouse small eye results from mutations in a paired-like homeobox-containing gene. *Nature* **354,** 522–525 (1991).

29. St-Onge, L., Sosa-Pineda, B., Chowdhury, K., Mansouri, A. & Gruss, P. Pax6 is required for differentiation of glucagon-producing alpha-cells in mouse pancreas. *Nature* **387,** 406–409 (1997).

30. Glaser, T. *et al.* PAX6 gene dosage effect in a family with congenital cataracts, aniridia, anophthalmia and central nervous system defects. *Nat. Genet.* **7,** 463–471 (1994).

31. Solomon, B. D. *et al.* Compound heterozygosity for mutations in PAX6 in a patient with complex brain anomaly, neonatal diabetes mellitus, and microophthalmia. *Am. J. Med. Genet. A.* **149A,** 2543–2546 (2009).

32. Gregory-Evans, C. Y. *et al.* Postnatal manipulation of Pax6 dosage reverses congenital tissue malformation defects. *J. Clin. Invest.* **124,** 111–116 (2014).

33. Tseng, S. C. & Li, D. Q. Comparison of protein kinase C subtype expression between normal and aniridic human ocular surfaces: implications for limbal stem cell dysfunction in aniridia. *Cornea* **15,** 168–178 (1996).

34. Li, G. *et al.* Transcription factor Paired Box 6 controls limbal stem cell lineage in development and disease. *J. Biol. Chem.* jbc.M115.662940 (2015). doi:10.1074/jbc.M115.662940

35. PAX6 homepage - MRC Human Genetics Unit LOVD at MRC IGMM - Leiden Open Variation Database. Available at: http://lsdb.hgu.mrc.ac.uk/home.php?select_db=PAX6. (Accessed: 3rd August 2016)

36. Tzoulaki, I., White, I. M. & Hanson, I. M. PAX6 mutations: genotype-phenotype correlations. *BMC Genet.* **6,** 27 (2005).

37. Fujita, Y. *et al.* Pax6 and Pdx1 are required for production of glucose-dependent insulinotropic polypeptide in proglucagon-expressing L cells. *Am. J. Physiol. Endocrinol. Metab.* **295,** E648-657 (2008).

38. Malandrini, A. *et al.* PAX6 mutation in a family with aniridia, congenital ptosis, and mental retardation. *Clin. Genet.* **60,** 151–154 (2001).

39. Davis, L. K. *et al.* Pax6 3′ deletion results in aniridia, autism and mental retardation. *Hum. Genet.* **123,** 371–378 (2008).

40. Ellison-Wright, Z. *et al.* Heterozygous PAX6 mutation, adult brain structure and fronto-striato-thalamic function in a human family. *Eur. J. Neurosci.* **19,** 1505–1512 (2004).

41. Martha, A., Strong, L. C., Ferrell, R. E. & Saunders, G. F. Three novel aniridia mutations in the human PAX6 gene. *Hum. Mutat.* **6,** 44–49 (1995).

42. Ahlqvist, E. *et al.* A common variant upstream of the PAX6 gene influences islet function in man. *Diabetologia* **55,** 94–104 (2012).

43. Sander, M. *et al.* Genetic analysis reveals that PAX6 is required for normal transcription of pancreatic hormone genes and islet development. *Genes Dev.* **11,** 1662–1673 (1997).

44. Hart, A. W., Mella, S., Mendrychowski, J., van Heyningen, V. & Kleinjan, D. A. The Developmental Regulator Pax6 Is Essential for Maintenance of Islet Cell Function in the Adult Mouse Pancreas. *PLoS ONE* **8,** (2013).

45. Ding, J. *et al.* Pax6 Haploinsufficiency Causes Abnormal Metabolic Homeostasis by Down-Regulating Glucagon-Like Peptide 1 in Mice. *Endocrinology* **150,** 2136–2144 (2009).

46. Umeda, T. *et al.* Evaluation of Pax6 Mutant Rat as a Model for Autism. *PLOS ONE* **5,** e15500 (2010).

47. Abouzeid, H. *et al.* PAX6 aniridia and interhemispheric brain anomalies. *Mol. Vis.* **15,** 2074–2083 (2009).

48. Panjwani, N. *et al.* A microRNA- 328 binding site in PAX6 is associated with centrotemporal spikes of rolandic epilepsy. *Ann. Clin. Transl. Neurol.* **3,** 512–522 (2016).

49. Chen, K.-C. *et al.* MicroRNA-328 may influence myopia development by mediating the PAX6 gene. *Invest. Ophthalmol. Vis. Sci.* **53,** 2732–2739 (2012).

50. Liang, C.-L. *et al.* A functional polymorphism at 3'UTR of the PAX6 gene may confer risk for extreme myopia in the Chinese. *Invest. Ophthalmol. Vis. Sci.* **52,** 3500–3505 (2011).

51. Yogarajah, M. *et al.* PAX6, brain structure and function in human adults: advanced MRI in aniridia. *Ann. Clin. Transl. Neurol.* **3,** 314–330 (2016).

52. Dellovade, T. L., Pfaff, D. W. & Schwanzel-Fukuda, M. Olfactory bulb development is altered in small-eye (Sey) mice. *J. Comp. Neurol.* **402,** 402–418 (1998).

53. Ashery-Padan, R. *et al.* Conditional inactivation of Pax6 in the pancreas causes early onset of diabetes. *Dev. Biol.* **269,** 479–488 (2004).

54. Hill, M. E., Asa, S. L. & Drucker, D. J. Essential requirement for Pax6 in control of enteroendocrine proglucagon gene transcription. *Mol. Endocrinol. Baltim. Md* **13,** 1474–1486 (1999).

55. Watts, M., Ha, J., Kimchi, O. & Sherman, A. Paracrine regulation of glucagon secretion: the β/α/δ model. *Am. J. Physiol. - Endocrinol. Metab.* **310,** E597–E611 (2016).

56. Gardner, D. S. & Tai, E. S. Clinical features and treatment of maturity onset diabetes of the young (MODY). *Diabetes Metab. Syndr. Obes. Targets Ther.* **5,** 101–108 (2012).

57. Chen, Y. *et al.* High-fat diet induces early-onset diabetes in heterozygous Pax6 mutant mice. *Diabetes Metab. Res. Rev.* **30,** 467–475 (2014).

58. Lee, H. J. & Colby, K. A. A review of the clinical and genetic aspects of aniridia. *Semin. Ophthalmol.* **28,** 306–312 (2013).

59. Bakhtiari, P. *et al.* Surgical and visual outcomes of the type I Boston Keratoprosthesis for the management of aniridic fibrosis syndrome in congenital aniridia. *Am. J. Ophthalmol.* **153,** 967–971.e2 (2012).

60. Acland, G. M. *et al.* Gene therapy restores vision in a canine model of childhood blindness. *Nat. Genet.* **28,** 92–95 (2001).

61. Cideciyan, A. V. *et al.* Human gene therapy for RPE65 isomerase deficiency activates the retinoid cycle of vision but with slow rod kinetics. *Proc. Natl. Acad. Sci. U. S. A.* **105,** 15112–15117 (2008).

62. Hauswirth, W. W. *et al.* Treatment of leber congenital amaurosis due to RPE65 mutations by ocular subretinal injection of adeno-associated virus gene vector: short-term results of a phase I trial. *Hum. Gene Ther.* **19,** 979–990 (2008).

63. Maguire, A. M. *et al.* Age-dependent effects of RPE65 gene therapy for Leber's congenital amaurosis: a phase 1 dose-escalation trial. *Lancet Lond. Engl.* **374,** 1597–1605 (2009).

64. Jacobson SG, Cideciyan AV, Ratnakaram R & et al. Gene therapy for leber congenital amaurosis caused by rpe65 mutations: Safety and efficacy in 15 children and adults followed up to 3 years. *Arch. Ophthalmol.* **130,** 9–24 (2012).

65. Nicoletti, A. *et al.* Molecular characterization of the human gene encoding an abundant 61 kDa protein specific to the retinal pigment epithelium. *Hum. Mol. Genet.* **4,** 641–649 (1995).

66. Znoiko, S. L., Crouch, R. K., Moiseyev, G. & Ma, J.-X. Identification of the RPE65 protein in mammalian cone photoreceptors. *Invest. Ophthalmol. Vis. Sci.* **43,** 1604–1609 (2002).

67. Schedl, A. *et al.* Influence of PAX6 gene dosage on development: overexpression causes severe eye abnormalities. *Cell* **86,** 71–82 (1996).

68. Ouyang, J. *et al.* Pax6 overexpression suppresses cell proliferation and retards the cell cycle in corneal epithelial cells. *Invest. Ophthalmol. Vis. Sci.* **47,** 2397–2407 (2006).

69. Yamaoka, T. *et al.* Diabetes and pancreatic tumours in transgenic mice expressing Pa × 6. *Diabetologia* **43,** 332–339

70. Aalfs, C. M. *et al.* Tandem duplication of 11p12-p13 in a child with borderline development delay and eye abnormalities: dose effect of the PAX6 gene product? *Am. J. Med. Genet.* **73,** 267–271 (1997).

71. Hug, N., Longman, D. & Cáceres, J. F. Mechanism and regulation of the nonsense-mediated decay pathway. *Nucleic Acids Res.* **44,** 1483–1495 (2016).

72. Keeling, K. M., Wang, D., Conard, S. E. & Bedwell, D. M. Suppression of premature termination codons as a therapeutic approach. *Crit. Rev. Biochem. Mol. Biol.* **47,** 444–463 (2012).

73. Welch, E. M. *et al.* PTC124 targets genetic disorders caused by nonsense mutations. *Nature* **447,** 87–91 (2007).

74. Lagos-Quintana, M., Rauhut, R., Lendeckel, W. & Tuschl, T. Identification of Novel Genes Coding for Small Expressed RNAs. *Science* **294,** 853–858 (2001).

75. Lee, R. C., Feinbaum, R. L. & Ambros, V. The C. elegans heterochronic gene lin-4 encodes small RNAs with antisense complementarity to lin-14. *Cell* **75,** 843–854 (1993).

76. Lewis, B. P., Burge, C. B. & Bartel, D. P. Conserved Seed Pairing, Often Flanked by Adenosines, Indicates that Thousands of Human Genes are MicroRNA Targets. *Cell* **120,** 15–20 (2005).

77. Baek, D. *et al.* The impact of microRNAs on protein output. *Nature* **455,** 64–71 (2008).

78. Lee, Y. *et al.* MicroRNA genes are transcribed by RNA polymerase II. *EMBO J.* **23,** 4051–4060 (2004).

79. Gregory, R. I. *et al.* The Microprocessor complex mediates the genesis of microRNAs. *Nature* **432,** 235–240 (2004).

80. Lund, E., Güttinger, S., Calado, A., Dahlberg, J. E. & Kutay, U. Nuclear Export of MicroRNA Precursors. *Science* **303,** 95–98 (2004).

81. Park, J.-E. *et al.* Dicer recognizes the 5′ end of RNA for efficient and accurate processing. *Nature* **475,** 201–205 (2011).

82. Wightman, B., Ha, I. & Ruvkun, G. Posttranscriptional regulation of the heterochronic gene lin-14 by lin-4 mediates temporal pattern formation in C. elegans. *Cell* **75,** 855–862 (1993).

83. Zeng, Y., Yi, R. & Cullen, B. R. MicroRNAs and small interfering RNAs can inhibit mRNA expression by similar mechanisms. *Proc. Natl. Acad. Sci. U. S. A.* **100,** 9779–9784 (2003).

84. Selbach, M. *et al.* Widespread changes in protein synthesis induced by microRNAs. *Nature* **455,** 58–63 (2008).

85. Ma, L. *et al.* Therapeutic silencing of miR-10b inhibits metastasis in a mouse mammary tumor model. *Nat. Biotechnol.* **28,** 341–347 (2010).

86. Poy, M. N. *et al.* A pancreatic islet-specific microRNA regulates insulin secretion. *Nature* **432,** 226–230 (2004).

87. Baroukh, N. *et al.* MicroRNA-124a regulates Foxa2 expression and intracellular signaling in pancreatic beta-cell lines. *J. Biol. Chem.* **282,** 19575–19588 (2007).

88. Kloosterman, W. P., Lagendijk, A. K., Ketting, R. F., Moulton, J. D. & Plasterk, R. H. A. Targeted Inhibition of miRNA Maturation with Morpholinos Reveals a Role for miR-375 in Pancreatic Islet Development. *PLoS Biol.* **5,** (2007).

89. Jopling, C. L. Regulation of hepatitis C virus by microRNA-122. *Biochem. Soc. Trans.* **36,** 1220–1223 (2008).

90. Jopling, C. L., Yi, M., Lancaster, A. M., Lemon, S. M. & Sarnow, P. Modulation of hepatitis C virus RNA abundance by a liver-specific MicroRNA. *Science* **309,** 1577–1581 (2005).

91. Randall, G. *et al.* Cellular cofactors affecting hepatitis C virus infection and replication. *Proc. Natl. Acad. Sci.* **104,** 12884–12889 (2007).

92. Lanford, R. E. *et al.* Therapeutic silencing of microRNA-122 in primates with chronic hepatitis C virus infection. *Science* **327,** 198–201 (2010).

93. van der Ree, M. H. *et al.* Long-term safety and efficacy of microRNA-targeted therapy in chronic hepatitis C patients. *Antiviral Res.* **111,** 53–59 (2014).

94. A Multicenter Phase I Study of MRX34, MicroRNA miR-RX34 Liposomal Injection - Full Text View - ClinicalTrials.gov. Available at: https://clinicaltrials.gov/ct2/show/NCT01829971. (Accessed: 4th August 2016)

95. Kelly, O. G. & Melton, D. A. Development of the pancreas in Xenopus laevis. *Dev. Dyn.* **218,** 615–627 (2000).

96. Turque, N., Plaza, S., Radvanyi, F., Carriere, C. & Saule, S. Pax-QNR/Pax-6, a paired box- and homeobox-containing gene expressed in neurons, is also expressed in pancreatic endocrine cells. *Mol. Endocrinol. Baltim. Md* **8,** 929–938 (1994).

97. Kapsimali, M. *et al.* MicroRNAs show a wide diversity of expression profiles in the developing and mature central nervous system. *Genome Biol.* **8,** R173 (2007).

98. de Chevigny, A. *et al.* miR-7a regulation of Pax6 controls spatial origin of forebrain dopaminergic neurons. *Nat. Neurosci.* **15,** 1120–1126 (2012).

99. Kredo-Russo, S. *et al.* Pancreas-enriched miRNA refines endocrine cell differentiation. *Development* **139,** 3021–3031 (2012).

100. Xu, H., Guo, S., Li, W. & Yu, P. The circular RNA Cdr1as, via miR-7 and its targets, regulates insulin transcription and secretion in islet cells. *Sci. Rep.* **5,** 12453 (2015).

101. Carè, A. *et al.* MicroRNA-133 controls cardiac hypertrophy. *Nat. Med.* **13,** 613–618 (2007).

102. Hutvágner, G., Simard, M. J., Mello, C. C. & Zamore, P. D. Sequence-Specific Inhibition of Small RNA Function. *PLoS Biol.* **2,** (2004).

103. Horwich, M. D. & Zamore, P. D. Design and Delivery of Antisense Oligonucleotides to Block microRNA Function in Cultured Drosophila and Human Cells. *Nat. Protoc.* **3,** 1537–1549 (2008).

104. Haraguchi, T., Ozaki, Y. & Iba, H. Vectors expressing efficient RNA decoys achieve the long-term suppression of specific microRNA activity in mammalian cells. *Nucleic Acids Res.* **37,** e43 (2009).

105. Bak, R. O., Hollensen, A. K., Primo, M. N., Sørensen, C. D. & Mikkelsen, J. G. Potent microRNA suppression by RNA Pol II-transcribed 'Tough Decoy' inhibitors. *RNA* **19,** 280–293 (2013).

106. Zhang, L., Li, Y.-J., Wu, X.-Y., Hong, Z. & Wei, W.-S. MicroRNA-181c negatively regulates the inflammatory response in oxygen-glucose-deprived microglia by targeting Toll-like receptor 4. *J. Neurochem.* **132,** 713–723 (2015).

107. Choi, W.-Y., Giraldez, A. J. & Schier, A. F. Target protectors reveal dampening and balancing of Nodal agonist and antagonist by miR-430. *Science* **318,** 271–274 (2007).

108. Staton, A. A. & Giraldez, A. J. Use of target protector morpholinos to analyze the physiological roles of specific miRNA-mRNA pairs in vivo. *Nat. Protoc.* **6,** 2035–2049 (2011).

109. Knauss, J. L., Bian, S. & Sun, T. Plasmid-based target protectors allow specific blockade of miRNA silencing activity in mammalian developmental systems. *Front. Cell. Neurosci.* **7,** (2013).

110. Ellis, B. L. *et al.* A survey of ex vivo/in vitro transduction efficiency of mammalian primary cells and cell lines with Nine natural adeno-associated virus (AAV1-9) and one engineered adeno-associated virus serotype. *Virol. J.* **10,** 74 (2013).

111. Kronenberg, S., Kleinschmidt, J. A. & Böttcher, B. Electron cryo-microscopy and image reconstruction of adeno-associated virus type 2 empty capsids. *EMBO Rep.* **2,** 997–1002 (2001).

112. Xiao, X., Li, J. & Samulski, R. J. Efficient long-term gene transfer into muscle tissue of immunocompetent mice by adeno-associated virus vector. *J. Virol.* **70,** 8098–8108 (1996).

113. Nathwani, A. C. *et al.* Adenovirus-associated virus vector-mediated gene transfer in hemophilia B. *N. Engl. J. Med.* **365,** 2357–2365 (2011).

114. Zincarelli, C., Soltys, S., Rengo, G. & Rabinowitz, J. E. Analysis of AAV Serotypes 1–9 Mediated Gene Expression and Tropism in Mice After Systemic Injection. *Mol. Ther.* **16,** 1073–1080 (2008).

115. Zhou, X. & Muzyczka, N. In vitro packaging of adeno-associated virus DNA. *J. Virol.* **72,** 3241–3247 (1998).

116. Samulski, R. J. *et al.* Targeted integration of adeno-associated virus (AAV) into human chromosome 19. *EMBO J.* **10,** 3941–3950 (1991).

117. Kotin, R. M. *et al.* Site-specific integration by adeno-associated virus. *Proc. Natl. Acad. Sci.* **87,** 2211–2215 (1990).

118. Penaud-Budloo, M. *et al.* Adeno-Associated Virus Vector Genomes Persist as Episomal Chromatin in Primate Muscle. *J. Virol.* **82,** 7875–7885 (2008).

119. Podsakoff, G., Wong, K. K. & Chatterjee, S. Efficient gene transfer into nondividing cells by adeno-associated virus-based vectors. *J. Virol.* **68,** 5656–5666 (1994).

120. Mingozzi, F. & High, K. A. Immune responses to AAV vectors: overcoming barriers to successful gene therapy. *Blood* **122,** 23–36 (2013).

121. Roberts, R. C. Small eyes—a new dominant eye mutant in the mouse. *Genet. Res.* **9,** 121–122 (1967).

122. Fantes, J. A. *et al.* Submicroscopic deletions at the WAGR locus, revealed by nonradioactive in situ hybridization. *Am. J. Hum. Genet.* **51,** 1286–1294 (1992).

123. Favor, J. *et al.* Analysis of Pax6 contiguous gene deletions in the mouse, Mus musculus, identifies regions distinct from Pax6 responsible for extreme small-eye and belly-spotting phenotypes. *Genetics* **182,** 1077–1088 (2009).

124. Glaser, T., Lane, J. & Housman, D. A mouse model of the aniridia-Wilms tumor deletion syndrome. *Science* **250,** 823–827 (1990).

125. Ramaesh, T. *et al.* Corneal abnormalities in Pax6+/- small eye mice mimic human aniridia-related keratopathy. *Invest. Ophthalmol. Vis. Sci.* **44,** 1871–1878 (2003).

126. Latreille, M. *et al.* MicroRNA-7a regulates pancreatic β cell function. *J. Clin. Invest.* **124,** 2722–2735 (2014).

127. Burré, J. *et al.* Alpha-synuclein promotes SNARE-complex assembly in vivo and in vitro. *Science* **329,** 1663–1667 (2010).

128. Poy, M. N. *et al.* miR-375 maintains normal pancreatic alpha- and beta-cell mass. *Proc. Natl. Acad. Sci. U. S. A.* **106,** 5813–5818 (2009).

129. El Ouaamari, A. *et al.* miR-375 targets 3'-phosphoinositide-dependent protein kinase-1 and regulates glucose-induced biological responses in pancreatic beta-cells. *Diabetes* **57,** 2708–2717 (2008).

130. Westmoreland, J. J., Wang, Q., Bouzaffour, M., Baker, S. J. & Sosa-Pineda, B. Pdk1 activity controls proliferation, survival, and growth of developing pancreatic cells. *Dev. Biol.* **334,** 285–298 (2009).

131. Hashimoto, N. *et al.* Ablation of PDK1 in pancreatic β cells induces diabetes as a result of loss of β cell mass. *Nat. Genet.* **38,** 589–593 (2006).

132. Bang-Berthelsen, C. H. *et al.* Independent component and pathway-based analysis of miRNA-regulated gene expression in a model of type 1 diabetes. *BMC Genomics* **12,** 97 (2011).

133. Mockenhaupt, S., Grosse, S., Rupp, D., Bartenschlager, R. & Grimm, D. Alleviation of off-target effects from vector-encoded shRNAs via codelivered RNA decoys. *Proc. Natl. Acad. Sci. U. S. A.* **112,** E4007–E4016 (2015).

134. Cheng, H. *et al.* Efficient and persistent transduction of exocrine and endocrine pancreas by adeno-associated virus type 8. *J. Biomed. Sci.* **14,** 585–594 (2007).

135. Jimenez, V. *et al.* In vivo genetic engineering of murine pancreatic beta cells mediated by single-stranded adeno-associated viral vectors of serotypes 6, 8 and 9. *Diabetologia* **54,** 1075–1086 (2011).

136. Wang, A. Y., Peng, P. D., Ehrhardt, A., Storm, T. A. & Kay, M. A. Comparison of adenoviral and adeno-associated viral vectors for pancreatic gene delivery in vivo. *Hum. Gene Ther.* **15,** 405–413 (2004).

137. Hippert, C. *et al.* Corneal Transduction by Intra-Stromal Injection of AAV Vectors In Vivo in the Mouse and Ex Vivo in Human Explants. *PLoS ONE* **7,** (2012).

138. Mohan, R. R., Sharma, A., Cebulko, T. C. & Tandon, A. Vector delivery technique affects gene transfer in the cornea in vivo. *Mol. Vis.* **16,** 2494–2501 (2010).

139. Dinculescu, A. *et al.* AAV-Mediated Clarin-1 Expression in the Mouse Retina: Implications for USH3A Gene Therapy. *PLoS ONE* **11,** (2016).

140. Sharma, A., Tovey, J. C. K., Ghosh, A. & Mohan, R. R. AAV serotype influences gene transfer in corneal stroma in vivo. *Exp. Eye Res.* **91,** 440–448 (2010).

141. Boye, S. E. *et al.* The human rhodopsin kinase promoter in an AAV5 vector confers rod- and cone-specific expression in the primate retina. *Hum. Gene Ther.* **23,** 1101–1115 (2012).

142. Mohan, R. R., Tandon, A., Sharma, A., Cowden, J. W. & Tovey, J. C. K. Significant inhibition of corneal scarring in vivo with tissue-selective, targeted AAV5 decorin gene therapy. *Invest. Ophthalmol. Vis. Sci.* **52,** 4833–4841 (2011).

143. Hackler, L., Wan, J., Swaroop, A., Qian, J. & Zack, D. J. MicroRNA Profile of the Developing Mouse Retina. *Invest. Ophthalmol. Vis. Sci.* **51,** 1823–1831 (2010).

144. Caglayan, A. O. & Robinson, D. Aniridia phenotype and myopia in a turkish boy with a PAX6 gene mutation. *Genet. Couns. Geneva Switz.* **22,** 155–159 (2011).

145. Naithani, P., Sinha, A. & Gupta, V. Inherited partial aniridia, microcornea with high myopia and Bergmeister′s papilla: A new phenotypic expression. *Indian J. Ophthalmol.* **56,** 145–146 (2008).

146. Biswas, J., Chakrabarti, A. & Das, D. Rare Association of Familial Aniridia, Microcornea with Myopia and Aphakia. *Middle East Afr. J. Ophthalmol.* **21,** 268–270 (2014).

147. Gomes, J. A. *et al.* Recurrent keratopathy after penetrating keratoplasty for aniridia. *Cornea* **15,** 457–462 (1996).

148. Ouyang, H. *et al.* WNT7A and PAX6 define corneal epithelium homeostasis and pathogenesis. *Nature* **advance online publication,** (2014).

Appendices

Appendix A- Supplementary data

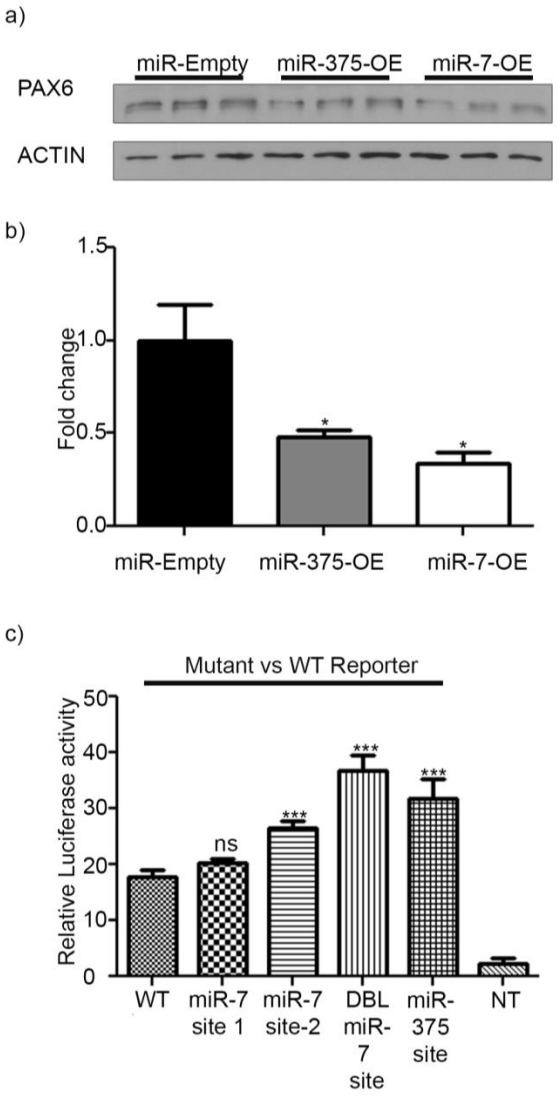

Appendix Figure 1: miRNA-375 and miRNA-7 regulate *Pax6* in αtc1-6 cells.
(a) Representative western blot analysis of the effect of miRNA-375 or miRNA-7 overexpression on PAX6 protein levels in αtc1-6 cells; each lane represents a protein sample extracted from a well of 6 well plate, β -actin was used as a loading control. (b) Quantification of densitometrey western blot data using Image J, showing fold change relative to miR-Empty. The fold change was calculated by dividing the ratio of PAX6:ACTIN signal of each condition (miR-Empty, miR-375-OE, miR-7-OE) by the average ratio of PAX6:ACTIN for miR-Empty. The resultant fold change for each condition was averaged. (c) Representative luciferase reporter assays of αtc1-6 cells 24 hours after transfection of the wild-type *Pax6* 3'UTR or mutated *Pax6* 3'UTR at miRNA 7 or miRNA-375 seed site. For panels (b) and (c), a one-way ANOVA was conducted with the following results: F [2,6] =8.519; P=0.0177 (b), F [5,12] =111.5; P<0.0001 (c). This was

followed by Dunnett's multiple comparison test comparing all column to control (miR-empty or WT) was used to determine whether there were significant differences between groups to controls, P<0.05=*, P<0.01=**, *P*<0.001=***, non-significant = n.s.

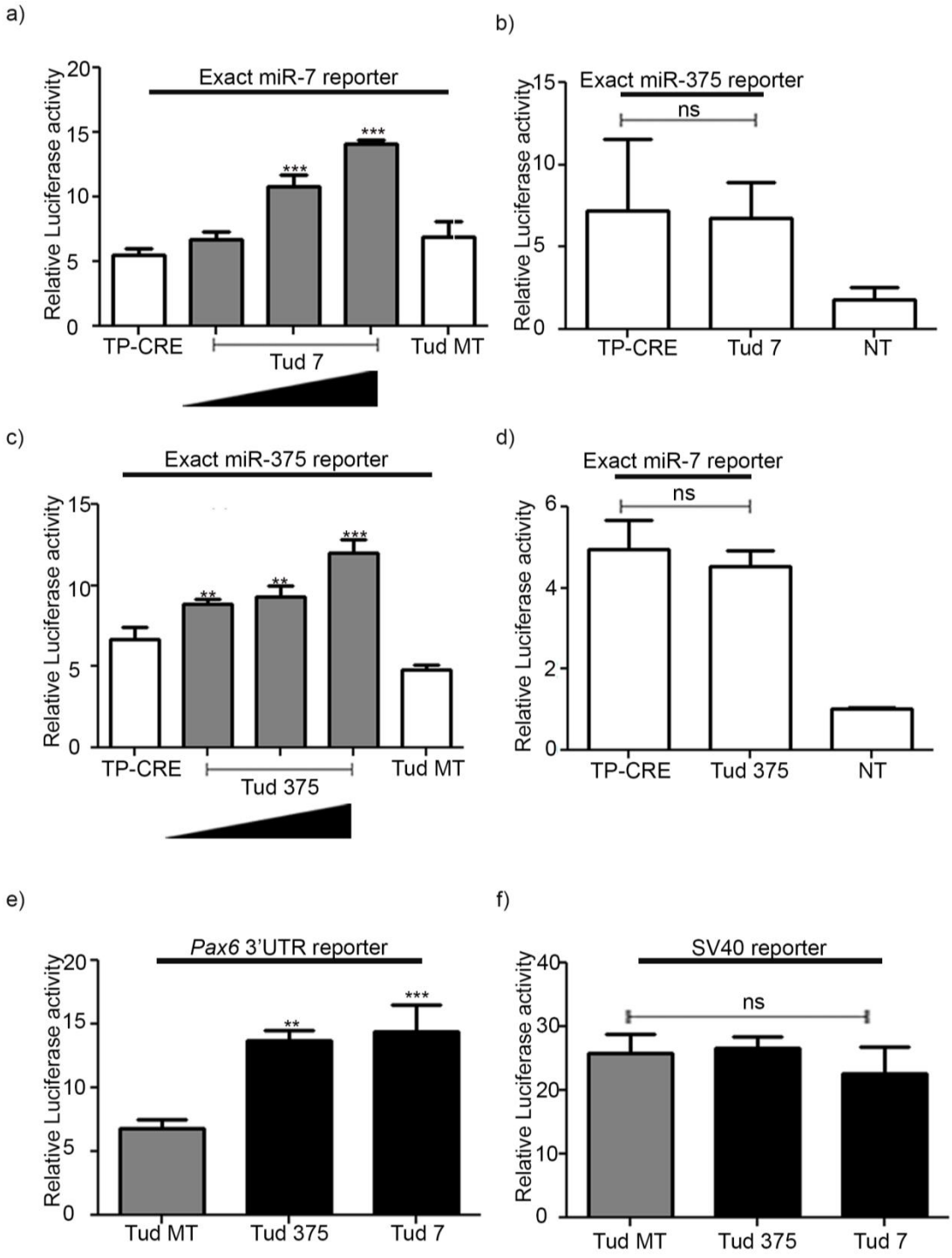

Appendix Figure 2: Tud-mediated miRNA inhibition increases *Pax6* 3'UTR reporter expression in αtc1-6 cells. (a) Representative luciferase reporter assays of αtc1-6 cells 24 hours

after co-transfection of the exact miRNA-7 seed site reporter and either control TP-CRE, Tud MT or increasing concentration of Tud 7. (b) Representative luciferase reporter assays of αtc1-6 cells 24 hours after co-transfection of the exact miRNA-375 seed site reporter and either control TP-CRE or Tud 7 (at the highest concentration). (c) Representative luciferase reporter assays of αtc1-6 cells 24 hours after co-transfection of the exact miRNA-375 seed site reporter and either control TP-CRE, Tud MT; or increasing concentration of Tud 375. (d) Representative luciferase reporter assays of αtc1-6 cells 24 hours after co-transfection of the exact miRNA-7 seed site reporter and either control TP-CRE or Tud 375 (at the highest concentration). (e) Representative luciferase reporter assays of αtc1-6 cells 24 hours after co-transfection of wild-type *Pax6* 3'UTR and Tud constructs. (f) Representative luciferase reporter assays of αtc1-6 cells 24 h after co-transfection of SV40 reporter and Tud constructs. For panels (a-f) a one-way ANOVA was conducted with the following results: F [4,10] =59.35; P<0.0001 (a), F [2,6] =3.327; n.s (b), F [4,10] =58.23; P<0.0001 (c), F [2,6] =58.87; P=0.0001 (d), F [2,6] =29.45; P=0.0008 (e), F [2,6] =1.335; n.s (f). This was followed by Dunnett's multiple comparison test comparing all column to control (Tud Mt or TP-CRE) was used to determine whether there were significant differences between groups to control, P<0.01=**, P<0.001=***, non-significant = n.s.

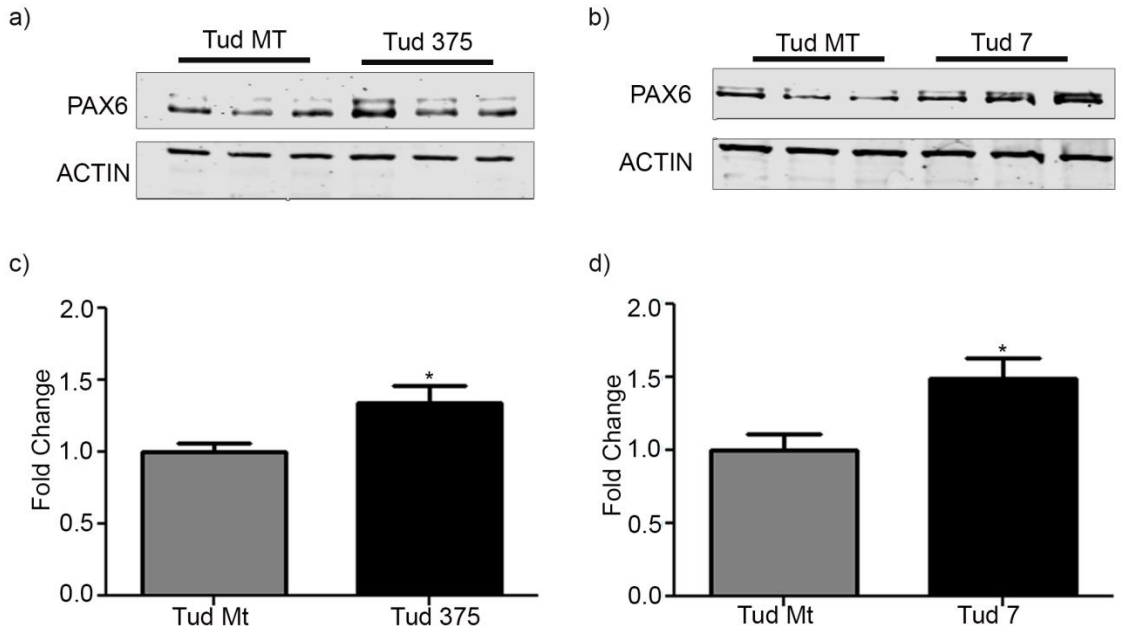

Appendix Figure 3: Tud-mediated miRNA inhibition increases *Pax6* protein levels in αtc1-6 cells. a) Representative western blot analysis of the effect of Tuds mediated suppression of miRNA-375 on PAX6 protein levels in αtc6 cells; each lane represents protein sample extracted from a well from a 6 well plate, β -actin was used as a loading control.
(b) Representative western blot analysis of the effect of Tuds-mediated suppression of miRNA-7 on PAX6 protein levels in βtc6 cells; each lane represents protein sample extracted from a well from a 6 well plate, β -actin was used as a loading control. (c) Quantification of western blot analysis by li-COR image studio of blot of Tud 375 treated cells, showing PAX6 fold change relative to Tud MT. (d) Quantification of western blot analysis by image studio of li-COR blot Tud 7 treated cells, showing PAX6 fold change relative to Tud MT. The fold change was calculated by dividing the ratio of PAX6:ACTIN li-Cor signal intensity from each condition by

the average ratio of li-Cor signal intensity of PAX6:ACTIN for Tud MT. The resultant fold change for each condition was then averaged. A two-tailed t-test was used to determine whether there was a significant difference between either Tud Mt and Tud 375 (c) or Tud 7 (d), in panel (c): t (4) =3.293 *P*=0.0301, panel (d): t (4) =3.281 *P*=0.0358, *P*<0.05=*.

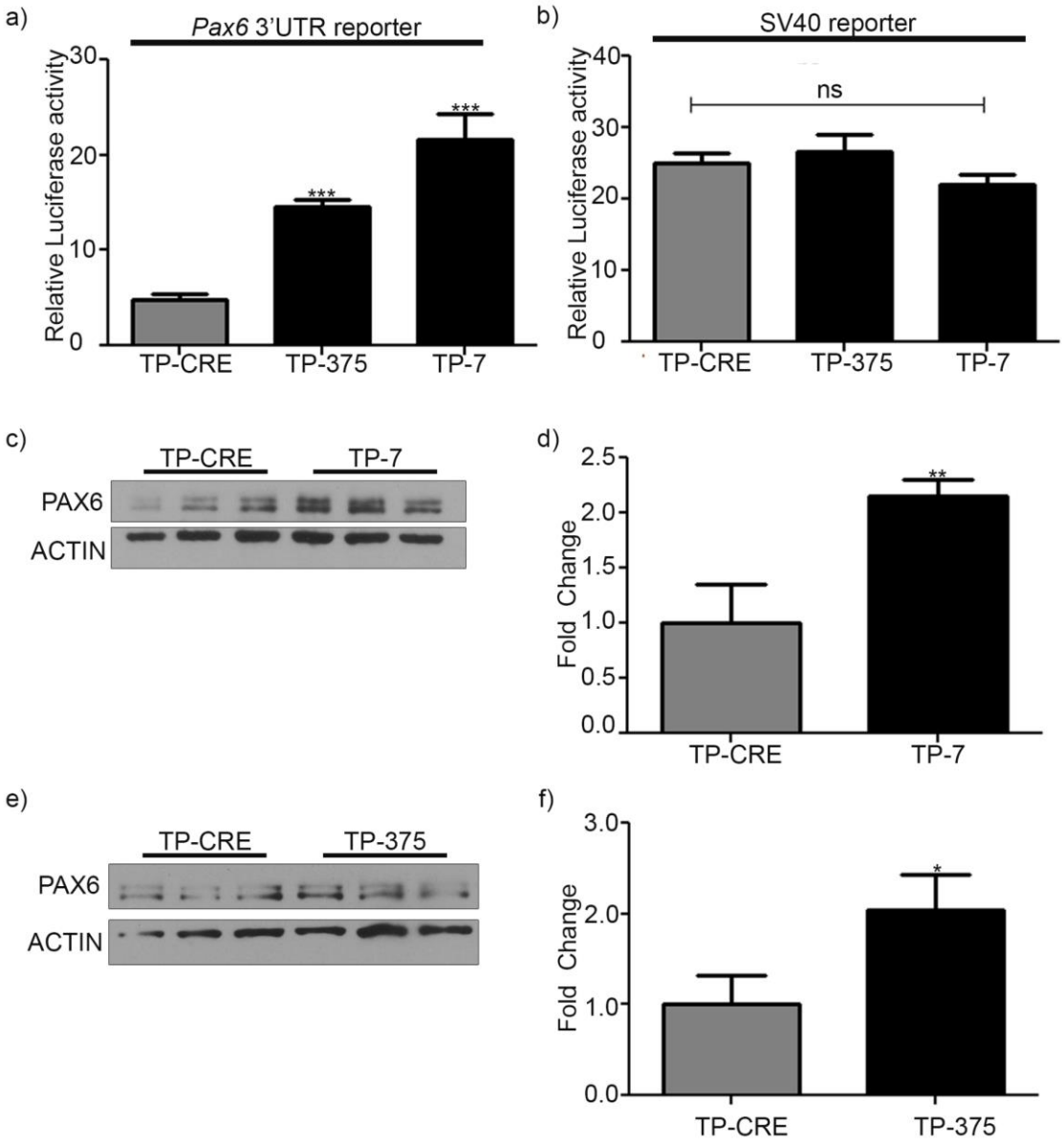

Appendix Figure 4: Target Protector mediated miRNA inhibition increases PAX6 levels in αtc1-6 cells. (a) Representative luciferase reporter assays of αtc1-6 cells 24 hour after co-transfection of wildtype *Pax6* 3'UTR reporter and TP constructs. (b) Representative luciferase reporter assays of αtc1-6 cells 24 h after co-transfection of SV40 reporter and TP constructs. (c and e) Representative western blot analysis of the effect of TP mediated repression of miRNA-7 (c) or miRNA-375 (e) on PAX6 protein levels in αtc1-6 cells, each lane represents protein sample extracted from a well from a 6 well plate, β -actin was used as a loading control. (d and f) Quantification of western blot analysis, fold change relative to TP-CRE by ImageJ of

densitometry data. . The fold change was calculated by dividing the ratio of PAX6:ACTIN LiCor signal from each condition by the average PAX6:ACTIN ratio signal of TP-CRE. The resultant fold change for each condition was averaged.For panels (a-b) a one-way ANOVA with the following results: F [2,6] =74.90; P<0.0001 (a), F [2,6] =2.915; n.s (b), followed by Dunnett's multiple comparison test comparing all column to control (TP-CRE) was used to determine whether there were significant differences between groups in panel, P<0.01=**, P<0.001=***, non-significant = n.s. A two-tailed t-test was used to determine whether there was a significant difference between either TP-CRE and TP-7 (d) or TP-375 (f), in panel (d): t (4) =5.154 P=0.0067, panel (d): t (4) =3.495 P=0.0250, P<0.05=*, P<0.01=**.

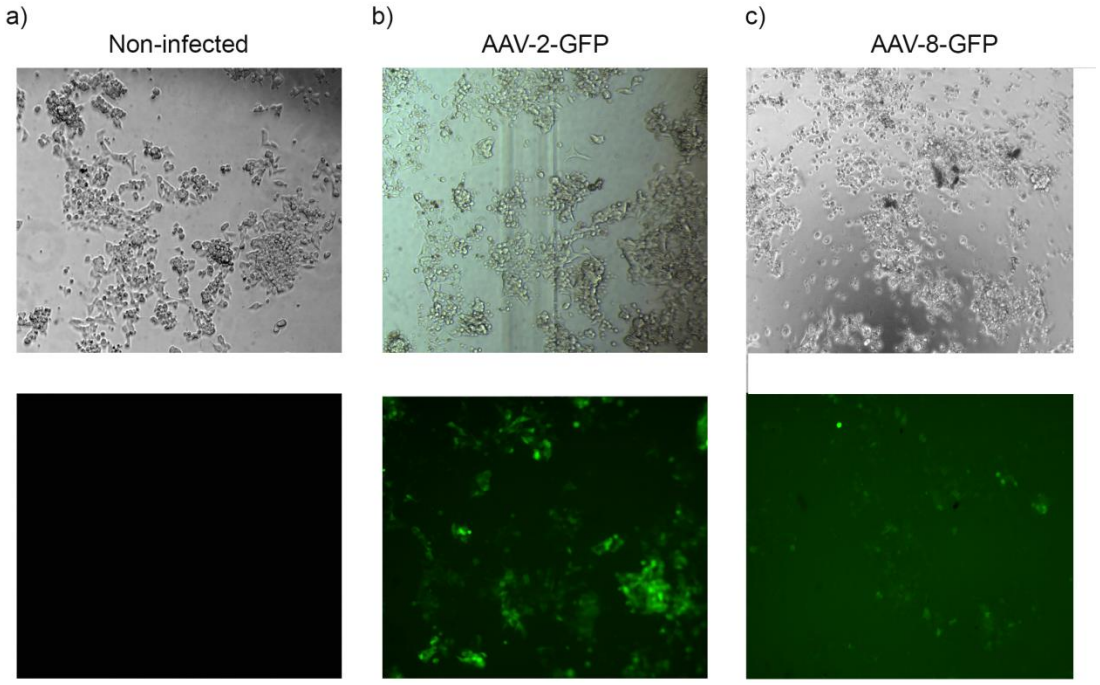

Appendix Figure 5: AAV-2 serotype efficiently infects αtc6-1 cells. (a) Non-infected αtc6-1 cells. (b) αtc6-1 cells infected with AAV-2 GFP serotype after 3 days of infection MOI 10^6. (c) αtc6-1 cells infected with AAV-8 serotype after 3 days of infection MOI 10^6.

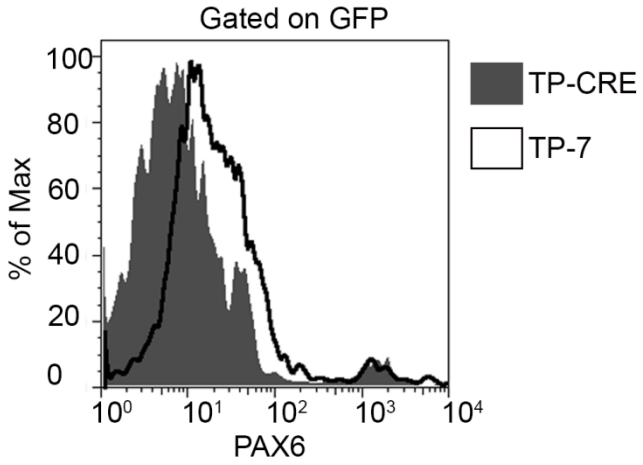

Appendix Figure 6: Blind tested Target Protector mediated miRNA inhibition increases PAX6 levels in islets. In order to ensure no bias was introduce, viral vector expressing either TP-CRE, or TP-7 were coded by another student without my knowledge. Islets were treated with coded samples, and processed as other flow cytometer experiment. After analysis samples were decoded. PAX6 histogram from GFP positive cells, the shaded histogram represents dissociated wildtype islet cells treated with TP-CRE the non-shaded histogram with the dark line represents wildtype islet cells treated with TP-7.

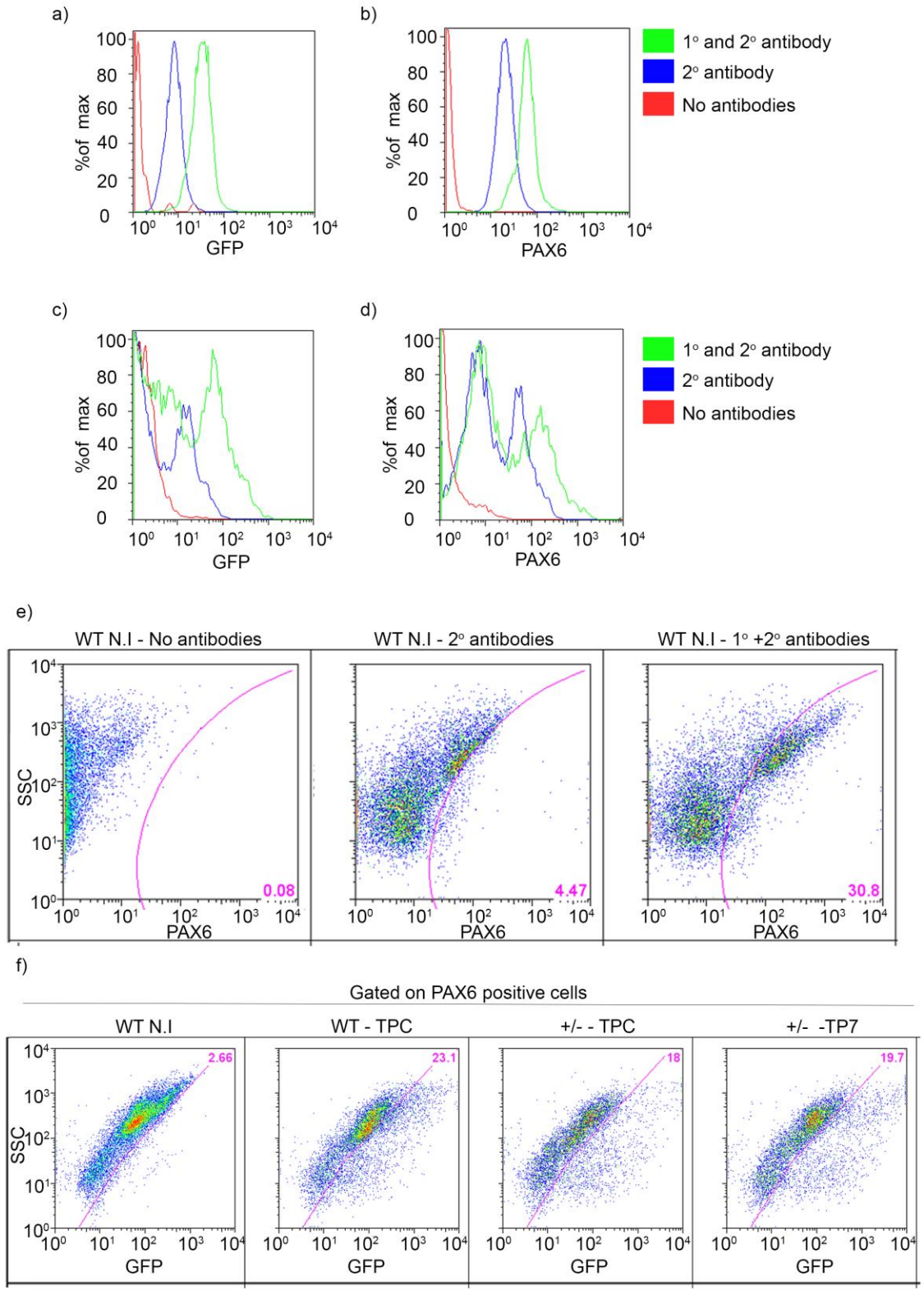

Appendix Figure 7: Flow cytometer controls and gating for PAX6 and GFP positive cells. a,c) Representative histogram showing GFP levels in nontransfected βtc-6 cells(a) or wildtype islets (c). The histogram with the red outline represent cell that were not labelled with any

antibody. The histogram with the blue outline represents cells that were labelled with the secondary antibody for GFP and PAX6. The histogram with the green outline represents cells that were label with both primary and secondary antibody for GFP and PAX6. b,d) Representative histogram showing PAX6 level in nontransfected βtc-6 cells(b) or wildtype islets (d). The histogram with the red outline represents cells that were not labelled with any antibody. The histogram with the blue outline represents cells that were labelled with the secondary antibody for GFP and PAX6. The histogram with the green outline represent cells that were label with both primary and secondary antibody for GFP and PAX6.e) Representative PAX6 positive gating control. PAX6 positive cells were determined by gating the region that did not contain any cells in samples that were labelled with secondary antibodies for PAX6 on the FL4 channel (2^{nd} panel). Cells residing in the pink outline represent PAX6 positive cells. In the 1^{st} panel – non-infected islets cells that were not labelled with any antibodies. In the 2^{nd} panel – non-infected islets cells that were labelled with secondary antibodies for PAX6 and GFP. In the 3^{rd} panel – non-infected islets that were labelled with primary and secondary antibodies for PAX6 and GFP. f) Representative GFP positive gating control. GFP positive cell were determined by gating the region that did not contain any cell in samples that were not treated and were labelled with primary and secondary antibodies for GFP and PAX6 on the FL1 channel (3^{rd} panel). Cells residing in the pink outline represent GFP positive cells. In the 1^{st} panel – non-infected wildtype islets cells that were labelled with primary antibodies for GFP and PAX6. In the 2^{nd} panel – wildtype islets cells that were treated with TP-CRE and were labelled with primary and secondary antibodies for PAX6 and GFP. In the 3^{rd} panel – heterozygous islets cells that were treated with TP-CRE and were labelled with primary and secondary islets for PAX6 and GFP. In the 4^{th} panel – heterozygous islets cells that were treated with TP-7 and were labelled with primary and secondary antibodies for PAX6 and GFP .